

**MAGEL2 regulates leptin receptor internalization through ubiquitination
pathways involving USP8 and RNF41**

by

Tishani Methsala Wijesuriya

A thesis submitted in partial fulfillment of the requirements for the degree of

Master of Science

Medical Sciences – Medical Genetics

University of Alberta

©Tishani Methsala Wijesuriya, 2017

Abstract

Children with Prader-Willi syndrome have neonatal feeding difficulties, developmental delay and excessive appetite. Loss of *MAGEL2* alone causes a related neurodevelopmental disorder (Schaaf-Yang syndrome) and may contribute to obesity in children with Prader-Willi syndrome who lack *MAGEL2* and other genes. *MAGEL2* is essential in neurons that sense levels of the adipose tissue-derived hormone leptin. The *MAGEL2* protein is important for recycling or degradation of proteins in the brain and interacts with and modifies the activity of E3 ubiquitin ligases. RNF41 is a E3 ubiquitin ligase that associates with a ubiquitin-specific protease (USP8). Together with USP8, RNF41 regulates the recycling of the leptin receptor by targeting it either for degradation or for recycling to the cell membrane. I hypothesized that *MAGEL2* regulates the interaction between RNF41 and USP8, and that loss of this regulation could impair leptin response pathways in the brain in children with PWS.

Human U2OS cells were transfected with recombinant constructs encoding epitope tagged versions of *MAGEL2* and wild type and mutant forms of RNF41. Immunofluorescence was used to visualize the co-localization of different forms of RNF41 with *MAGEL2* in intracellular compartments. I expressed recombinant *MAGEL2*, RNF41 and USP8 in combinations in human U2OS cells and examined the relative abundance of each protein in the presence or absence of the other components of the complex. The interactions between *MAGEL2* and other proteins were examined by the Bio ID system.

I identified interactions among components of the RNF41-USP8 complex that depended either on the activity of the RING domain of RNF41 (RNF-SQ mutant form) or the binding domain of

RNF41 (RNF-AE mutant form). Co-expression of MAGEL2 with components of the RNF41-USP8 complex modified the abundance of proteins in the complex. My results suggest that RNF41 enhances USP8 ubiquitylation, and I found that MAGEL2 diminishes the ability of RNF41 to auto-ubiquitinate or to ubiquitinate. Co-expression of MAGEL2 also modified the intracellular localization of components of the RNF41-USP8 complex. Levels of endogenous RNF41 and USP8 level in brain tissues from *Magel2* knockout mice were different from levels found in tissues from wild type littermates.

My results suggest that MAGEL2 could modify the activity of the RNF41-USP8 ubiquitination complex in leptin sensing neurons, providing a possible mechanism for dysregulation of leptin sensing in neurons in children with Prader-Willi syndrome.

Preface

This thesis is an original work by Tishani Methsala Wijesuriya. The research project, of which this thesis is a part, received research ethics approval from the University of Alberta Research Ethics Board, Project Name “Murine homologues of Prader-Willi Syndrome (PWS) Genes”, No. AUP00000359, June 22, 2016.

The project was done in collaboration with Dr. Jan Tavernier and Dr. Leetnje De Ceuninck at the University of Ghent, Belgium. They performed a set of experiments parallel with the experiments I performed. For simplicity, I will present their experiments as preliminary results.

Acknowledgements

First and foremost, I would like to thank Professor Rachel Wevrick for giving me an opportunity to work under her guidance. I am really privileged to have her as my supervisor. I was able to complete my research with her immense support and encouragement. She was always there to help me whenever I was doubtful and stressed. I would also like to thank my committee members Dr. Emmanuelle Cordat and Dr. Gary Eitzen for helping and guiding me throughout my research. Your suggestions and comments were valuable to improve my project. Also, my special thank goes to our collaborators Dr. Jan Tavernier and Dr. Leentje De Ceuninck for providing me valuable suggestions and ideas to fill up the gaps I had in my project and also, for providing plasmids for experiments. I would also like to thank our graduate coordinator Dr. Hughes. I am lucky to have her as my instructor for my first ever journal club as she helped and guided me a lot. Thank you for providing me with all the support and guidance needed to succeed.

I would like to thank our lab technician, Jocelyn Bischof for the support given throughout my degree specially with the mice work. Specially I would like to thank Herman Cortes, our former lab technician. He was always there to teach me whenever I needed help. I also would like to thank all the Wevrick lab members: Vanessa Carias, Dila Kamaludin, Chloe Luck, Matthea Sanderson for all the support they have given throughout. I would like to thank my summer student Kelly Fagan, for helping me to finish up experiments. It was a great experience to teach and guide an undergraduate. I thank Ensaf Almomani from Dr. Cordat's lab and Katie Badior from Dr. Casey's lab for helping me with reagents and suggestions for the cell surface biotinylation assay.

I am also very grateful to Canadian Institute of Health Research, Faculty of Medicine and Dentistry, University of Alberta for funding my research. Also, I would like to thank all the other faculty members, nonacademic staff and all the graduate students in Department of Medical Genetics for their support. Finally, I would like to thank my parents and family and especially my husband Kasun, for believing in me, and encouraging me throughout these years.

Table of Contents

Chapter 1 : Introduction	1
1.1 Prader-Willi Syndrome	1
1.2 Genetics of PWS.....	2
1.3 MAGEL2	4
1.4 NDN.....	6
1.5 Ubiquitination	7
1.6 Obesity in PWS	9
1.6.1 Nutritional phases in PWS	10
1.7 Energy homeostasis.....	11
1.7.1 Leptin	11
1.7.2 Hypothalamic control of energy homeostasis	12
1.8 Leptin receptor (LepR).....	14
1.8.1 Leptin receptor activation.....	15
1.8.2 Leptin receptor trafficking and recycling.....	17
1.8.3 Membrane protein trafficking	20
1.9 Leptin resistance	22
1.10 Rationale and Hypothesis.....	23
1.11 Preliminary results.....	25
1.11.1 Identifying interactions of MAGEL2 and necdin with leptin receptor associated proteins using MAPPIT assay	25
Chapter 2 : Methods	29
2.1 Plasmids	29
2.1.1 Preparation of new plasmids	29

2.2	Transfections	31
2.3	Protein collection.....	32
2.4	BioID assay	32
2.5	Ubiquitylation assay.....	33
2.6	Protein stability assay using cycloheximide.....	34
2.7	Cell surface biotinylation assay	34
2.8	Immunoblotting.....	35
2.9	Immunofluorescence (IF)	36
2.10	Mouse strains.....	37
2.10.1	Genotyping	37
2.10.2	Crude protein preparation.....	38
Chapter 3 : Results		41
3.1	Necdin and MAGEL2 form a bridge between leptin receptor and RNF41-USP8....	42
3.2	MAGEL2 regulates the stability of the USP8-RNF41 complex.....	47
3.3	RNF41 and USP8 alter the abundance of MAGEL2.....	54
3.4	Mutations that disrupt the MHD of MAGEL2 disrupt the mutual effects of co-expression on stability.....	57
3.5	MAGEL2 regulates the subcellular localization of RNF41, USP8 and the leptin receptor.....	59
3.6	Abundance of LepR at the cell surface is sensitive to the presence of MAGEL2.	65
3.7	Lysosomal degradation of LepR (CTS formation) is prevented by RNF41 and MAGEL2	67

3.8 Endogenous levels of murine Rnf41, Usp8, Stam1, LepR and necdin are altered in the brain of mice with a loss of function of Magel2.	72
Chapter 4 : Discussion	78
References	92

List of Tables

Table 1: List of newly prepared plasmids.....	30
Table 2 : Summary of primary antibodies	39
Table 3 : Summary of secondary antibodies.....	40

List of Figures

Figure 1.1: Molecular classes of PWS and their frequencies.	2
Figure 1.2: Summary of the genetic and expression map of chromosomal region 15q11.2-q13. ..	3
Figure 1.3 : Map of full length (FL) <i>MAGEL2</i> and C-terminal MAGEL2 (C-term).....	5
Figure 1.4 : Ubiquitin Proteasome system.	7
Figure 1.5 : Classic morphological features observed in patients with Prader-Willi syndrome... ..	10
Figure 1.6 : CNS neurocircuits regulating energy homeostasis by leptin.....	12
Figure 1.7 : Structure of Leptin receptor.	14
Figure 1.8: Leptin receptor signaling pathways.....	16
Figure 1.9 : Leptin receptor trafficking.....	19
Figure 1.10 : Trafficking of membrane proteins.....	21
Figure 1.11: Schematic outline of the MAPPIT technique using a chimeric EpoR-LepR bait receptor.	27
Figure 1.12 : Preliminary results- MAPPIT assay.....	28
Figure 3.1 : Biotinylation of interacting proteins by BirA-FLAG-MAGEL2	45
Figure 3.2 : Biotinylation of interacting proteins by BirA-FLAG-NDN	46
Figure 3.3 : Abundance of USP8 with RNF41-WT and mutant forms.	48
Figure 3.4: MAGEL2 regulates the stability of the USP8-RNF41 complex.	48
Figure 3.5 : Abundance of USP8 with MAGEL2.....	50
Figure 3.6 : Abundance of RNF41 with MAGEL2.	51
Figure 3.7 : MAGEL2 co-expression reduces the ubiquitination of RNF41.....	52
Figure 3.8 : Role of MAGEL2 in altering the stability of RNF41.....	53
Figure 3.9 : Abundance of MAGEL2 with RNF41.	55
Figure 3.10 : Abundance of MAGEL2 with USP8.....	56
Figure 3.11 : Mutations that disrupt the MHD of MAGEL2 disrupt the mutual effects of co-expression on stability.....	58
Figure 3.12 : Subcellular localization of MAGEL2 and RNF41.	60
Figure 3.13 : Change in subcellular localization of MAGEL2 with RNF41.	60
Figure 3.14 : Expression of HA-MAGEL2 reverses the stabilizing effect of USP8 on RNF41.. .	61

Figure 3.15: Change in subcellular localization of the LepR with other interacting proteins in relation to early endosomes labelled by antibody against EEA1.....	63
Figure 3.16 : Change in subcellular localization of the LepR with other interacting proteins in relation to late endosomes labelled by antibody against lysosomal marker LAMP1.....	64
Figure 3.17: Abundance of LepR at the cell surface is sensitive to the presence of MAGEL2... ..	66
Figure 3.18 : Lysosomal degradation of LepR (CTS formation) is prevented by RNF41 and MAGEL2.....	68
Figure 3.19 : Role of MAGEL2 in altering the stability of LepR.....	70
Figure 3.20 : Abundance of STAM1 with MAGEL2.....	71
Figure 3.21 : Endogenous levels of murine Rnf41 and Usp8 are altered in the brain of mice with a loss of function of <i>Magel2</i>	73
Figure 3.22 : Endogenous levels of murine Stam1 are altered in the brain of mice with a loss of function of <i>Magel2</i>	74
Figure 3.23 : Endogenous levels of murine Lepr is altered in the brain of mice with a loss of function of <i>Magel2</i>	76
Figure 3.24 : Endogenous levels of murine necdin is altered in the brain of mice with a loss of function of <i>Magel2</i>	77
Figure 4.1: Summary of the abundance results.....	90
Figure 4.2 : Summary of the interaction results.....	90
Figure 4.3 : Model for leptin receptor trafficking in the presence (A) or absence (B) of MAGEL2.....	91

List of Abbreviations

AgRP	agouti-related peptide
ARC	arcuate nucleus
AS	Angelman syndrome
BP	Breakpoints
CRH	cytokine receptor homology
CTS	C terminal stub
DMEM	Dulbecco's modified Eagle medium
DMH	dorsomedial hypothalamus
DNA	Deoxyribonucleic acid
DTT	Dithiothreitol
DUB	Deubiquitinating enzymes
EDTA	Ethylenediaminetetraacetic acid
EpoR	erythropoietin receptor
ERK	extracellular signal-regulated kinase
ESCRT	endosomal complex required for transport
FBS	Fetal bovine serum
FEZ1	Facciculation and elongationprotein zeta 1
FN III	fibronectin type III
GABA	gamma-aminobutyric acid
HEK	Human embryonic kidney
HEPES	4-(2-hydroxyethyl)-1-piperazineethanesulfonic acid
Hrs	hepatocyte growth factor-regulated substrate
IC	Imprinting center
ID	Imprinting defect
Ig	Immunoglobulin
IRS	insulin receptor substrate
JAK	Janus kinases
LB	Lysogeny broth
LepR	leptin receptor

LHA	lateral hypothalamic area
MAGE	Melanoma-associated antigen
MAGEL2	Melanoma antigen (MAGE)-like 2
MAPPIT	Mammalian protein-protein interaction trap
MC3R	melanocortin receptors
MFMR	multifunctional mosaic region
MG132	N-Benzylloxycarbonyl-L-leucyl-L-leucyl-L-leucinal
MHD	MAGE homology domain
MKRN3	makorin ring finger protein 3
mTOR	mammalian Target of Rapamycin
MVB	multivesicular bodies
NDN	Necdin
NPY	neuropeptide Y
NTS	nucleus of the solitary tract
OPTI-MEM	Reduced-Serum Medium
P13K	phosphatidylinositide 3-kinase
PBS	Phosphate-buffered saline
PCR	Polymerase chain reaction
PFA	Paraformaldehyde
POMC	pro-opiomelanocortin
PTPB1	protein tyrosine phosphatase
PVN	paraventricular nucleus
PWS	Prader-Willi syndrome
SDS	Sodium dodecyl sulfate
SH2	Src homology 2
SH2B1	SH2B adapter protein 1
snoRNA	Small nucleolar RNAs
SNRPN	Small nuclear ribonucleoprotein polypeptide N
SNURF	<i>SNRPN</i> upstream reading frame protein
SOC	Super Optimal Broth
SOCS3	suppressor of cytokine signaling 3

STAM	signal transducing adaptor molecule
STAT3	signal transducer and activator of transcription 3
Sulfo-NHS-SS	sulfosuccinimidyl-2-(biotinamido) ethyl-1,3-dithiopropionate
TBS	tris-buffered saline
U2OS	Human osteosarcoma cells
UBD	ubiquitin-binding domains
UBE3A	Ubiquitin-protein ligase E3A
UPD	Uniparental disomy.
VMH	ventromedial hypothalamus
VTA	ventral tegmental area
α -MSH	melanocyte- stimulating hormone

Chapter 1 : Introduction

1.1 Prader-Willi Syndrome

Prader-Willi syndrome (PWS) is a human genetic obesity disorder formally identified in 1956 by Andrea Prader, Alexis Labhart and Heinrich Willi (Prader et al., 1956). PWS is a multisystem disorder affecting the nervous, endocrine and musculoskeletal systems. The prevalence of PWS has been estimated between 1 in 10,000 to 1 in 30,000 live births. PWS occurs equally in both males and females among all races (Cassidy et al., 1997).

It is not easy to diagnose PWS, as phenotypical features differ with age. Previously clinical features of PWS were not well-defined. The clinical diagnostic criteria were revised and validated in 1993 by Holm and a group of experienced healthcare professionals. They established three different categories of clinical findings: major, minor and supportive. One point was given for major criteria and half point to minor criteria. No points were given to supportive criteria, but these supportive clinical findings increased confidence and strengthen likelihood of diagnosis (Holm et al., 1993).

Major criteria consist feeding problems, poor suckling in infancy, causing failure to thrive, low muscle tone, weight gain between age two to four, characteristic facial features (including low set ears, narrow forehead, almond shaped and down slanted eyes, narrow face, small mouth with thin upper lip), hypogonadism, developmental and intellectual disability, and hyperphagia leading to severe obesity if uncontrolled. Minor criteria include decreased fetal movement, sleep disturbance of sleep apnea, short stature, hypopigmentation, small hands and feet, eye abnormalities (cross eyed appearance, shortsightedness), Speech defects and skin picking. Supportive criteria include less frequent and nonspecific clinical features like scoliosis or kyphosis, increased pain threshold, and decreased vomiting. Children aged 3 years and younger require 5 points for diagnosis, with 4 of these criteria coming from the major group and children over 3 years of age require 8 points for diagnosis, with 5 or more of these criteria coming from the major group. These clinical diagnostic criteria for PWS was developed before genetic testing was available.

After the genetic basis of PWS was discovered, these criteria were revised in 2001 to assist diagnosis through DNA testing (Gunay-Aygun, et al., 2001).

1.2 Genetics of PWS

Prader-Willi syndrome results from the loss of expression of a group of paternally expressed genes on chromosome 15q11.2-q13. This group of genes is maternally silenced. The loss of the paternal copy leads to the complete loss of expression (Cassidy et al., 2012). Paternal deletion, maternal uniparental disomy (UPD) and imprinting defects are the three major molecular mechanisms that lead to PWS (Glenn et al., 1997; Ledbetter et al., 1982; Nicholls et al., 1989).

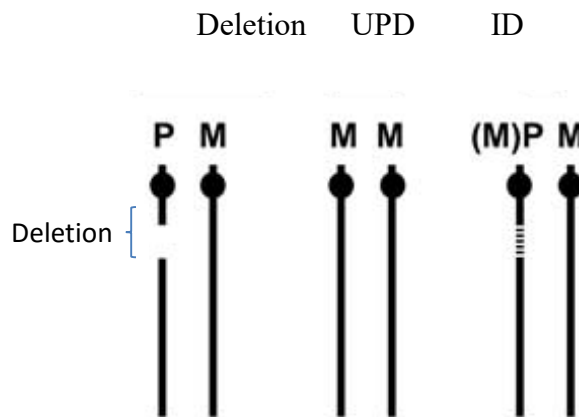


Figure 1.1: Molecular classes of PWS and their frequencies.

Deletion 15q11.2 – q13, maternal uniparental disomy (UPD), imprinting defect (ID) The parent of origin of each chromosome is indicated with P (paternal) or M (maternal) (Modified from Cassidy et al., 2012).

The majority of PWS cases (65-75%) result from a microdeletion on the long-arm of the paternal chromosome 15 (Cassidy et al., 2012). The microdeletion can be 5-6 Mb in size. 20-30% of cases result from maternal UPD for chromosome 15, in which both copies of chromosome 15 are inherited from the mother and none from the father. The remaining 2-5% of cases result from imprinting defects or chromosome 15 translocations that lead to altered methylation and/or disruption of the paternal 15q11-q13 region (Cassidy et al., 2012; Grugni et al., 2008).

The 15q11.2–q13 region can be divided into four distinct regions that are separated by three common deletion breakpoints (BP). The four regions are:

- 1) non-imprinted region between BP1 and BP2 containing four biparentally expressed genes,
- 2) ‘PWS paternal-only expressed region’ containing five protein coding genes (MKRN3, MAGEL2, NDN, SNURF-SNRPN) and cluster of five snoRNA genes that are subjected to genomic imprinting,
- 3) Angelman syndrome (AS) region containing the preferentially maternally expressed genes,
- 4) distal non-imprinted region.

Paternal deletions can be further divided into Type 1 deletion (between breakpoints BP1 and BP3) and Type 2 deletion (between breakpoints BP2 and BP3).

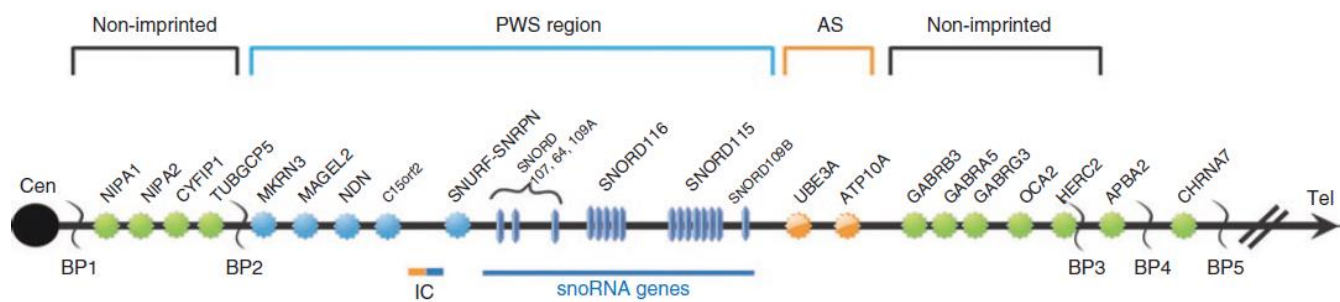


Figure 1.2: Summary of the genetic and expression map of chromosomal region 15q11.2–q13.

The PWS region genes (shown in blue) are paternally expressed and not expressed in PWS patients. The AS region genes shown in orange are maternally expressed and not expressed in AS patients. AS is caused by maternal deficiency of the imprinted gene UBE3A. It is characterized by intellectual disability, developmental delay, speech impairment, seizures and ataxia. Gene names in green (non-imprinted region) are expressed on both maternal and paternal chromosomes. Breakpoints (BP) are where the deletions usually occur, imprinting center (IC), centromere (Cen), telomere (Tel). Adapted from (Cassidy et al., 2012).

1.3 MAGEL2

As described above, the PWS region consists of five imprinted protein-coding genes and several snoRNA genes (Cassidy, 1997). Among the affected protein-coding genes is *MAGEL2*. It is a type II MAGE protein, a member of the greater melanoma antigen (MAGE) family. These proteins act in intracellular signaling pathways that regulate protein modification, protein degradation, cytoskeletal rearrangement, and transcription (Doyle et al., 2010). The MAGE family of proteins are divided into two classes, the type I MAGEs and the type II MAGEs (Barker and Salehi, 2002). Type I MAGEs comprise more than 45 genes encoded which are clustered on the X chromosome. They are expressed in the testes, trophoblast, and placenta and cancer cells (Chomez et al., 2001). Type II MAGEs consist of 15 genes that are expressed in a variety of tissues. The physiological function of MAGE proteins remains largely unknown. It was published that members of the MAGE protein family have the ability to regulate various signaling pathways, leading to changes in physiological functions such as cell cycle regulation and hypothalamic regulation. MAGEs can regulate ubiquitination of different proteins as well (Doyle et al., 2010).

The MAGE gene that is the primary focus of our laboratory and this research project is *MAGEL2*. The exact function of the MAGE protein MAGEL2 has yet to be determined. A recent publication revealed a role of MAGEL2 in endosomal protein recycling, which involves an interaction with an E3 RING ubiquitin ligase (Doyle et al., 2010; Hao et al., 2015). MAGEL2 could influence the fate of specific proteins and the loss of MAGEL2 could influence how proteins are targeted within the cell.

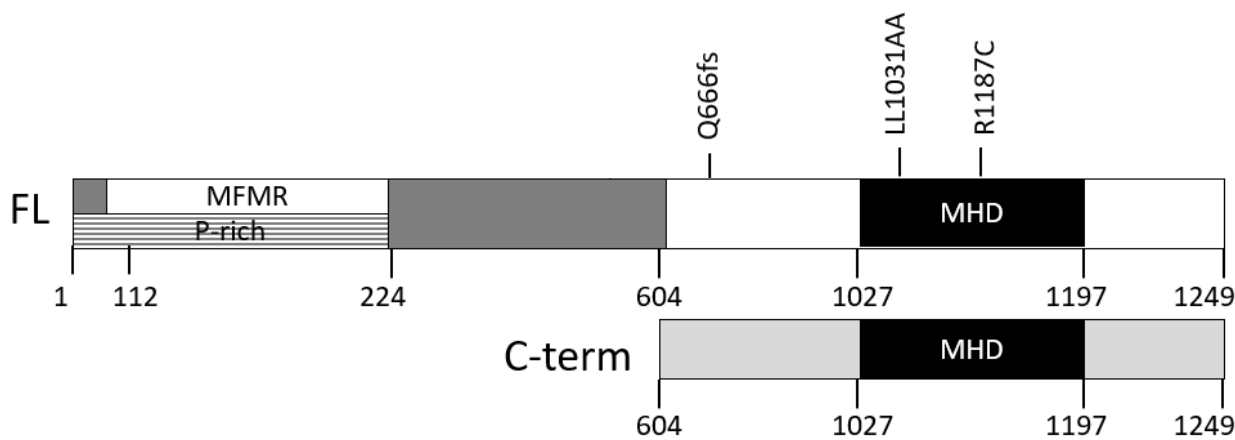


Figure 1.3 : Map of full length (FL) *MAGEL2* and C-terminal *MAGEL2* (C-term).

Locations of site directed mutations R1187C and LL1031AA and Schaaf-Yang syndrome mutation hotspot p.Q666fs. Domains are indicated: proline-rich (P-rich), multifunctional mosaic region (MFMR), MAGE homology domain (MHD).

MAGEL2 is a gene that spans 4298 bp and contains a single exon. The protein contains three conserved domains: a proline-rich domain (residues 53-225), a multifunctional mosaic region (MFMR) (residues 112-224), and a MAGE homology domain (MHD) (residues 1027-1197) that defines its inclusion in the MAGE family of proteins. Recently, with the improved genomic sequence it is predicted that *MAGEL2* encodes a 1249 amino acid protein with a predicted molecular weight of 133 kDa (Fig 1.3). Endogenous *MAGEL2* has not yet been detected in tissue samples due to lack of a specific antibody to detect *MAGEL2*.

Inactivation of genes in the Prader-Willi region causes PWS, but the loss of *MAGEL2* alone is sufficient to produce a PWS-like phenotype renamed Schaaf-Yang Syndrome (Schaaf et al., 2013). Protein truncating mutations have been detected throughout the coding sequence in children with Schaaf-Yang syndrome. A mutational hotspot (*MAGEL2* c.1996delC; p.Q666fs) leading to frameshift and a premature stop codon causes a prenatal lethal form of arthrogryposis or congenital joint contractures (Mejlachowicz et al., 2015; Schaaf et al., 2013). The orthologous mouse gene, *Magel2*, encodes a predicted protein of 1284 residues, with a predicted molecular weight of 138 kDa. In mice, the homologous *Magel2* protein shares a 77 % overall similarity to the human protein (Boccaccio et al., 1999).

1.4 NDN

NDN is another gene that is located in the PWS deletion region (MacDonald and Wevrick, 1997). It is an imprinted gene and is expressed exclusively from the paternal allele (Chapman and Knowles, 2009). The *NDN* gene produces a 325-amino acid protein necdin, which was first identified in mouse stem cells (Maruyama et al., 1991). Like *MAGEL2*, necdin is a member of the greater melanoma antigen (MAGE) family and it is a type II MAGE protein (Barker and Salehi, 2002).

There was no *NDN* expression in the brain and fibroblasts from PWS patients. This gene is expressed exclusively from the paternal allele in these tissues. Therefore necdin might have a possible role in PWS (Jay et al., 1997). Necdin is ubiquitously expressed in many tissues. It can be detected in fetal brain, lung, liver and kidney; in adult heart, brain, placenta, lung, liver, skeletal muscle, kidney, pancreas, spleen, thymus, prostate, testis, ovary, small intestine and colon. The necdin protein is expressed in almost all postmitotic neurons in the CNS (Maruyama, 1996; Uetsuki et al., 1996).

The amino acid sequence of the functional domain of the necdin protein (the MHD, aa 83–292) is highly conserved between human and mouse suggesting an evolutionary conservation (MacDonald and Wevrick, 1997). Recent publications revealed strong similarities in terms of morphological, behavioral modifications, between the effects of *Ndn* mutated mice and key features of PWS (Muscatelli et al., 2000). Neurons from mice lacking necdin display reduced differentiation and increased apoptosis (Bush and Wevrick, 2012). Necdin interacts with various cytoplasmic and nuclear proteins. Therefore, this protein might have several functions. It binds to many regulatory proteins that are involved in the proliferation, differentiation, survival and destruction of mammalian neurons and neural stem cells. Necdin acts as a growth inhibitor, that helps cells to undergo cell cycle arrest and which allows cells to no longer involved in duplication and division. Some of the interactors of necdin are p53, FEZ1 (Lee et al., 2005), MAGEL2 and MAGED1 (Tcherpakov et al., 2002).

1.5 Ubiquitination

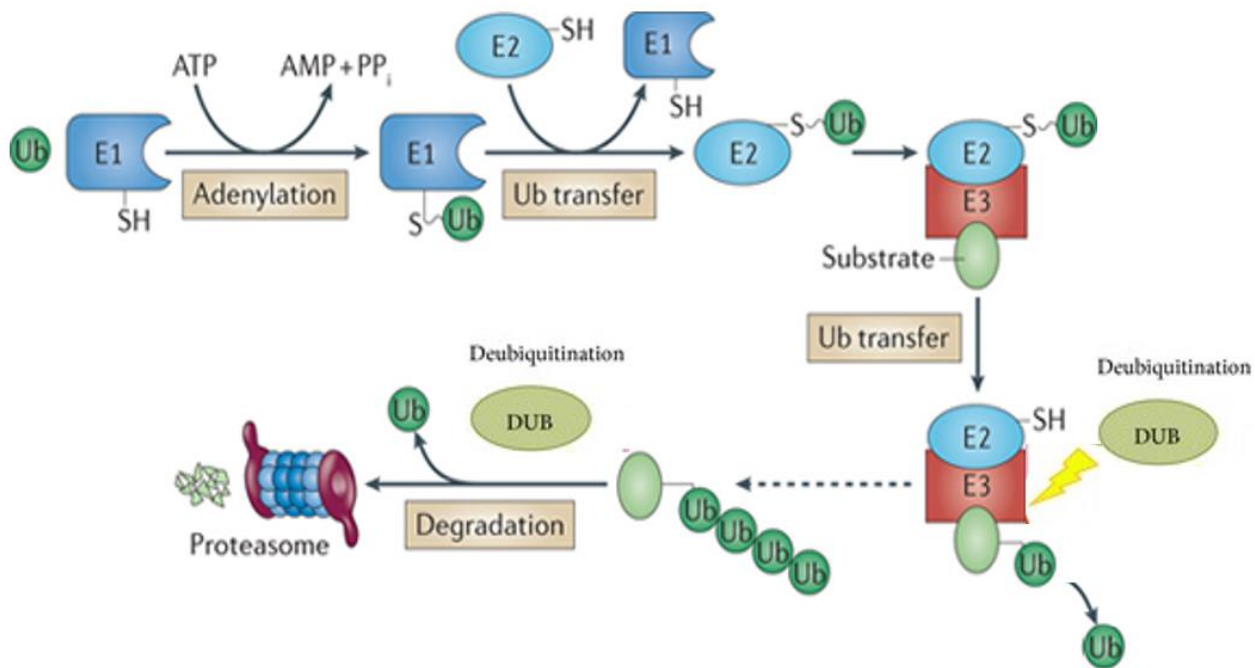


Figure 1.4 : Ubiquitin Proteasome system.

Ubiquitin (Ub), Ubiquitin-activating enzymes (E1), ubiquitin conjugating enzymes (E2) and ubiquitin ligases (E3), deubiquitinases (DUB). Modified from (Fang and Weissman, 2004).

Ubiquitination is a posttranslational modification that regulates a wide range of cellular functions. This mechanism can change the stability of a protein by promoting or preventing protein interactions, and alter their cellular localization. It is a major mechanism that controls membrane protein internalization and intracellular trafficking and targets proteins for proteasomal or lysosomal degradation (Niendorf et al., 2007). Ubiquitin (Ub) is a small regulatory protein which is a 76 amino acid polypeptide. The ubiquitination process begins by a covalent attachment of Ub to the lysine residue of a target protein. Ub acts as an internalization signal that decides the intracellular destiny of a protein. Ub sends the modified substrate to the endocytic or sorting compartments, followed by recycling to the plasma membrane or degradation in the lysosome (d'Azzo et al., 2005). Ub is attached to substrate proteins through a three step enzymatic cascade (Fang and Weissman, 2004). Each of these enzyme types has an important role to play in ubiquitination and the labeling of proteins to be degraded by the proteasome.

Ub binds to the E1- ubiquitin activating enzyme through a cysteine residue. ATP is the form of energy that is used for the process. Next the activated Ub in E1 is transferred to E2- conjugating enzyme. Finally, E3 -ligating enzyme recognizes the E2 and helps to transfer the Ub from E2 to the target substrate protein. E3s play important roles in the formation of chains of Ub molecules on substrates. This can either be monoubiquitination or polyubiquitination that are crucial for recognition by proteasomes (Fang and Weissman, 2004; Hao et al., 2013). Ubiquitination can have multiple effects on its substrates depending on the length and type of ubiquitin chains. K48-linked ubiquitin chains typically target proteins for degradation by proteasomes (Schrader et al., 2009). K63-linked ubiquitin chains target proteins for degradation by lysosomes. (Hao et al., 2013; Sun and Chen, 2004). Deubiquitinating enzymes (DUBs) reverse the ubiquitylation of target proteins by removing the Ub, and alter the modification of the target proteins. More than 90 DUBs have been identified so far (Berlin et al., 2010).

Ubiquitination process is highly regulated and controlled by the E3 ubiquitin ligases (Deshaies and Joazeiro, 2009). There are E3 ubiquitin ligase enhancers that increase its function and activity, known as MAGE family proteins (Doyle et al., 2010). Ring domain proteins are a big family of E3 ligases, that bind to the conserved MHD of the MAGE proteins. There are many E3 ligases that are coupled with many MAGE proteins to enhance endosomal protein recycling and trafficking. I will describe some examples. MAGEL2 binds to an E3 RING ubiquitin ligase, TRIM27, and enhances the ubiquitin ligase activity of TRIM27 (Doyle et al., 2010; Hao et al., 2013). The MAGEL2-TRIM27 complex localizes to endosomes through interactions with retromer complex. This enhances retromer-mediated transport, which is recycling of transmembrane proteins from endosomes to transgolgi network. MAGED1 was identified to bind RING domain protein XIAP, and facilitates the apoptosis of neural progenitors (Feng et al., 2011). Recent evidence showed that MAGEG1, MAGED1 and MAGEC2 could enhance the activity of NSE1, Praja-1 and TRIM28 respectively (Doyle et al., 2010; Feng et al., 2011). The specificity of the RING protein that binds to MAGE is determined by recognizing unique regions in the RING partner by the MHD. These E3 ligases play an important role in the ubiquitination process (d'Azzo et al., 2005).

The mechanisms behind the enhancement of the RING protein ubiquitination activity by MAGEL2 are currently not fully understood. One possible mechanism is a change in the structure of the RING protein as MAGE proteins binds, and this conformational change can increase its activity. A second possible mechanism is that MAGE proteins may facilitate the substrate protein to be bound to the E2-E3 ubiquitin complex. Another possible mechanism is that MAGE proteins can help E2 ubiquitin conjugating enzyme by binding to it and enhance its recruitment on the E3-substrate complex. Therefore, the role of MAGE proteins in protein ubiquitination remains unclear.

1.6 Obesity in PWS

Obesity is caused by a chronically positive energy balance resulting in increased fat mass (Stunkard, 1996). Although genetic and epigenetic factors can predispose an individual to store more fat, it is commonly accepted that hyperphagia or excessive appetite is the major cause of obesity (Morton et al., 2006). PWS is a genetic disease characterized by early onset childhood hyperphagia with lack of fullness, and reduced energy expenditure (Colmers and Wevrick, 2013). Children with PWS have higher proportion of fat mass to lean mass. These children tend to steal food, eat inappropriate food like pet food, spoiled food or sometimes garbage. They can become very obese if their food intake is not strictly controlled which will lead to life threatening conditions as well (Butler, 2011; Colmers and Wevrick, 2013).



Figure 1.5 : Classic morphological features observed in patients with Prader-Willi syndrome.

Central obesity of PWS in (a) a 2 ½ year old girl and (b) a 21-year-old male. Note the central obesity and typical facial appearance Adapted from (Cassidy and Driscoll, 2008)

1.6.1 Nutritional phases in PWS

PWS has been described as having two distinct nutritional phases in different developmental stages. Individuals with PWS undergo hypotonia or low muscle tone and failure-to-thrive state in infancy, followed by a period of excessive feeding leading to obesity in later childhood (Gunay-aygun, et al., 2001; Tauber et al., 2014). Miller in 2011 identified a total of seven different nutritional phases, with five main phases and sub-phases in phases 1 and 2 (Miller et al., 2011). I have explained some of the clinical features in different phases below. Growth restrictions and low fetal movements can be observed prenatally. Infant have low muscle tone, difficulties in feeding but they are not obese. At the age of 9-25 months the infant with PWS grows steadily with improved feeding and along with weight increasing at a normal rate. At the age of 2-8 years, they become more interested in food and show increased weight gain. At the age of 8 and above, children have an excessive appetite with the lack of feeling full. The hyperphagia and increased body weight are indicators of PWS that categorize it as a form of genetic obesity (Butler et al., 2007).

1.7 Energy homeostasis

When an individual's food intake is greater than the energy expenditure, the excess energy is stored as fat. There is a tight regulation of the energy inflow through food intake and energy outflow, through burning energy in normal physiological functions. This biological process that maintain this stability is called energy homeostasis. Energy balance refers to the process whereby energy reserves are maintained over a long period through many regulators, but primarily insulin and leptin (Morton et al., 2006). Importantly, leptin has a more crucial role in long term energy homeostasis than insulin. It is one of the most important and widely studied hormones in the modulation of energy balance. The subsequent discussion focuses on leptin signaling pathways.

1.7.1 Leptin

Leptin is a 16 kDa peptide hormone. Leptin is encoded by a gene located in human chromosome 7q31.3 (Considine and Caro, 1997). Leptin protein has 146 amino acid residues and it circulates in blood similar to other hormones (Frederich et al., 1995; Margetic et al., 2002). Adipocytes are the major source of leptin synthesis and secretion (Sweeney, 2002). Leptin is expressed in brain, pituitary glands, stomach, liver and muscles in low levels. Leptin serves as a critical indicator of long term energy status (Frederich et al., 1995). Leptin circulates at levels proportionate to body fat content and enters the brain through the blood brain barrier. The brain cells can sense how much fat the body has by measuring leptin levels in the bloodstream (Mercer et al., 2013). Leptin promotes weight loss by acting on neuronal systems that are involved in energy homeostasis. If leptin function is disrupted, it will prevent neuronal actions which will lead to impaired energy balance (Morton et al., 2006). Leptin action is mediated by leptin receptors (LepR) that are located in the hypothalamus and in many peripheral tissues (Belouzard et al., 2004).

1.7.2 Hypothalamic control of energy homeostasis

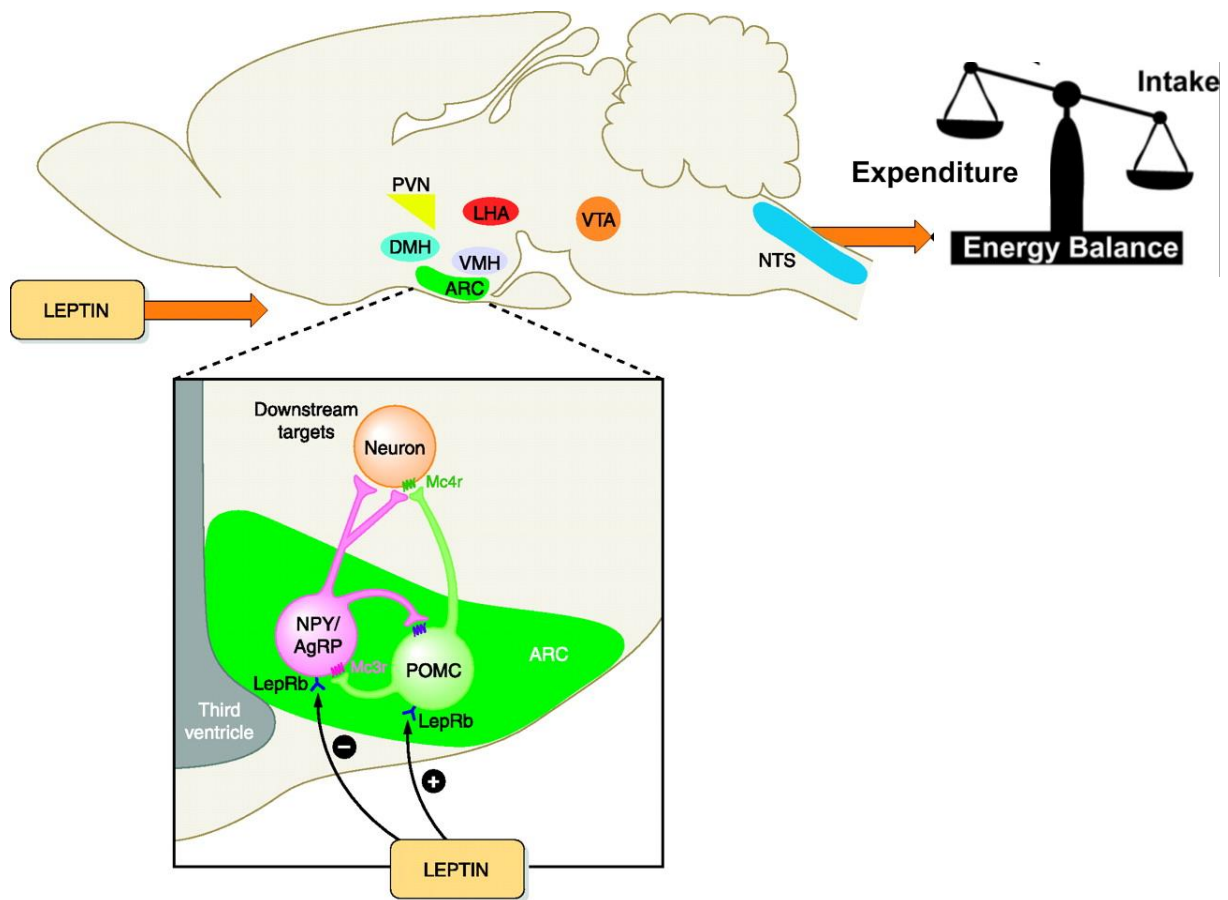


Figure 1.6 : CNS neurocircuits regulating energy homeostasis by leptin.

Modified from (Morton and Schwartz, 2011).

The hypothalamic ARC contains neuropeptide Y and agouti-related peptide (NPY/AgRP) neurons that stimulate food intake and are inhibited by leptin, and proopiomelanocortin (POMC) neurons that reduce food intake and are stimulated by leptin.

(ARC-arcuate nucleus; LepRb- leptin receptor; Mc4r -melanocortin-4 receptor; VMH- ventromedial hypothalamus; LHA- lateral hypothalamic area; PVN- paraventricular nucleus; DMH- dorsomedial hypothalamus; VTA- ventral tegmental area; NTS- nucleus of the solitary tract)

The hypothalamus is the main monitoring and control center for energy balance in the body. It responds to nutrient and hormone levels to regulate homeostatic processes including appetite and energy expenditure. Numerous peripheral signals circulate in the blood stream and act on the hypothalamus, to stimulate or inhibit the production of peptides that are involved in energy balance regulation (Boguszewski et al., 2010). Leptin appears to be the major peripheral hormone involved in regulating energy balance. It acts on LepR to perform its regulatory function. LepR is present in several neural tissues, but is highly expressed in multiple hypothalamic regions including the arcuate nucleus (ARC), the ventromedial hypothalamus (VMH), the paraventricular nucleus (PVN), the dorsomedial hypothalamus (DMH), the lateral hypothalamic area (LHA) and the ventral premammillary nucleus (PMV). All these hypothalamic nuclei have their own role in energy homeostasis (Suzuki et al., 2012). The coordinated action of these nuclei likely contributes to central regulation of energy homeostasis by leptin. However, the ARC is the key hypothalamic region involved in energy balance regulation and it is leptin's main site of action (Mercer et al., 2013; Woods and D'Alessio, 2008). There are two distinct neuronal subtypes that respond to leptin within the ARC. One population synthesizes the appetite stimulating neuropeptide Y (NPY) and agouti-related peptide (AgRP), while the other population synthesizes the appetite depressing neuropeptide pro-opiomelanocortin (POMC). A state of excess calories increases circulating leptin levels, allowing it to bind LepR in ARC in sufficient quantity to trigger a physiological response. Leptin hyperpolarizes or inhibits AgRP/ NPY neurons and suppresses the secretion of appetite-inducing peptides like gamma-aminobutyric acid (GABA). In contrast, leptin depolarizes or excites POMC neurons, promoting the release of appetite-suppressing peptides. One such peptide is α -MSH (melanocyte- stimulating hormone), which acts on melanocortin receptors MC3R and MC4R to promote energy expenditure (Colmers and Wevrick, 2013).

Another major peripheral signal of energy balance is insulin, produced by the pancreas (Benoit et al., 2004). Although both leptin and insulin influence energy homeostasis, the subsequent discussion is restricted to leptin because the experiments described in this thesis focus on LepR and its associated proteins.

1.8 Leptin receptor (LepR)

Leptin receptor (LepR) is a class I cytokine membrane spanning receptor (Wauman and Tavernier, 2011). There are several isoforms of LepR: several short isoforms, one long isoform LepRb with a long cytosolic C-terminus tail and one soluble isoform. The long isoform has three main sections. They are the extra cellular domain which included the leptin binding site, the transmembrane domain and the cytoplasmic intracellular domain (Roujeau et al., 2014). The cytoplasmic domain of LepR has three conserved tyrosine residues corresponding to positions Y985, Y1077, and Y1138 (Allison and Myers, 2014; Wauman and Tavernier, 2011). LepR expression is more restricted with high levels in hypothalamic nuclei such as the ARC, LHA, VMH, DMH and PVN (Bjørbaek et al., 1998). The biological function of the short isoforms is still not known, but long isoform LepR in ARC is mainly responsible for the effect of leptin on body weight control (Roujeau et al., 2014; Schwartz et al., 2000).

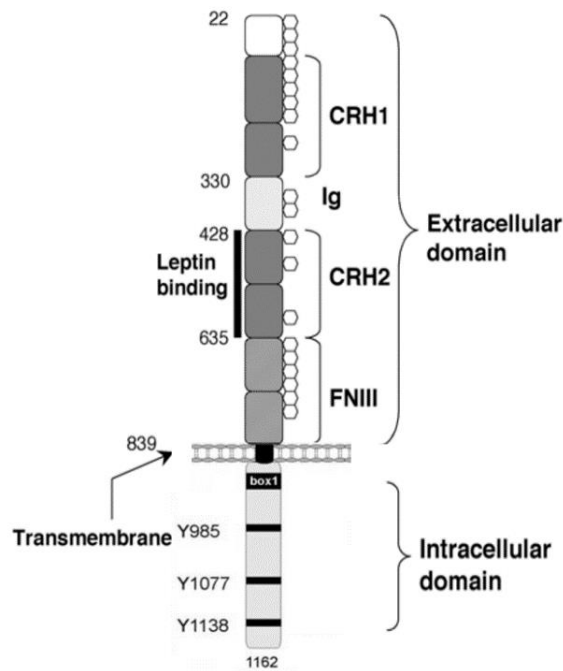


Figure 1.7 : Structure of Leptin receptor.

Extracellular domain (residues 22–839), transmembrane domain (residues 840- 862) and intracellular domain (residues 863-1162). cytokine receptor homology (CRH) immunoglobulin (Ig)-like domain, fibronectin type III (FNIII) domains. Modified from (Kamikubo et al., 2008).

1.8.1 Leptin receptor activation

The leptin signaling pathway is critical to maintaining energy homeostasis. When leptin binds to the leptin receptors many downstream signal transduction pathways are activated. LepR is present on the cell membrane as a mixture of monomers and dimers. Unlike many other cytokine receptors, ligand binding does not appear to activate LepR by promoting receptor dimerization, but it promotes a change in its structure. Both these actions are required for receptor activation and subsequent signal transduction. Once leptin is bound to the extra cellular domain of LepR, it in turn phosphorylates the three intracellular residues (Y985, Y1077, and Y1138) which mediates ERK, STAT5 and STAT3 signaling respectively. I will describe briefly about the signaling pathways that are activated by leptin.

Upon binding of leptin, LepRb-associated Janus kinase 2 (Jak2) is activated through auto-phosphorylation. In turn, JAK2 phosphorylates several tyrosine residues on LepRb (Y985 and Y1138). Phosphorylation of Y985 activates extracellular signal-regulated kinase (ERK) which leads to increased transcription of *c-fos*. This pathway mediates the anorectic action of leptin in the hypothalamus (Rahmouni et al., 2009). Phosphorylation of Y1138 through activation of JAK2, in turn activates STAT3 (signal transducer and activator of transcription 3). Activation of STAT3 causes it to dimerize and translocate into the nucleus. STAT3 serves as a transcription factor to produce pro-opiomelanocortin (POMC) and suppressor of cytokine signalling-3 (SOCS3) mRNA. SOCS3 is a negative feedback regulator of LepR/Jak2 signal transduction (White et al. 1997, Banks et al. 2000). Phosphorylated Tyr1077 promotes the recruitment and activation of STAT5; Tyr1138 may also contribute to STAT5 activation (Banks et al., 2000; Allison and Myers 2014). The significance of its contribution to the regulation of energy homeostasis is less clear.

Other than the JAK/STAT pathway, leptin is also able to activate the IRS/PI3K (Insulin receptor substrate/ phosphatidylinoside 3-kinase) pathway that is important in glucose homeostasis (Morton et al., 2005). It is known that the hypothalamic PI3K pathway of leptin signaling is also impaired during the development of diet-induced obesity (Li et al., 2016).

In addition, the mammalian target of rapamycin (mTOR) has emerged as a key downstream pathway in LepR signaling. Leptin increases hypothalamic mTOR activity, and the inhibition of mTOR signaling reduces leptin's appetite suppressing effect (Wauman and Tavernier, 2011). The roles for each signaling pathway in leptin action and the control of energy balance are complicated. Therefore, mechanisms of how LepR modulates these pathways remains unclear.

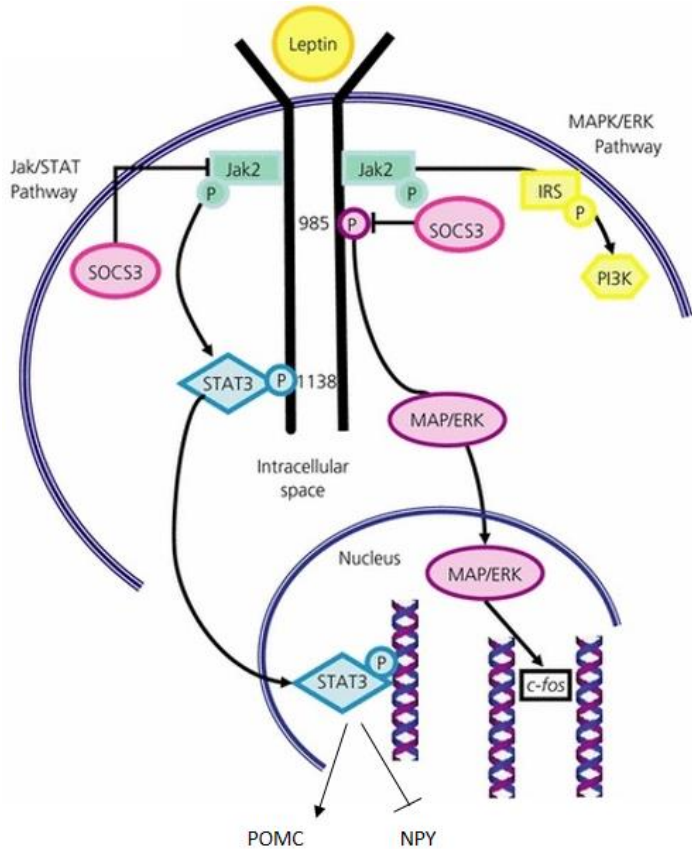


Figure 1.8: Leptin receptor signaling pathways.

Modified from(Sweeney, 2002).

Leptin binding activates Janus kinase 2 (Jak2), resulting in auto-phosphorylation as well as phosphorylation (P) at tyrosine residues 985 and 1138 of LepR. Activation of JAK2 recruits STAT3 signaling as well as IRS/PI3K pathway. Phosphorylation of tyrosine 985 recruits the MAPK/ERK signaling pathway. Phosphorylation of STAT3 translocate into the nucleus where it serves as a transcription factor to produce POMC.

1.8.2 Leptin receptor trafficking and recycling

The majority of LepR is localized in intracellular compartments, including endoplasmic reticulum, trans -Golgi apparatus, and endosomes, with only a minor fraction of LepR present at the plasma membrane, which is approximately 10%-20% (Belouzard et al., 2004). Reasons for this might be due to retention of receptors in the pathways after they are synthesized and may be due to removal of receptors at the membrane via ligand independent constitutive endocytosis. (Belouzard et al., 2004). Whether alteration in LepR trafficking affects cell surface expression and, in turn, leptin signaling has not been investigated thoroughly. The amount of receptors at the cell surface is determined by the equilibrium between receptor synthesis and transport to the plasma membrane, internalization and the receptor being processed for degradation or efficiently recycled back to the cell surface and ectodomain shedding (Roujeau et al., 2014).

LepR are internalized by budding of membrane into a vesicle by coating with clathrin protein after leptin is bound (Sweeney, 2002). Some studies have described LepR being constitutively internalized, which is independent from ligand binding (Barr et al., 1999; Belouzard et al., 2004). Internalized receptors are targeted to early endosomal compartments, followed by sorting to recycling vesicles, signaling endosomes or multivesicular bodies (MVBs) (Jovic et al., 2010). Within the MVB, LepR are cleaved and remains are sent to the lysosomes for degradation. The degradation products of LepR are called C-terminal stubs (Wauman et al., 2011). Newly synthesized leptin receptors are partially retained in the Golgi complex or in a post-Golgi intracellular compartments. They could be transported to lysosomes directly by different intracellular pathways without transporting them to cell surface. The remaining fraction is transported to the cell surface before being constitutively endocytosed and degraded (Belouzard et al., 2004; Wauman and Tavernier, 2011).

After LepR are internalized the early endosomal compartments act as checkpoints that regulate further transportation within the cells. Also, the decision to recycle receptors back to the plasma membrane, where receptors are likely to be removed from cell surface as ectodomain shedding, or to direct them towards the lysosomes for degradation is largely a function of ESCRT complex (endosomal complex required for transport).

The ESCRT complex can also be divided into sub-complexes. The ESCRT-0 complex consists of hepatocyte growth factor-regulated substrate (Hrs), and signal transducing adaptor molecule STAM1. ESCRT-0 binds ubiquitin via its ubiquitin-binding domains (UBD) (Berlin et al., 2010; Wauman et al., 2011). As I described earlier in the ubiquitination process, Ub serves as a trafficking signal and mediates the sorting and fate of receptors. Ubiquitinated proteins are concentrated before sorting them for lysosomal degradation. Increasing evidence suggests that ubiquitin ligase and DUB interaction with ESCRT members can modify trafficking outcomes of membrane proteins (Shields et al., 2009).

A recent study identified RING finger protein RNF41 as an interaction partner of the LepR (Wauman et al., 2011). They showed that the level of LepR at the cell surface and its signaling can be influenced by RNF41. They showed that RNF41 is important in LepR exposure and shedding as it can act as a controller for these mechanisms. They demonstrated that RNF41 prevents the degradation of endocytosed LepR and re-routes them to cellular compartments for ectodomain shedding with the help of metalloproteases. It was also known that Ubiquitin-specific protease 8 (USP8) which is an RNF41-interacting deubiquitylating enzyme (DUB), stabilizes RNF41. Also, USP8 is known to be involved in trafficking of various transmembrane proteins. USP8 interacts and stabilizes STAM, which is a component of the ESCRT complex. This complex is in-charge of the early steps of LepR receptor trafficking (Niendorf et al., 2007; Row et al., 2006).

As described earlier, the decision to recycle LepR back to the plasma membrane, or to direct them towards the lysosomes for degradation is largely a function of the ESCRT complex. The regulation and stability of this complex is mediated by RNF41 and USP8, therefore the regulation of the LepR cell surface expression is probably mediated by different mechanisms involving many other associated proteins.

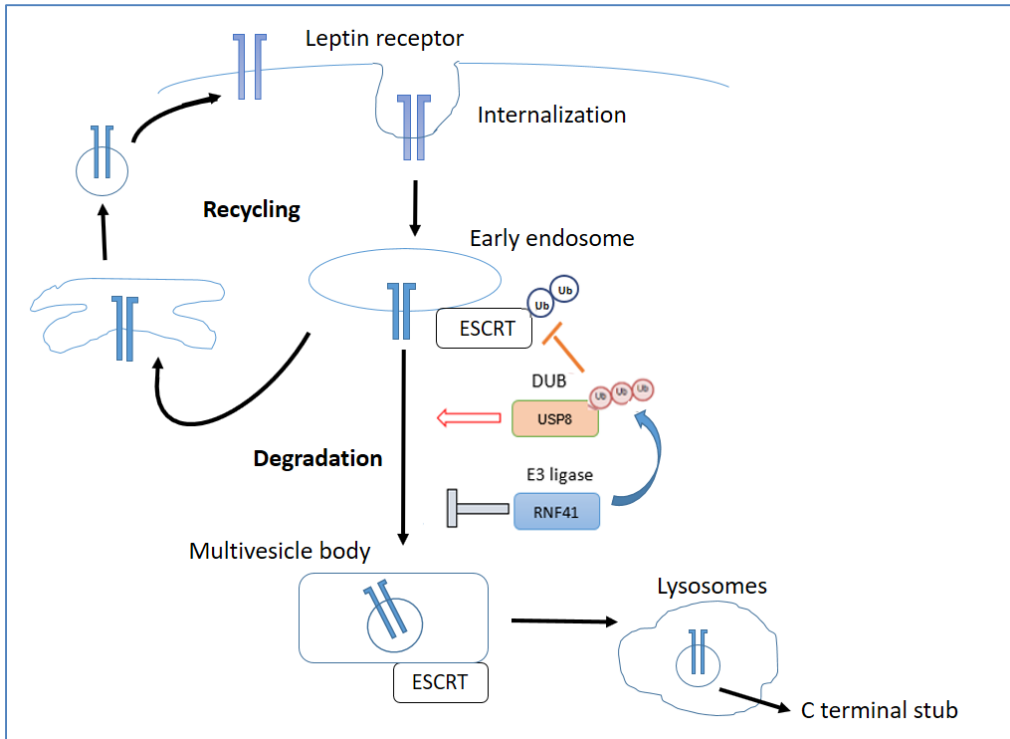


Figure 1.9 : Leptin receptor trafficking.

Modified from (De Ceuninck et al., 2013)

LepR are constitutively internalized from the plasma membrane towards early endosomes. USP8 interaction with STAM stabilizes the ESCRT-0 complex by de-ubiquitylating STAM. This allows receptor to move towards multi-vesicular bodies (MVB). Fusion of MVBs with lysosomes eventually causes lysosomal receptor degradation. USP8 destabilization upon ubiquitination by RNF41 eliminates LepR sorting towards lysosomes as the ESCRT complex gets destabilized. Therefore, LepRs are transported back to the plasma membrane as recycling (De Ceuninck et al., 2013).

1.8.3 Membrane protein trafficking

The diversity of membrane trafficking is the key underlying biological process responsible for the relocation of membrane proteins into different compartments of a cell. The presence and abundance of proteins on the plasma membrane is regulated by uptake of cell surface receptors into endocytic vesicles, sorting them either to the lysosome for degradation or recycled back to the plasma membrane (d'Azzo et al., 2005; Wright et al., 2011). Trafficking these membrane proteins within the cell depends on the various endosomes, membranous organelles and interaction of different proteins involve in this process.

Membrane proteins are internalized by clathrin-dependent pathway as well as clathrin-independent pathways (Mayor et al., 2014; Wauman and Tavernier, 2011). Endocytic vesicles along with the proteins are rapidly targeted to membrane-bound endocytic organelles also known as the early endosomes. This is the key trafficking control site that consists with the ESCRT complex. The fate of the internalized proteins is determined by the early endosomes, which is the starting point of protein sorting. Depending on the sorting process the internalized proteins are sent for recycling to the plasma membrane or degradation in lysosomes or delivery to the trans-Golgi network (Jovic et al., 2010).

The recycling pathway is pivotal for returning proteins to the cellular surface. There are two methods of recycling. The fast recycling pathway mediates trafficking of the proteins directly from the early endosomes to the plasma membrane. The slow recycling pathway mediates trafficking of the channel from the early endosomes to a recycling compartment and then to the plasma membrane (de Souza and Ambudkar, 2014). The other pathway is the retrograde transport of internalized proteins, where proteins are sent towards the trans golgi network from the early endosomes.

The membrane proteins that are destined to be degraded, are transported to lysosomes with the help of the MVB. Once committed to degradation, these proteins are deubiquitinated and deposited into intraluminal vesicles, which are then released to fuse with the proteolytic organelle carrying proteolytic enzymes (MacDonald et al., 2012).

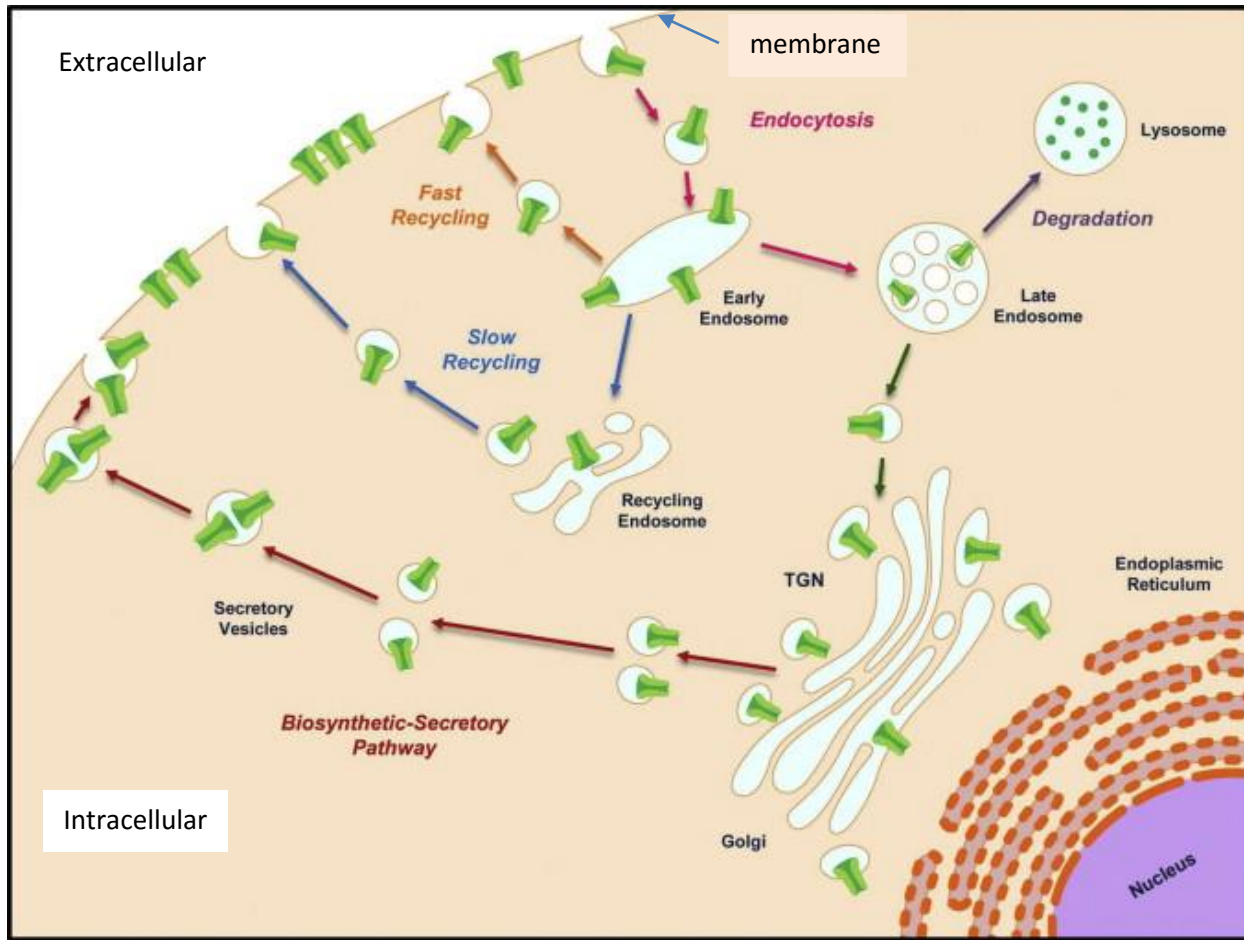


Figure 1.10 : Trafficking of membrane proteins.

At the plasma membrane, the membrane proteins are internalized by endocytosis and can be recycled back to the plasma membrane from early endosomes or degraded by the fusion of MVB to lysosomes. Modified from (de Souza and Ambudkar, 2014).

1.9 Leptin resistance

Leptin resistance is the reduced ability of circulating leptin to suppress appetite and weight gain and to promote energy expenditure. It is a primary risk factor for the development of obesity. Leptin resistance results from mutations in leptin, mutations in LepR, defects in leptin signaling, and/or defects in the hypothalamic neural circuitry that regulates energy homeostasis.

Congenital leptin deficiency is a rare autosomal recessive obesity syndrome caused by mutations in the leptin gene. In humans, eight distinct leptin mutations have been described in the literature (Funcke et al., 2014; Morris and Rui, 2009). On the cellular level, these mutations result in defects in the synthesis and/or secretion of leptin. Rapid weight gain after birth, severe early onset obesity, impaired satiety and impaired production of sex hormone are some of the clinical phenotypes in patients with congenital leptin deficiency (Montague et al., 1997). Mice homozygous for the deletion of leptin known as *ob/ob* or *obese* mice, exhibit hyperphagia leading to obesity. These mice are glucose intolerant, have reduced fertility, and hypometabolic (Morris and Rui, 2009; Xia and Grant, 2013).

Another cause of obesity is the non-functional LepR due to homozygous mutations in the human leptin receptor gene. This occurs as a result of truncated leptin receptor that does not have both the transmembrane and the intracellular domains. Patients homozygous for LepR mutation have hyperphagia, severe obesity, alterations in immune function, alterations in glucose homeostasis, elevation of plasma cholesterol and delayed puberty due to lack of hormones that normally stimulate the ovaries or testes (Clément et al., 1998). Leptin receptor knockout mice (*db/db* or *diabetes* mice) have a similar phenotype to that of the *ob/ob* mice (Farooqi et al., 2007; Xia and Grant, 2013). These *db/db* mice show excess adipose tissue and no significant difference in food intake or energy balance, even after exogenous administration of leptin. This suggest that these mice have reduce leptin sensitivity, even though they have high levels of circulating leptin (Pravdivyi et al., 2015). Other than the previously described phenomena, leptin resistance can be a result of impaired LepR signaling. In a normal condition, leptin stimulates the expression SOCS3, which provides a negative feedback mechanism to prevent overactivation of leptin-signaling pathways. SOCS3 binds to JAK2 and inhibits JAK2 activity. It also binds to Tyr985 in LepR and inhibits leptin signaling (Bjørbaek, 2009; Morris and Rui, 2009).

Another negative regulator is PTP1B (protein tyrosine phosphatase 1B). It binds to and dephosphorylates JAK2, thereby inhibiting leptin signaling (Morris and Rui, 2009). The expression of hypothalamic SOCS3 and PTP1B is increased in leptin-resistant animals, suggesting that both these might contribute to leptin resistance. Also, MC4R (melanocortin-4 receptor) mutations cause impaired hypothalamic regulation which leads to leptin resistance (Butler and Cone, 2002; Farooqi et al., 2003). These MC4R are known to be interacting with POMC in regulation of food intake and energy expenditure.

Therefore, a disruption of any cellular or molecular process in the leptin-melanocortin system, as well as mutations in the leptin and LepR would result in leptin resistance or insensitivity by blocking signal transduction leading to obesity.

1.10 Rationale and Hypothesis

PWS patients have a wide range of clinical features including intellectual disabilities, autism spectrum disorders, hypothalamic defects causing endocrine dysregulation and severe hyperphagia leading to obesity (Cassidy and Driscoll, 2008; Mercer and Wevrick, 2009). Obesity is caused by the imbalance of food intake and energy. This homeostasis is mainly regulated by leptin, a peptide hormone crucial to hypothalamic control of energy metabolism.

Previous publications showed that mice lacking *Magel2* are obese with reduced muscle mass, endocrine deficits including infertility, and behavioral deficits (Bischof et al., 2007; Kozlov et al., 2007; Mercer and Wevrick, 2009). Even though these mutant mice lacking *Magel2* have increased circulating leptin, they exhibit leptin insensitivity. Also, leptin-induced depolarization of POMC neurons in the arcuate nucleus of the hypothalamus is impaired in these mice (Maillard et al., 2016; Mercer and Wevrick, 2009). These observations strongly support that loss of *MAGEL2* contributes to obesity in PWS through pathways that involve leptin sensing.

It has been hypothesized that defects in leptin signaling pathway or defects in transport of leptin across the blood-brain barrier or defects in intracellular trafficking of LepR that could lead to an altered LepR expression at the cell surface might be the leading causes for leptin resistance in PWS patients (Belouzard et al., 2004; Roujeau et al., 2014). The mechanisms that underlie this problem remains unclear, and the molecular basis is not yet clearly understood.

Low LepR expression level at the cell surface may be due to constitutive internalization of receptors or intracellular retention of LepR or it may be due to lower recycling rate of receptors back to the cell surface. All these possibilities can be critical for leptin sensitivity. A recent study identified a relationship between LepR, deubiquitinase USP8 and ubiquitin ligase RNF41, in controlling LepR trafficking (De Ceuninck et al., 2013). RNF41 leads to an increase of LepR recycling to the plasma membrane than lysosomal targeting. USP8 interacts with and stabilizes the E3 ligase RNF41. Stabilizing RNF41 will in turn increase the activity of RNF41 through deubiquitination (Wu et al., 2004). In contrast, RNF41 ubiquitinates and destabilizes USP8, ultimately regulating LepR sorting through effects on the stability of the ESCRT complex (De Ceuninck et al., 2013; Wauman et al., 2011). It is also confirmed that the deubiquitinase USP8, the ubiquitin ligase RNF41 interacts with MAGEL2 (see below). However, the importance of those interactions has not yet been assessed properly.

I hypothesized that MAGEL2 modifies the activity of RNF41-USP8 ubiquitination complex and modifies the regulation of intracellular sorting of leptin receptor. Therefore, loss of MAGEL2 contributes to obesity in PWS because it acts as an adaptor protein by bridging the leptin receptor to the ubiquitination complex RNF41- USP8.

1.11 Preliminary results

1.11.1 Identifying interactions of MAGEL2 and necdin with leptin receptor associated proteins using MAPPIT assay

Mammalian protein-protein interaction trap (MAPPIT) is a cytokine receptor-based two-hybrid system that operates in mammalian cells. This method allows identification and analysis of protein-protein interactions *in vivo* through a bait-prey interaction based on a cytokine receptor signaling pathway (Fig.1.11).

MAPPIT bait receptors are designed chimeric proteins consisting of the extracellular part of the erythropoietin receptor (EpoR) and intracellular part of the leptin receptor (LepR). In the intracellular part, all three tyrosines (Y985, Y1077 and Y1138) are mutated to phenylalanine (F) residues (LR-F3), which inhibit Signal Transducer and Activator of Transcription 3 (STAT3) recruitment. The prey protein is fused to functional STAT3 recruitment sites of a FLAG-tagged gp130 chain. The bait-receptor is incapable of recruiting STAT3 upon stimulation. However, when bait and prey proteins interact, the C-terminal part of the gp130 chain is brought in close proximity to the JAK kinases which allows activation of the JAK–STAT signaling pathway. In summary bait-prey interaction leads to restoration of the signaling pathway, and activates STAT3 molecules, which stimulate STAT3-dependent reporter activity. Read-out is based on a STAT3-responsive luciferase reporter construct expressed as fold induction relative to the signal generated by a control prey, which binds to endogenous JAK2 associated with the bait receptor.

To determine whether MAGEL2 and necdin contribute to the regulation of LepR trafficking by RNF41 and USP8, our collaborators from Belgium used MAPPIT assay to examine interactions among MAGEL2, necdin, RNF41, USP8 and LepR and its adapter proteins. I have summarized their results below.

They tested whether MAGEL2 interacts with the LepR-associated protein complex (Fig. 1.12 A). MAGEL2 interacted weakly with RNF41. The MAGEL2-RNF41 interaction was dependent on the presence of the LepR tail. The interaction was weak when a large part of the LepR tail is deleted, which may indicate an indirect interaction between MAGEL2 and RNF41. Similar results were obtained by using a mutant form of RNF41 (RNF41-AE) that does not bind

to USP8 as the bait. This confirmed that MAGEL2-RNF41 interaction was independent of the interaction between RNF41 and USP8. They also found that MAGEL2 did not interact with the LepR intracellular domain, but it interacted strongly with USP8. This strong interaction between MAGEL2 and USP8 was lost in the absence of the LepR intracellular domain. From these results, they suggested that MAGEL2 can form a tight complex with USP8 and RNF41.

Next, they tested whether necdin interacts with the LepR-associated protein complex (Fig. 1.12B). Necdin interacts with every bait receptor, independent of the bait protein attached to it, but does not interact with a bait receptor in which the largest part of the LepR tail is deleted (pSEG short). This indicated that necdin interacts with the LepR tail. Necdin does not interact with USP8. Necdin recruitment to the LepR is between amino acids E1041-L1092. Necdin showed an interaction with LepR that has a mutation in the Y1077, [Y1077(F)] which is a tyrosine residue important for LepR signaling through STAT5. This indicated that LepR interaction with necdin is independent of phosphorylation at Y1077. In summary, necdin forms a weaker complex with RNF41 and USP8.

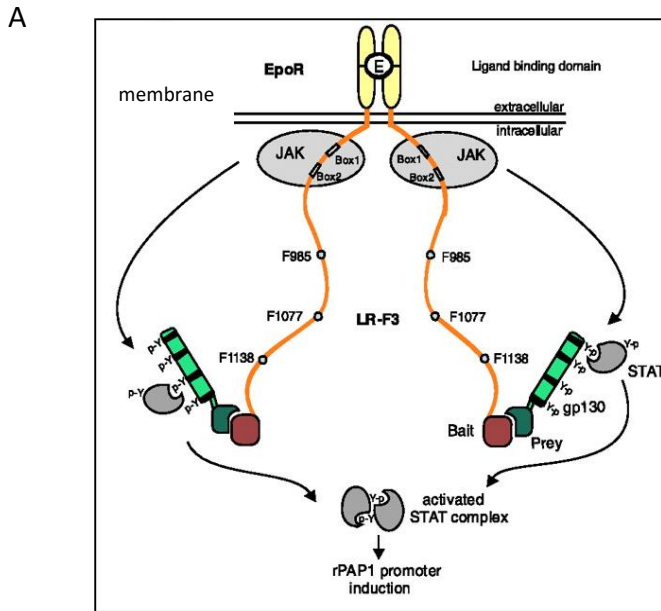
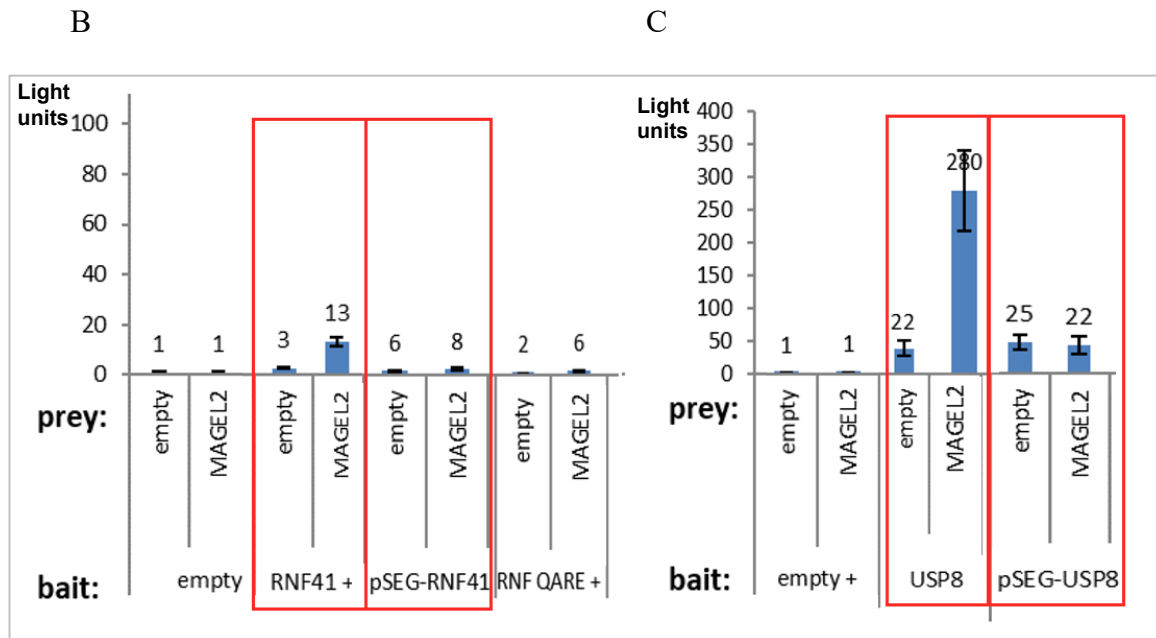


Figure 1.11: Schematic outline of the MAPPIT technique using a chimeric EpoR-LepR bait receptor.

Adapted from (Wauman et al., 2011)



B) MAGEL2 interacts weakly with RNF41.

C) MAGEL2 interacts strongly with USP8

(pSEG: Large part of the cytosolic LepR tail is deleted)

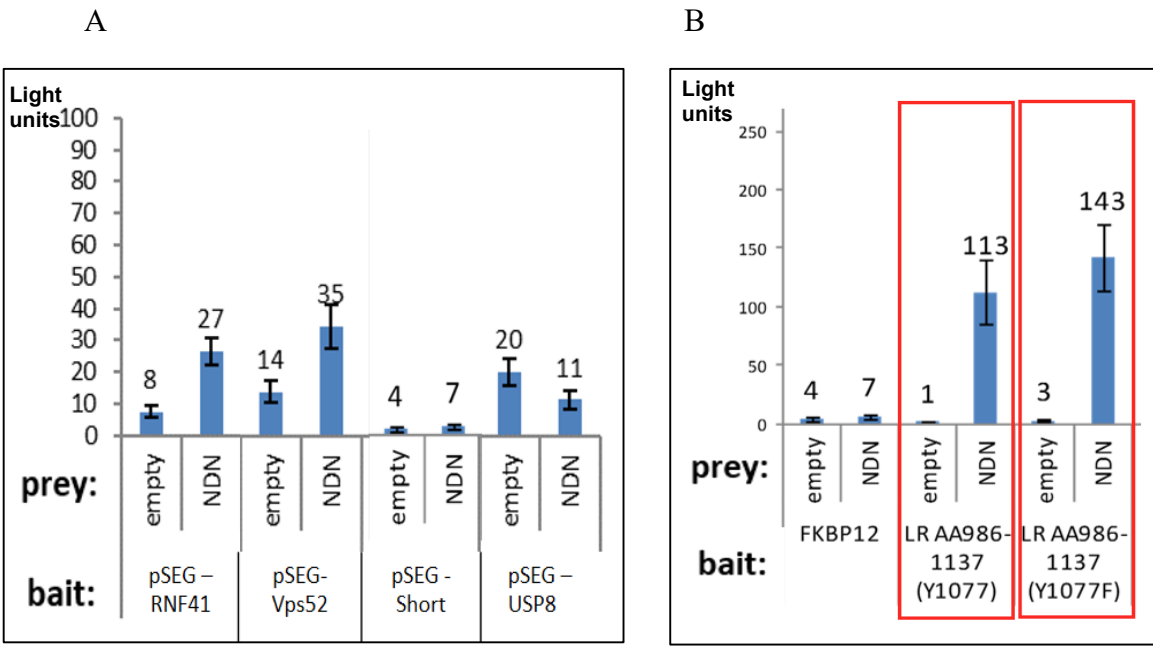


Figure 1.12 : Preliminary results- MAPPIT assay.

- A) Necdin interacts with any bait protein attached to LepR tail, but does not interact with bait proteins if the LepR tail is deleted (pSEG short). Necdin does not interact with USP8.
- B) LepR interaction with necdin is independent of phosphorylation at Y1077 tyrosine residue. (Y1077F: mutant form)

Chapter 2 :Methods

2.1 Plasmids

RNF41 constructs - RNF41-WT (wildtype), RNF41-SQ (RING E3 ligase domain is inactivated), RNF41-AE (no longer binds to USP8), leptin receptor construct (LepR- HA) and a USP8 construct (USP8- FLAG) were generously donated by Dr. Jan Tavernier and Dr. Leetnje De Ceuninck from Ghent University, Belgium. RNF41-V5, RNF41-FLAG, LepR-V5, USP8-V5, MAGEL2-V5, NDN-HA and NDN-Xpress plasmids were created using the Gateway clonase reaction by using relevant destination and entry vectors. Different MAGEL2 constructs (MAGEL2-HA partial and full length, MAGEL2-FLAG partial and full length, GFP-MAGEL2) were previously created in our laboratory. The full length MAGEL2 has both the PGQ rich region and the MAGE homology domain (MHD), but the partial MAGEL2 has only the MAGE homology domain that interacts with E3 ligases. Two new MAGEL2 point mutation forms in the MHD were created recently in our laboratory. The two mutants are a dileucine to dialanine substitution at amino acid positions #1031-1032 of MAGEL2 (MAGEL2p.LL1031AA) and a arginine to cysteine substitution at amino acid position #1187 (MAGEL2p.R1187C). An empty vector plasmid was used to make the DNA amount equal when co-transfected. For BioID experiments, new plasmids were created in the laboratory. BirA-MAGEL2-FLAG, BirA-NDN-HA and BirA-NDN-FLAG. FEZ1-HA, FEZ1-Xpress, EID1- HA, TRIM27-V5 and USP7-FLAG plasmids were created and used as positive controls. KANK4-V5 and KANK4-FLAG were created and used as a negative control in BioID technique. All the plasmids were confirmed by restriction digestion with relevant enzymes followed by gel electrophoresis (Table 1).

2.1.1 Preparation of new plasmids

10 μ l of clonase mixture was prepared with DNA of the relevant destination vector (concentration -75 ng/ μ l), DNA of relevant entry vector (50 ng/ μ l), 2 μ l of LR Clonase enzyme (Thermo Fisher) and nuclease free H₂O. The mixture was incubated for 1 h in room temperature. 5 μ l of the mixture was added directly into the 25 μ l of pre-thawed One Shot TOP10 Chemically Competent E. coli cells (Thermo Fisher) by swirling very gently.

It was incubated for 20 min on ice, then incubated for exactly 30 sec in 42°C water bath and again incubated for 2 min on ice. 175 µl of pre-warmed S.O.C media (Super Optimal Broth) was added to the mixture. The tube was placed on floating tube rack and incubated for 30 min in the warm room (37°C) on countertop shaker. 25 µl of relevant antibiotic was spread on two pre-dried LB (Lysogeny broth) plates using a plastic spreader. The plates were kept in room temperature for 30 min. After the 30min incubation in the warm room, 20 µl and 180 µl bacterial suspension was spread separately on the two LB agar plates. The plates were kept in room temperature for 30 min to dry, then kept in warm room (37°C) overnight. The next day, the plates were wrapped in parafilm and refrigerated until they were used. To make DNA from the transformed bacteria, one colony from each plate was picked and sub cultured in a new LB agar plate which was already spread with a relevant antibiotic. The plates were incubated in warm room (37°C) overnight. Then next day a single colony was picked and cultured in sterile culture tubes with 5 ml of LB broth with antibiotics. Two culture tubes were prepared for each transformation. The culture tubes were kept at 37°C for overnight in a shaker. Next day, DNA was made by using the QIAprep Miniprep Kit (QIAGEN). The DNA concentration of each new plasmid was measured using the spectrophotometer.

Plasmid name	Entry vector	Destination vector
MAGEL2-V5	MAGEL2 in pENTR 223.1 (Hscd00295122- DNASU)	pcDNA3.1/nV5-DEST (Thermo Fisher)
LepR -V5	LEPR in pENTR 223.1 (Hscd00351288- DNASU)	pcDNA3.1/nV5-DEST (Thermo Fisher)
USP8-V5	USP8 in pENTR 223 (Hscd00505996- DNASU)	pcDNA3.2/cV5-DEST (Invitrogen)
KANK4-V5	KANK4 in pENTR 223 (Hscd00516395- DNASU)	pcDNA3.2/cV5-DEST (Invitrogen)
RNF41-FLAG	RNF41 in pENTR 223 (Hscd00513773- DNASU)	pcDNA3.0/cSF-TAP-DEST
USP7-FLAG	USP7 in pENTR 223.1 (Hscd00294955- DNASU)	pcDNA3.0/nSF-TAP-DEST

Table 1: List of newly prepared plasmids

2.2 Transfections

Human osteosarcoma cells (U2OS cells) and human embryonic kidney cells (HEK cells) were cultured in Dulbecco's modified Eagle medium (DMEM) (Invitrogen) supplemented with 10% Fetal bovine serum (FBS), 1% l-glutamine and 1% penicillin/streptomycin at 37°C with 5% CO₂.

U2OS cells were seeded at 3.8 x10⁵- 4.0 x10⁵ cells/well in sterile 6 well plates. After 24 h, cells were transfected with recombinant constructs encoding epitope-tagged proteins using Effectene (QIAGEN) with a ratio of 1:8:10 = DNA(μg): Enhancer (μl): Effectene (μl). Plasmid DNA was diluted in 100 μl of EC buffer provided in the Effectene kit and incubated at room temperature for 5 min after enhancer was added. Subsequently Effectene reagent was added to the transfection mixture and mixed by vortexing. The mixture was then incubated for 10 min at room temperature. Next 600 μl of serum-free media was added to the mixture. The media was removed from the plates and the cells were washed gently with 1 ml of phosphate-buffered saline (PBS) and then 1.6 ml of fresh DMEM was added to each well before the addition of the transfection reagent drop-wisely onto the cells. The plates were incubated at 37°C for 24 h before protein collection. For BioID experiments the procedure was the same except for the addition of 75 μl of 1 mM Biotin solution to the transfection mixture.

HEK cells were seeded at 2.0 x10⁵ cells/well in sterile 6 well plates. After 24 h, cells were transfected with recombinant constructs using FuGENE6 (Promega) with a ratio of 1:3:50 = DNA (μg): FuGene6 (μl): serum free media (μl). FuGENE6 was added to the serum-free media and incubated for 5 min in room temperature. Then DNA was added and the mixture was incubated for 15 min in room temperature. The mixture was added to the plates drop-wise and then incubated at 37°C for 48 h before collection.

For the ubiquitination assay, HEK cells were seeded at 8.0x10⁵ cells/dish in sterile 100 mm dishes with 10 ml of DMEM media. The ratio of transfecting reagents and the procedure was similar, except that 24 h after transfection cells, were treated with 25 μM chloroquine and 5 μM MG 132 in serum-free OPTIMEM media to inhibit any lysosomal and proteasomal degradation.

2.3 Protein collection

24 h after the cells were transfected, the media was removed from the plates and the cells were washed with PBS. 250 μ l of Trypsin was added to each well and incubated at 37°C for 2 min. Then 2 ml of DMEM was added per well and the cells were collected separately into 1.5 ml eppendorf tubes. They were centrifuged at 420xg for 6 min and the supernatant was discarded. The cell pellet was washed with PBS three times. The cells were lysed in 100 μ l of 2x modified sample buffer (20% glycerol, 4% SDS of 20% stock, 0.13 M Tris HCl pH 7.8) with Complete Mini protease inhibitor tablet (Roche). Next the lysates were sonicated on ice (3 times for 5 sec with 5 sec pauses). Then they were incubated at 65°C for 5 min and centrifuged 10 min at 20800xg, at room temperature. The supernatants were transferred to new micro-centrifuge tubes. For immunoblots, 2 μ l/100 μ l of 2% β -mercaptoethanol and 1 μ l/100 μ l of saturated bromophenol blue were added, then the lysates were boiled for 5 min in a boiling water bath and stored at -20°C. When the LepR were to be detected via immunoblotting, the protein lysates were not boiled.

2.4 BioID assay

U2OS cells were seeded at 3.0×10^5 cells/well in 6 well plates. Two wells were seeded for each reaction. Effectene was used as the transfection reagent. 75 μ l of 1 mM biotin mixture (12.2 mg biotin in 50 ml of serum-free DMEM) was added to the transfection mixture to induce biotinylation. 24 h after transfection DMEM was removed from the plates and the cells were washed twice with 3 ml of PBS per well to remove excess biotin. 400 μ l of lysis buffer (50 mM Tris HCl (pH 7.5), 500 mM NaCl, 0.2% SDS, 2% Triton-X, 1 mM DTT with Complete Mini protease inhibitor tablet) was added and the lysates were incubated at room temperature for 10 min in a rocker. Lysates were transferred to 1.5 ml eppendorf tubes. The lysates were sonicated on ice (3 times for 5 sec with 5 sec pauses) and centrifuged at 16500xg at 4°C for 10 min. The lysates were filtered using Amicon Ultra Centrifugal units (Millipore # UFC500324). While the samples were spinning 30 μ l of streptavidin sepharose beads (GE product code: 17-5113-01) per sample was added to 200 μ l of lysis buffer and 200 μ l of 50 mM of Tris-Cl (pH 7.4). The beads were kept in the mixture for 3 min to be equilibrated. The supernatant was removed from the beads after centrifuging at 800xg for 2 min at RT.

From the filtered lysates, 30 μ l was removed into a new eppendorf tubes as input (30 μ l of 2x modified sample buffer was added and processed as for any other protein sample). The remaining filtered lysate was added to the beads and incubated at 4°C overnight on a rotator. The next day, the sample tubes were centrifuged at 800xg at RT for 2 min and the supernatants were discarded. The beads were then incubated for at room temperature for 8 min in three different wash buffers separately: [(Wash Buffer 1- 2% SDS, Milli Q water), (Wash Buffer 2- 0.1% deoxycholic acid, 1% Triton X, 1mM EDTA, 500mM NaCl, 50mM HEPES (pH 7.5), Milli Q water), (Wash Buffer 3- 0.5% deoxycholic acid, 0.5% NP-40, 1mM EDTA, 250 mM LiCl, 10 mM Tris Cl (pH 7.4), Milli Q water)]. The tubes were centrifuged at 800xg at RT for 2 min to pellet the beads then they were resuspended in 30 μ l 50mM Tris Cl and 30 μ l 2x modified sample buffer. For immunoblots, 5 μ l of 1 mM Biotin, 2 μ l/100 μ l of 2% β -mercaptoethanol and 1 μ l/100 μ l of saturated bromophenol blue were added, then the lysates were boiled for 5 min in a boiling water bath and stored at -20°C.

2.5 Ubiquitylation assay

HEK cells were seeded at 8.0×10^5 cells/well in 100 mm petri dishes with 10 ml of DMEM. FuGENE 6 was used as the transfection reagent. After 24 h, cells were incubated overnight with 25 μ M chloroquine and 5 μ M MG132 in serum-free OPTIMEM media to inhibit any lysosomal and proteosomal degradation. Next the media was removed and the cells were washed with PBS. 250 μ l of modified lysis buffer (2% SDS, 150 mM NaCl, 10 mM Tris-HCl, pH 8.0, 1 mM Sodium orthovanadate, 1 mM Sodium fluoride, 20 mM β -glycerophosphate phosphatase, 10 mM N-ethylmaleimide and Complete Mini protease inhibitor (Roche) was added to each well and incubated for 30 min in a rocker at room temperature to lyse the cells. Lysates were collected separately into 1.5 eppendorf tubes and were sonicated on ice (3 times for 5 sec with 5 sec pauses). Then the lysates were boiled for 10 min in a boiling water bath. From the lysate 40 μ l was removed into a new eppendorf tubes as input and 10 μ l of 5x Laemmli buffer (156 mM Tris-HCl, pH 6.8, 2% SDS, 25% glycerol)) was added and processed as for any other protein sample. The rest of the lysate was added to a 5 ml eppendorf tubes and incubated for 1 h in a rotator at 4°C with 2250 μ l dilution buffer (10 mM Tris-HCl, pH 8.0, 150 mM NaCl, 2 mM EDTA, 1% Triton). Next the diluted lysates were centrifuged at 20000xg for 30 min and precleared by incubating with 20 μ l of

sepharose 4B beads (Sigma) for 1 h at 4°C in a rocker. The supernatant was separated from the sepharose beads by centrifuging at 3000 rpm for 3 min. Next the supernatant was incubated with 30 µl of anti-FLAG M2 Affinity Gel (Sigma) at 4°C in a rocker overnight. The supernatant was separated from the anti-FLAG beads by centrifuging at 3000 rpm for 3 min. After cleaning the beads twice with wash buffer (10 mM Tris-HCl, pH 8.0, 1 M NaCl, 1 mM EDTA, 1% NP-40), the beads were eluted in 80 µl of 2X Laemmli buffer. For immunoblots, 2 µl /100 µl of 2% β-mercaptoethanol and 1 µl /100 µl of saturated bromophenol blue were added, then the lysates were boiled for 10 min in a boiling water bath and stored at -20°C.

2.6 Protein stability assay using cycloheximide

HEK cells were seeded at 2.0×10^5 cells/well in 6 well plates in 2 ml of DMEM. FuGENE 6 was used as the transfection reagent. 48 h after transfection cells were treated with 10 µg/ml cycloheximide for 0, 30, 60, 90, 120, 150, 180 min. Proteins were collected at each time point separately using the method explained above.

2.7 Cell surface biotinylation assay

HEK cells were seeded at 2.0×10^5 cells/well in 6well plates in DMEM. FuGENE 6 was used as the transfection reagent. Cells were transfected with a LepR construct either alone, with RNF41 or with MAGEL2. Cell surface proteins were labeled with 1 mg/ml Sulfo-NHS- SS-Biotin* (Pierce) in borate buffer (10 mM Boric acid, 145 mM NaCl, 7.2 mM KCl, 1.8 mM CaCl₂, pH 9) for 15 min at 4°C. Biotinylation solution was renewed for another 15 min incubation. Excess biotin was quenched with 100 mM ice cold glycine in borate buffer. Next the cells were washed with 1 ml of cold PBS twice. The cells were lysed in 300 µl TNT lysis buffer pH 7.2 (50 mM Tris-HCl, 150 mM NaCl, 1 % Triton X-100, 0.2 % SDS, 1 µg and Complete Mini protease inhibitor tablet) for 20 min at 4°C. Ten percent of the lysate was kept as total lysate and the remaining 90 percent was incubated with 100 µl streptavidin sepharose beads (GE product code: 17-5113-01) for 1 h at 4°C on a rotator.

After 1 h, the supernatant was separated from the streptavidin beads by centrifuging at 1000rpm for 2 min. 60 µl of the supernatant was taken as the cytosolic portion. The rest of the supernatant was discarded. 60 µl of 2x modified sample buffer was added to the cytosolic portion and processed as any other protein sample. The beads were washed with 1 ml of TNT lysis buffer for three times. Cell surface proteins were eluted with 50 µl 2x modified sample buffer that contained 15 % beta-mercaptoethanol. The beads were mixed thoroughly with the sample buffer. The amount bound (biotinylated and internalized) was compared to the total amount with anti-LepR to calculate the percentage at cell surface.

2.8 Immunoblotting

Experiments involving protein abundance, protein interaction using BioID assay, cycloheximide assay, ubiquitylation assay and cell surface biotinylation assay were performed in triplicate and analyzed by SDS-PAGE and protein immunoblotting. A range of 10 µg to 15 µg of protein depending on the experiment was loaded on a 7.5% polyacrylamide along with Precision Plus Protein Dual colour standard (Bio-RAD). The lysates were electrophoresed at 80 milliamps for roughly 45 min, or until the ladder had separately appropriately. Resolved proteins were then transferred to Immobilon-P polyvinylidene fluoride membranes (Millipore) at 100 volts for 90 min and blocked at room temperature for 1 hour with TBSTM (5% skim milk powder in TBST (137 mM NaCl, 0.1% Tween-20, 20 mM Tris pH 7.5) The membranes were incubated overnight at 4°C with relevant primary antibody in TBSTM, or for 2 hours at room temperature with mouse anti- β actin (Sigma A3854, 1:50000 dilution). After three 10-15 min washes in TBST, the membranes were incubated for 1 h at room temperature in anti-rabbit or anti-mouse HRP secondary antibodies in TBSTM. Again, the membranes were washed three times with TBST. Finally, they were incubated at room temperature in Immobilon Western Chemiluminescent HRP substrate (Millipore) for 5 min and imaged using Kodak Image Station. Immunoblot analysis was performed using ImageJ software and protein quantities were calculated as the ratio of band intensity from the protein of interest to band intensity from β actin.

2.9 Immunofluorescence (IF)

Autoclaved coverslips were placed on to 6 well plates separately and treated with 500 μ l of poly-l-lysine for 15 minutes. HEK cells were seeded at 1.0×10^5 cells/well onto cover slips with 2ml of DMEM. After 24 h cells were transfected with FuGene6 (Promega). For U2OS cells, poly-l-lysine treatment was not done. U2OS cells were seeded at 1.8×10^5 cells/well onto cover slips with 2 ml of DMEM. After 24 h cells were transfected with Effectene (QIAGEN). 24 h after transfection, the media was removed and the coverslips were washed twice with PBS with a 5 min incubation at room temperature. Then cells were fixed onto the cover slips for 15 min with 1 ml/well of 4% paraformaldehyde (PFA) or with ice cold methanol. Cells were washed twice with PBS with a 5-min incubation at room temperature. Next the cells were blocked with PBSX (PBS containing 0.05% Triton X-100) to minimize nonspecific binding, for 15 min at room temperature. Cells were incubated at room temperature for 1 h or 4°C overnight with relevant primary antibodies prepared in 5% bovine serum albumin in PBSX. Next the cells were washed twice with PBSX, then incubated with fluorescently tagged secondary antibodies (Alexa Fluor 546 and 488) prepared in 1% normal goat serum in PBSX for 1 h in room temperature. The cells were again washed twice with PBSX and then treated for 15 min with PBSX containing the nuclear stain Hoechst 33342 (Invitrogen) at a ratio of 0.24 μ L Hoechst 33342: 10 ml PBSX. The cells were washed twice with PBSX before the coverslips were mounted onto glass microscope slides using ProLong Gold antifade reagent without DAPI (Life Technologies). Slides were sealed with clear nail polish, left to dry, and stored at -20 °C until they were imaged using the 40x / 1.00-0.50 objective lens in Leica DMRE fluorescence microscope.

2.10 Mouse strains

The *Magel2*-null mice were originally developed by Serguei Kozlov (Kozlov et al., 2007) and also available from The Jackson Laboratory (C57BL/6-Magel2tm1Stw/J, stock 009062). This mouse strain was developed by inserting a LacZ reporter cassette into the open reading frame of the *Magel2* gene leaving a mouse that expresses LacZ in place of *Magel2* (Kozlov et al., 2007), (Bischof et al., 2007). *Magel2*-carrier males were bred with wildtype females. *Magel2* is maternally silenced (maternally-inherited imprinted) with only the paternal copy leading to the expression of the protein. This cross produces *Magel2*-null offspring, heterozygous for *Magel2* and LacZ, and homozygous wildtype control littermates expressing endogenous *Magel2*. Mice were housed in the University of Alberta Health Science Laboratory Animal Services (HSLAS) facilities under standard conditions (12 hr light / dark cycle, lights on from 6 am – 6 pm and temperature maintained at 21 °C). The University of Alberta Animal Care and Use Committee in accordance with the guidelines of the Canadian Council on Animal Care approved all procedures involving animals.

2.10.1 Genotyping

Wildtype and *Magel2*-null mutant mice were differentiated by genotyping. Genotyping was done by polymerase chain reaction (PCR) of ear notch biopsies by our laboratory technician Jocelyn Bischof (Bischof et al., 2007). Ear notches were stored in 1.5 ml eppendorf tubes at -20°C until further processing. DNA from frozen tissue was extracted using the DNeasy Blood & Tissue Kit (Qiagen) following the manufacturer's instructions. Then DNA was amplified in a PCR in a Veriti 96 well thermal cycler (Applied Biosystems). The primer sequences (Gibco BRL) are as follows:

forward common primer (ATGGCTCCATCAGGAGAAC),
mutant reverse primer (GGGATAGGTACGTTGGTGT),
wild type reverse (GATGGAAAGACCCTTGAGGT).

This reaction resulted in 233 bp amplicons for wildtype mice, and 233 bp and 336 bp amplicons for mutants. PCR products were loaded onto a 2% agarose gel and run at 100 V for 60 minutes. Bands were visualized by using Kodak Image Station.

2.10.2 Crude protein preparation

The mice were euthanized by administering a lethal dose of euthanyl into the peritoneum. Hypothalamus and cortex were collected, transferred into a micro-centrifuge tube, and snap frozen in liquid nitrogen. The samples were stored in -80°C until they were used. The tissues were ground using pre-chilled disposable plastic pestles and re-suspended in 500 µl of 2X modified sample buffer (20% glycerol, 4% SDS, 0.13 M Tris, pH 7.8) with Complete Mini protease inhibitor (Roche). The tissues were sonicated on ice (3 times for 5 sec with 5 sec pauses), then incubated at 65°C for 5 min and centrifuged 10 min at 20000xg, RT. The supernatants were transferred to new micro-centrifuge tubes and the protein concentration was quantified using the Pierce™ BCA protein assay kit (Thermo Fisher). For immunoblots, 2 µl/100 µl of 2% β-mercaptoethanol and 1 µl/100 µl of saturated bromophenol blue were added, then the lysates were boiled for 5 min in a boiling water bath and stored at -20°C.

Primary Antibodies	Host	Supplier	WB Concentration	IF Concentration
HA-probe Antibody (Y-11): sc-805	Rabbit polyclonal	Santa Cruz	1:500	1:500
ANTI-FLAG, antibody F7425	Rabbit polyclonal	Sigma	1:1000	1:500
FLRF/RNF41 Antibody, A300-049A	Rabbit polyclonal	Bethyl	1:5000	
USP8 Antibody, A302-929A	Rabbit polyclonal	Bethyl	1:2000	1:500
Anti-V5 Epitope Tag Antibody AB3792	Rabbit polyclonal	Millipore	1:3000	
V5 Tag Antibody MA5-15253	Mouse monoclonal	Sigma	1:3000	1:500
Xpress Monoclonal Antibody PN 46-0528	Mouse monoclonal	Sigma	1:2000	
STAM Antibody (H-175)	Rabbit polyclonal	Santa Cruz	1:2000	
Anti-Necdin Antibody AB9372	Mouse monoclonal	Sigma	1:2000	
Anti-Leptin Receptor antibody ab104403	Rabbit polyclonal	Abcam		1:500
Anti-LAMP1 antibody [H4A3] ab25630	Mouse monoclonal	Abcam		1:500
Anti-EEA1 antibody [1G11] - ab70521	Mouse monoclonal	Abcam		1:500
Anti (RNF41) Nrdp1 Antibody (A-6) sc-365622	Mouse monoclonal	Santa Cruz		1:500
Monoclonal Anti-β-Actin– Peroxidase antibody	Mouse monoclonal	Sigma	1:50000	

Table 2 : Summary of primary antibodies

Secondary Antibodies	Host	Supplier	WB Concentration	IF Concentration
Sheep Anti-Mouse IgG - Horseradish Peroxidase	Sheep	Amersham	1:5000	
Donkey Anti-Rabbit IgG - Horseradish Peroxidase	Donkey	Amersham	1:5000	
Goat anti-Rabbit IgG (H+L) Highly Cross-Adsorbed Secondary Antibody, Alexa Fluor 488	Goat	Life Technologies		1:5000
Goat anti-Rabbit IgG (H+L) Cross-Adsorbed Secondary Antibody, Alexa Fluor 594	Goat	Life Technologies		1:5000
Goat anti-Mouse IgG (H+L) Cross-Adsorbed, Secondary Antibody, Alexa Fluor 594	Goat	Life Technologies		1:5000
Goat anti-Mouse IgG (H+L) Cross-Adsorbed, Secondary Antibody, Alexa Fluor 488	Goat	Life Technologies		1:5000

Table 3 : Summary of secondary antibodies

Chapter 3 :Results

LepR can be internalized by two different mechanisms. One is the ligand-dependent pathway, in which LepR signaling is activated through the JAK/STAT pathway by binding of leptin (Bates et al., 2003). The other method is constitutive internalization and trafficking of LepR in the absence of ligand stimulation. The abundance of LepR on the cell surface is an important factor for ligand-independent LepR internalization (Wauman and Tavernier, 2011). Among the large collection of deubiquitylating enzymes and E3 ligases present in mammalian cells, USP8 and RNF41 have an important role in LepR recycling and degradation pathway. RNF41 interacts with LepR and reduces its cell surface expression. RNF41 controls internalization, recycling and degradation of LepR by regulating the USP8 and ESCRT-0 complex. Both MAGEL2 and necdin, which belong to the melanoma antigen (MAGE) protein family, interact with and bind to E3 RING ubiquitin ligases, promoting protein trafficking and recycling (Doyle et al., 2010; Kozlov et al., 2007). To determine whether MAGEL2 and necdin contribute to the regulation of LepR by RNF41 and USP8, I performed BioID experiments using U2OS cells. The BioID assay is a proximity dependent biotin labelling technique used to detect protein-protein interactions *in vivo*. I used MAGEL2 and necdin, which were fused with biotin ligases (also known as BirA) as bait in BioID. The interacting proteins that bind the bait proteins are known as prey proteins. The interaction between bait and prey protein occur only when the prey proteins are in close proximity to the BirA-tagged bait. Both the bait itself and the prey are labelled by covalent attachment of biotin. Only the biotinylated proteins are separated by streptavidin affinity purification and they can be detected by immunoblotting.

3.1 Necdin and MAGEL2 form a bridge between leptin receptor and RNF41-USP8.

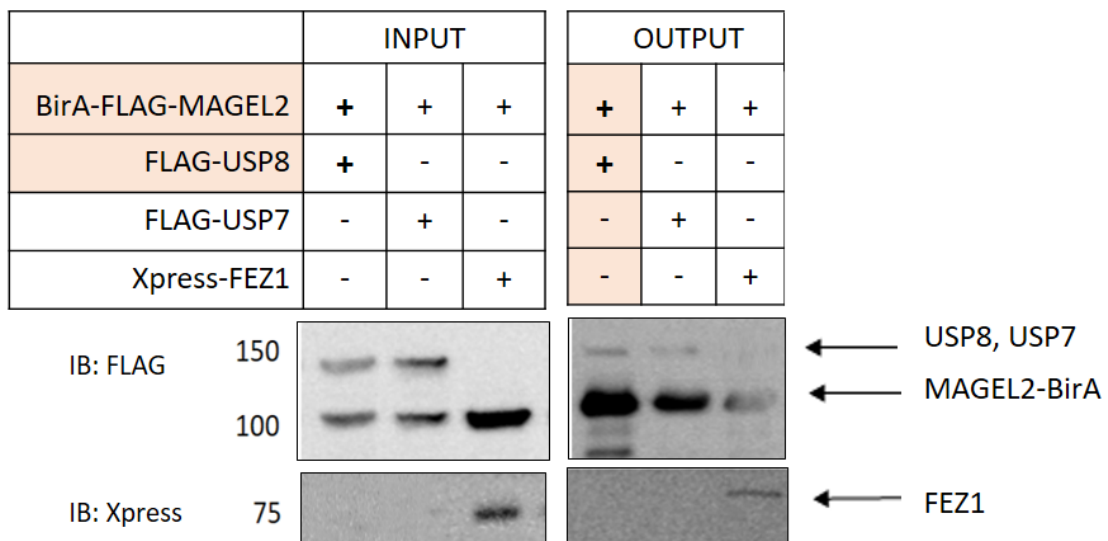
I transiently co-transfected cells with BirA-MAGEL2 and BirA-NDN (bait) and a second construct expressing epitope-tagged MAGEL2, NDN, TRIM27, RNF41, USP7, USP8, FEZ1, KANK4 (prey), and cultured in media with excess biotin. After streptavidin affinity purification using the streptavidin sepharose beads, the input and the bound proteins were immunoblotted to detect proteins originally in proximity to the BirA-fusion baits. FEZ1 and EID1 were used as positive controls and KANK4 was used as a negative control for both MAGEL2 and necdin biotinylation experiments.

I could detect USP8 and USP7 in the “bound” fraction, indicating that these proteins were biotinylated by BirA-MAGEL2 (Fig. 3.1A). USP8 and BirA-MAGEL2 had the same epitope tag (FLAG). I blot the membrane using an anti-FLAG antibody. When I imaged the blot, I detected only USP7 protein expression in the bound fraction but couldn’t detect USP8. When imaging the blot, bands for BirA-MAGEL2 was more intense than the bands of interacting proteins. To overcome this issue, I used interacting proteins with a different epitope tag than the BirA bait protein. Therefore, I confirmed the biotinylation of USP8 by MAGEL2 by using a different construct (V5-USP8) along with V5-TRIM27 as a positive control (Fig.3.1B). The interaction between MAGEL2 and USP8 was consistent with MAPPIT results (previously explained in Chapter 1). Both USP7 and TRIM27 were biotinylated by BirA-MAGEL2 (Fig.3.1A,B), consistent with published evidence of protein-protein interaction (Hao et al., 2015).

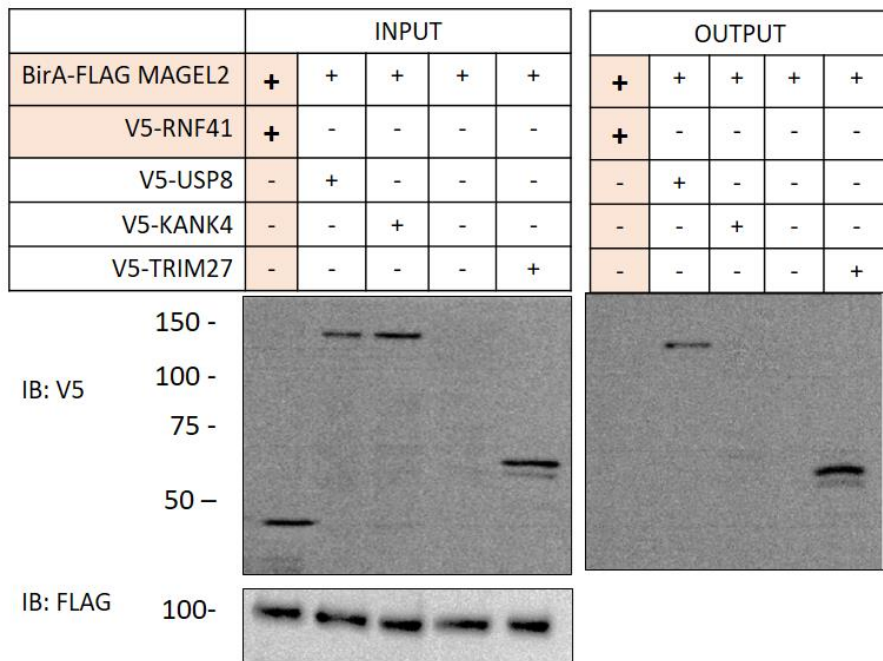
I could not detect any RNF41 protein in the bound fraction, when co-transfected with BirA-MAGEL2 (Fig.3.1B). Surprisingly, biotinylation of RNF41 by BirA-MAGEL2 was detected in the presence of co-transfected USP8, LepR, both USP8 and LepR or TRIM27 (Fig.3.1C). The interaction of RNF41 with MAGEL2 in the presence of USP8 is consistent with the MAPPIT results. I wanted to assess the relationship of necdin and MAGEL2 using BioID. I detected that necdin was biotinylated by BirA-MAGEL2 (Fig. 3.1D), and MAGEL2 was biotinylated by BirA-NDN (Fig. 3.2).

To assess if necdin was biotinylated by RNF41, USP8 and LepR, more BioID experiments were done using NDN-BirA. I could not detect any bound RNF41 and USP8, indicating that these proteins do not strongly interact with necdin. In contrast, LepR and MAGEL2 proteins were detected in the bound fraction, indicating that these proteins do interact with necdin (Fig.3.2). In combination, the BioID and the MAPPIT results support a role for MAGEL2 and necdin in regulation of leptin receptor with the involvement of RNF41 and USP8.

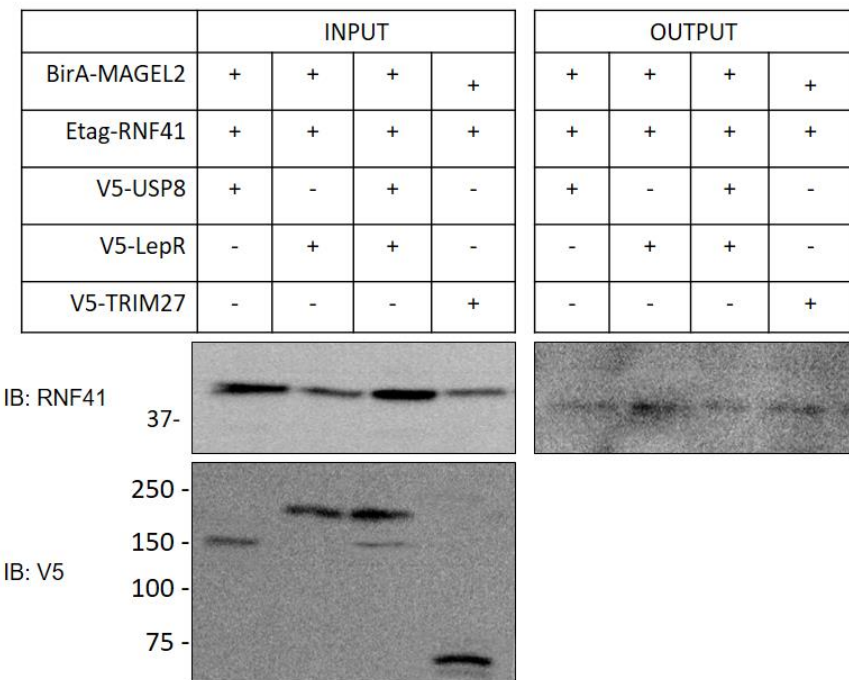
A



B



C



D

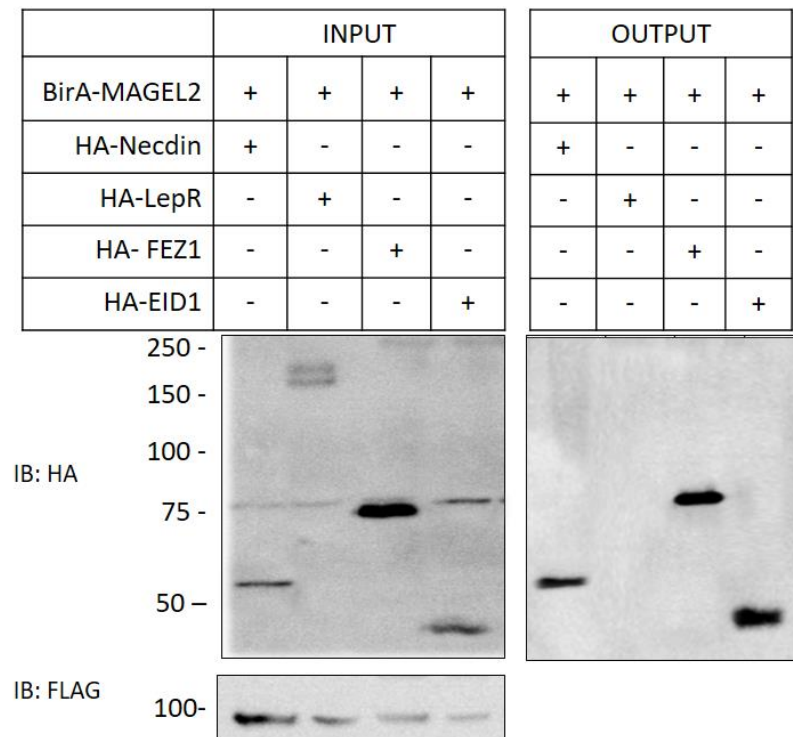


Figure 3.1 : Biotinylation of interacting proteins by BirA-FLAG-MAGEL2

HEK cells were co-transfected with BirA-FLAG-MAGEL2 along with a second construct expressing epitope tagged USP8, USP7, FEZ1, RNF41, KANK4, TRIM27, LepR, NDN and EID1 and cultured in media with 1mM biotin. Lysates were purified using streptavidin beads, and input and bound proteins were immunoblotted against relevant antibodies.

- A) USP8 and USP7 interact with MAGEL2. FEZ1 was a positive control.
- B) USP8 and TRIM27 interact with MAGEL2.
- C) RNF41 interacts with MAGEL2 in the presence of USP8, LepR or TRIM 27.
- D) Necdin interacts with MAGEL2. LepR does not interact with MAGEL2. FEZ1 and EID1 were positive controls.

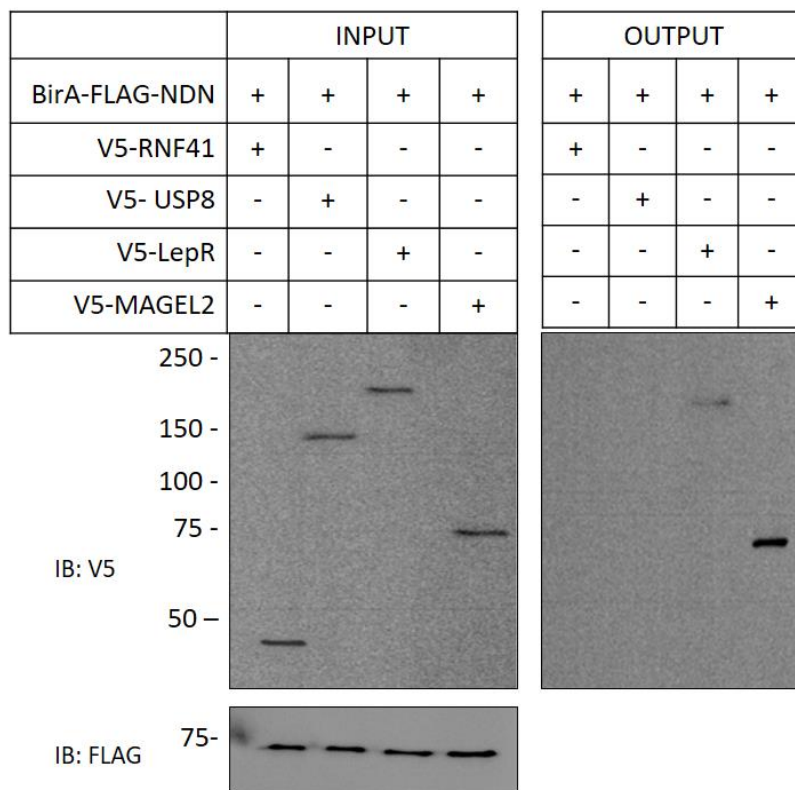


Figure 3.2 : Biotinylation of interacting proteins by BirA-FLAG-NDN .

HEK cells were co-transfected with BirA-FLAG-NDN along with a second construct expressing epitope tagged RNF41, USP8, LepR, MAGEL2 and cultured in media with 1mM biotin. Lysates were purified using streptavidin beads, and input and bound proteins were immunoblotted against anti V5 antibody.

LepR and MAGEL2 interact with necdin. RNF41 and USP8 do not interact with necdin.

3.2 MAGEL2 regulates the stability of the USP8-RNF41 complex.

To assess whether MAGEL2 has an influence on the abundance of the USP8-RNF41 complex, I used U2OS cells and transiently co-transfected MAGEL2 with a second construct expressing epitope tagged USP8 or RNF41. I then measured the changes in the protein expression levels. Quantification of relative protein abundance was carried out relative to β -actin controls. Three different RNF41 forms were used. They are RNF41 wild type, the RNF41-AE mutant that no longer binds to USP8, and the RNF-SQ form that has inactivation of E3 ligase activity. USP8 is a ubiquitination substrate of RNF41 and USP8 physically interacts with RNF41 (Wu et al., 2004). The endogenous USP8 levels were reduced in cultured cells by RNF41 (De Ceuninck et al., 2013). I transfected U2OS cells with USP8, and assessed the changes in the expression level when RNF41 was co-transfected. Consistent with the published results, I detected less USP8 protein when RNF41 was co-transfected compared to cells transfected with USP8 alone. To determine whether the RNF41 mutant forms change the expression level of USP8, I co-transfected U2OS cells with USP8 and different RNF41 mutant forms. A similar result as RNF41-wildtype was detected in RNF41-SQ mutant form with impaired E3 ubiquitin ligase activity. Conversely, RNF41-AE mutant expression no longer lowered USP8 protein levels, indicating that suppression of USP8 by RNF41 depends on direct interaction between RNF41 and USP8 (Fig. 3.3).

To examine whether abundance of RNF41 changes with USP8, I co-transfected cells with each of the three forms of RNF41 along with USP8. I observed a significant increase in all the RNF41 levels, indicating that USP8 stabilizes RNF41, RNF41-AE and an RNF41-SQ. Interestingly, co-transfection with MAGEL2 reversed the stabilizing effect of USP8 on RNF41 and its mutant forms (Fig 3.4).

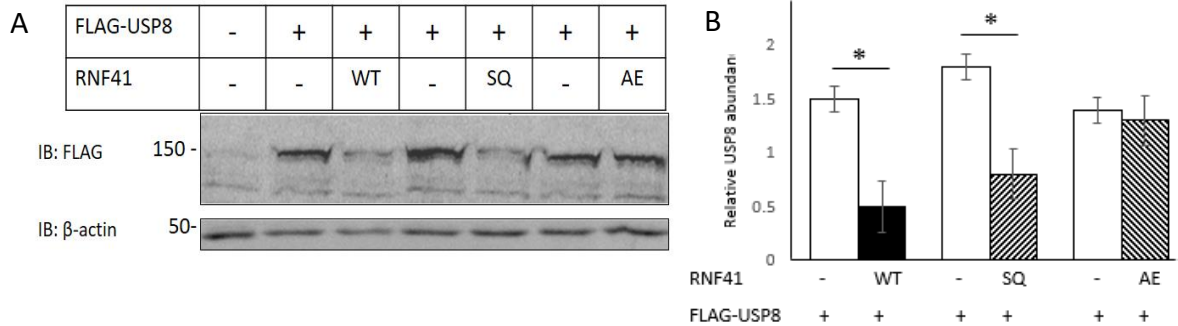


Figure 3.3 : Abundance of USP8 with RNF41-WT and mutant forms.

- A) Co-expression of RNF-WT and RNF-SQ reduces USP8 abundance.
- B) Quantification of the USP8 protein abundance relative to the β -actin control. (mean \pm SD of biological triplicates).

* P<0.05 different by student t-test

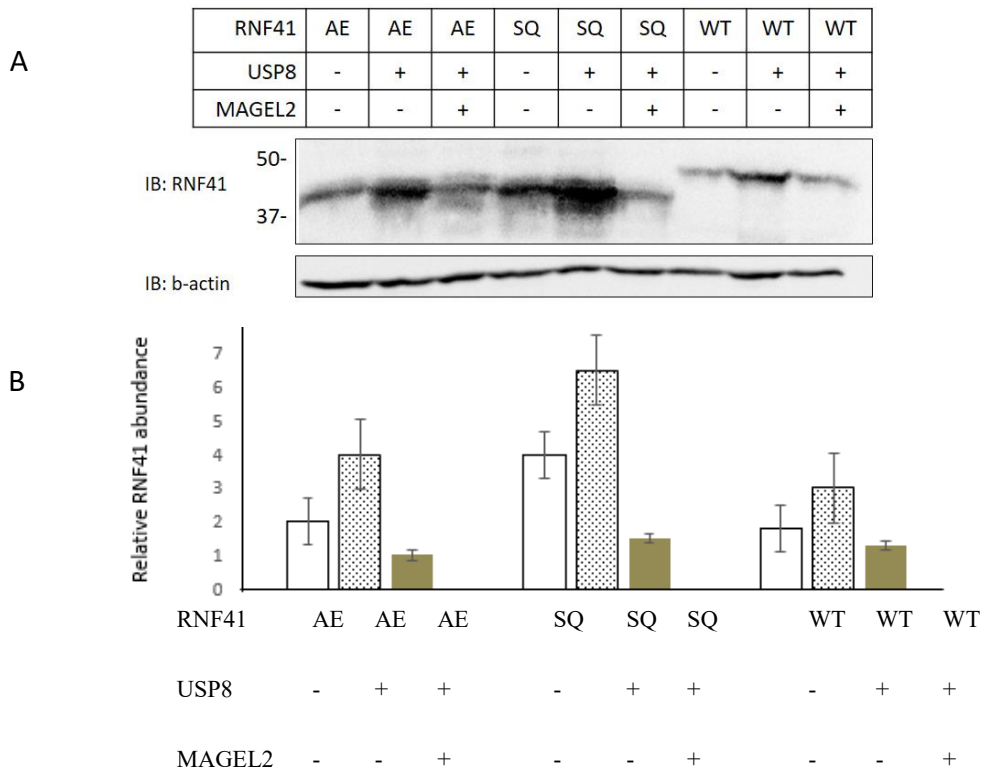


Figure 3.4: MAGEL2 regulates the stability of the USP8-RNF41 complex.

- A) USP8 stabilizes RNF41, but MAGEL2 reverses this effect.
- B) Quantification of the RNF41 protein abundance relative to the β -actin control. (mean \pm SD of biological triplicates).

As I observed that MAGEL2 made a significant difference in the abundance of RNF41-USP8 complex, next I wanted to assess whether MAGEL2 modulates the stability of USP8 or RNF41 separately. Co-expression of MAGEL2 significantly reduced the abundance of USP8 (Fig. 3.5). Conversely, co-expression of MAGEL2 increased the abundance of RNF41-WT (Fig 3.6A) as well as mutant forms (Fig.3.6C, 3.6E).

To determine if MAGEL2 could stabilize RNF41 through a process that involves ubiquitination, I co-transfected constructs encoding MAGEL2, RNF41, and HA-ubiquitin. The cells were cultured overnight with 25 μ M chloroquine and 5 μ M MG 132 in serum-free media to inhibit any lysosomal and proteasomal degradation. I performed an immunoprecipitation using anti-FLAG and then I immunoblotted for either anti-FLAG or anti-HA antibodies to detect RNF41 and ubiquitin respectively. The immunoblotting for ubiquitin revealed that RNF41 is ubiquitinated and co-expression of MAGEL2 reduced the extent of RNF41 ubiquitination (Fig. 3.7). From the above result, I could conclude that MAGEL2 stabilizes RNF41 by diminishing its auto-ubiquitination or, alternatively, by increasing de-ubiquitination by endogenous deubiquitinating enzymes.

To examine the role of MAGEL2 in altering the stability of RNF41, I performed a protein stability assay using cycloheximide. Cells were transiently transfected with RNF41 or with a combination of RNF41 and MAGEL2. An empty vector was used to equalize the DNA amount of the double transfections. 24 h after transfection, cells were treated with 5 mM cycloheximide to block *de novo* protein synthesis. The abundance of RNF41 was measured every 30 min for 3 h after treatment. The abundance was monitored by immunoblotting against RNF41. I was able to detect at 3 h, more than half of the total RNF41 was degraded, whereas RNF41 that was co-transfected with MAGEL2 degraded less than half of the starting RNF41 protein level (Fig. 3.8A). Also, co-expression of MAGEL2 doubled the half-life of RNF41 from 1.5 h to 3 h (Fig. 3.8B) indicating that MAGEL2 can stabilize RNF41 within the cells.

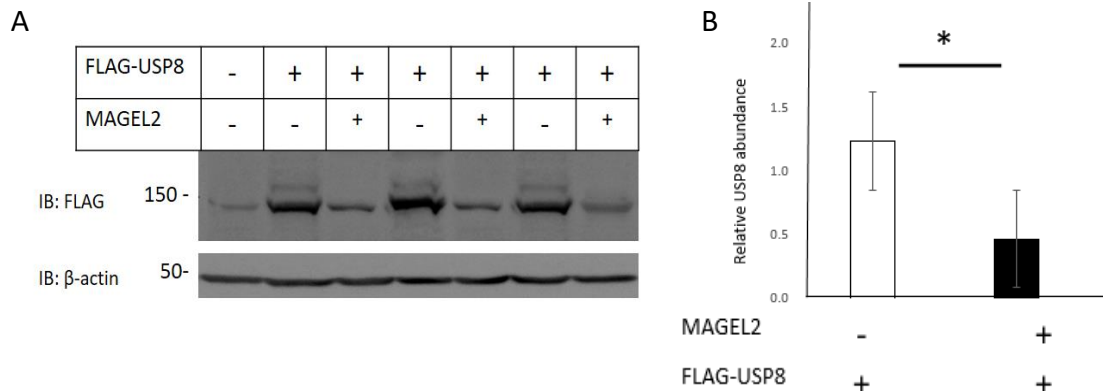
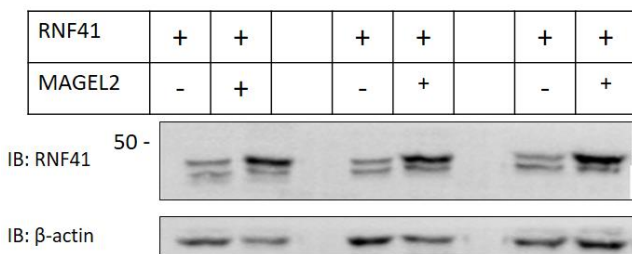


Figure 3.5 : Abundance of USP8 with MAGEL2.

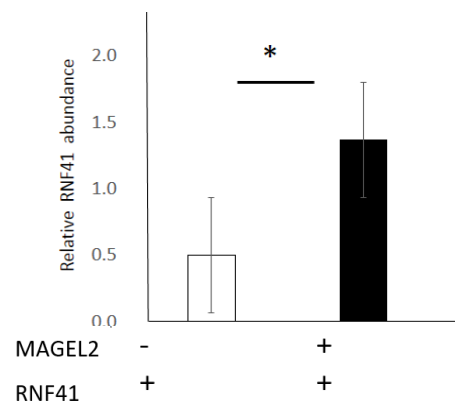
- A) Co-expression of MAGEL2 reduces the USP8 abundance. Cell lysates were immunoblotted against anti-FLAG antibody.
- B) Quantification of the USP8 protein abundance relative to the β -actin control. (mean \pm SD of biological triplicates).

* P<0.05 different by student t-test

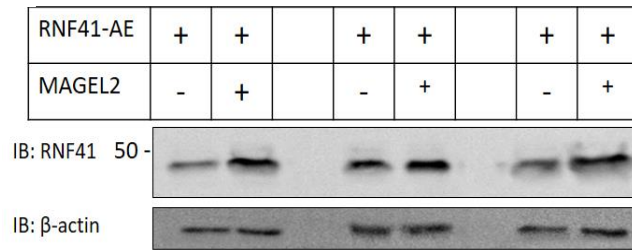
A



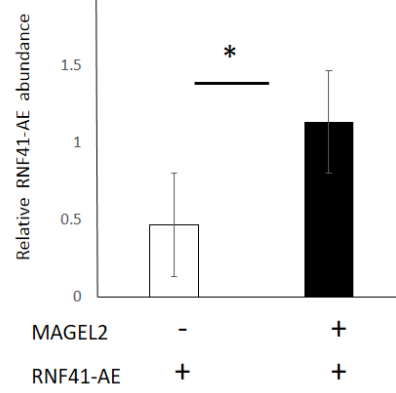
B



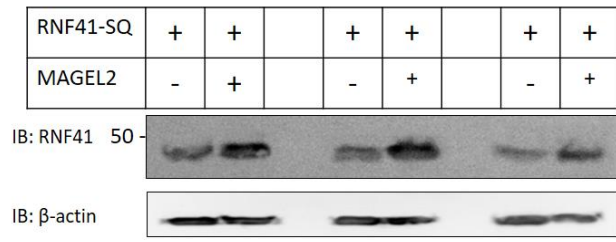
C



D



E



F

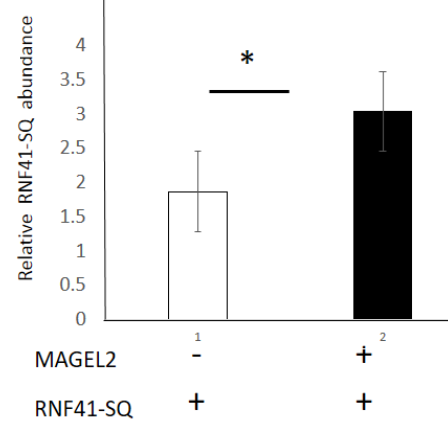


Figure 3.6 : Abundance of RNF41 with MAGEL2.

(mean ± SD of biological triplicates, * P<0.05 different by student t-test)

- A) Co-expression of MAGEL2 increases RNF41-WT abundance.
- B) Quantification of the RNF41-WT abundance relative to the β -actin control
- C) Co-expression of MAGEL2 increases RNF41-AE abundance.
- D) Quantification of the RNF-AE abundance relative to the β -actin control.
- E) Co-expression of MAGEL2 increases RNF41-SQ abundance.
- F) Quantification of the RNF-SQ abundance relative to the β -actin control.

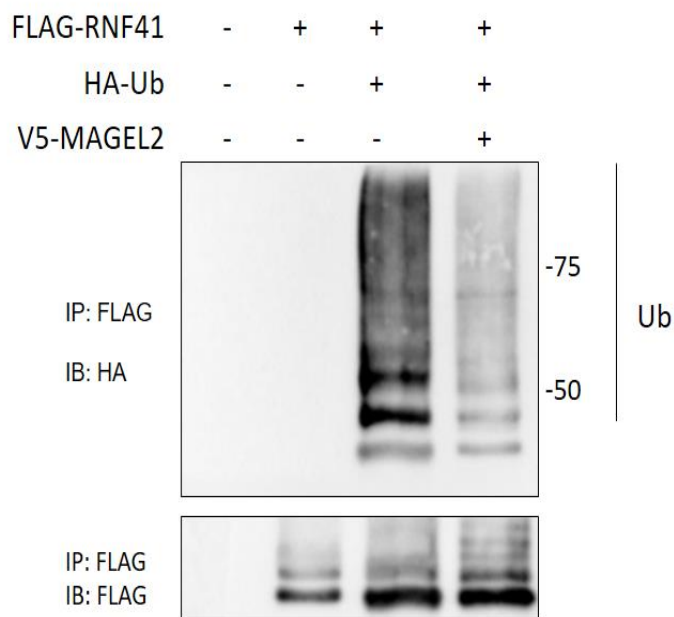
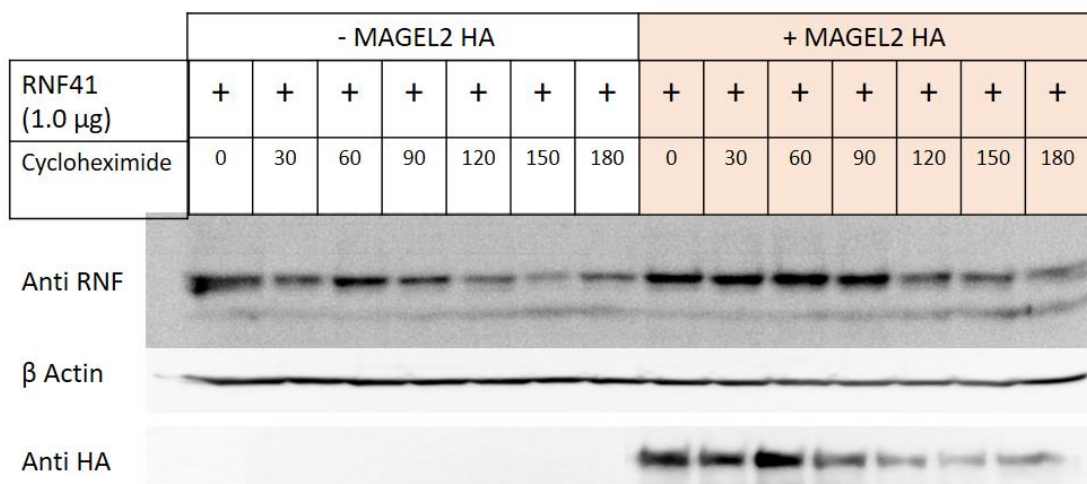


Figure 3.7 : MAGEL2 co-expression reduces the ubiquitination of RNF41.

HEK cells were co-transfected with FLAG-RNF41, HA-Ubiquitin and V5-MAGEL2. Cells were treated overnight with 5 μ M MG132 and 25 μ M chloroquine.

FLAG-RNF41 was immunoprecipitated and its ubiquitination status was assessed by immunoblotting against anti-HA.

A



B

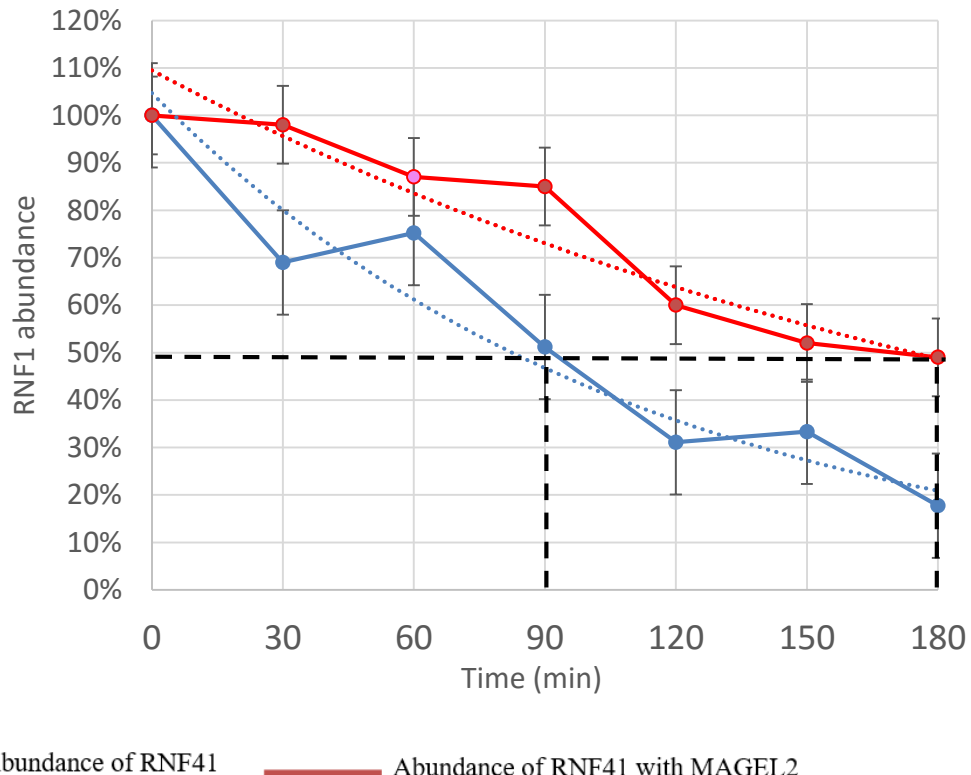


Figure 3.8 : Role of MAGEL2 in altering the stability of RNF41.

- A) In the presence of cycloheximide, degradation of RNF41 was slower when MAGEL2 was co-expressed.
- B) MAGEL2 co-expression doubled the half-life of RNF41 from 1.5 h to 3 h, indicating that MAGEL2 can stabilize RNF41 within the cells. (mean \pm SD of biological triplicates).

3.3 RNF41 and USP8 alter the abundance of MAGEL2.

I previously described the results of how MAGEL2 can influence the stability of RNF41 and USP8. Next I assessed whether the abundance of MAGEL2 changes with RNF41 and USP8 when they are co-transfected. I used all three forms of RNF41 and noted that MAGEL2 protein levels were significantly lower when co-expressed with RNF41-WT or RNF41-AE (Fig. 3.9A and Fig.3.9B). Surprisingly, MAGEL2 protein levels were higher when co-expressed with RNF41-SQ that lacks the E3 ligase activity. The destabilization of MAGEL2 by RNF41 depends on the activity of the RING domain. This suggest that the ability of RNF41 to destabilize MAGEL2 requires the ubiquitination activity (Fig. 3.9C). In contrast, to the change in USP8 abundance with MAGEL2, co-expression of USP8 significantly increased the abundance of MAGEL2 (Fig. 3.10A)

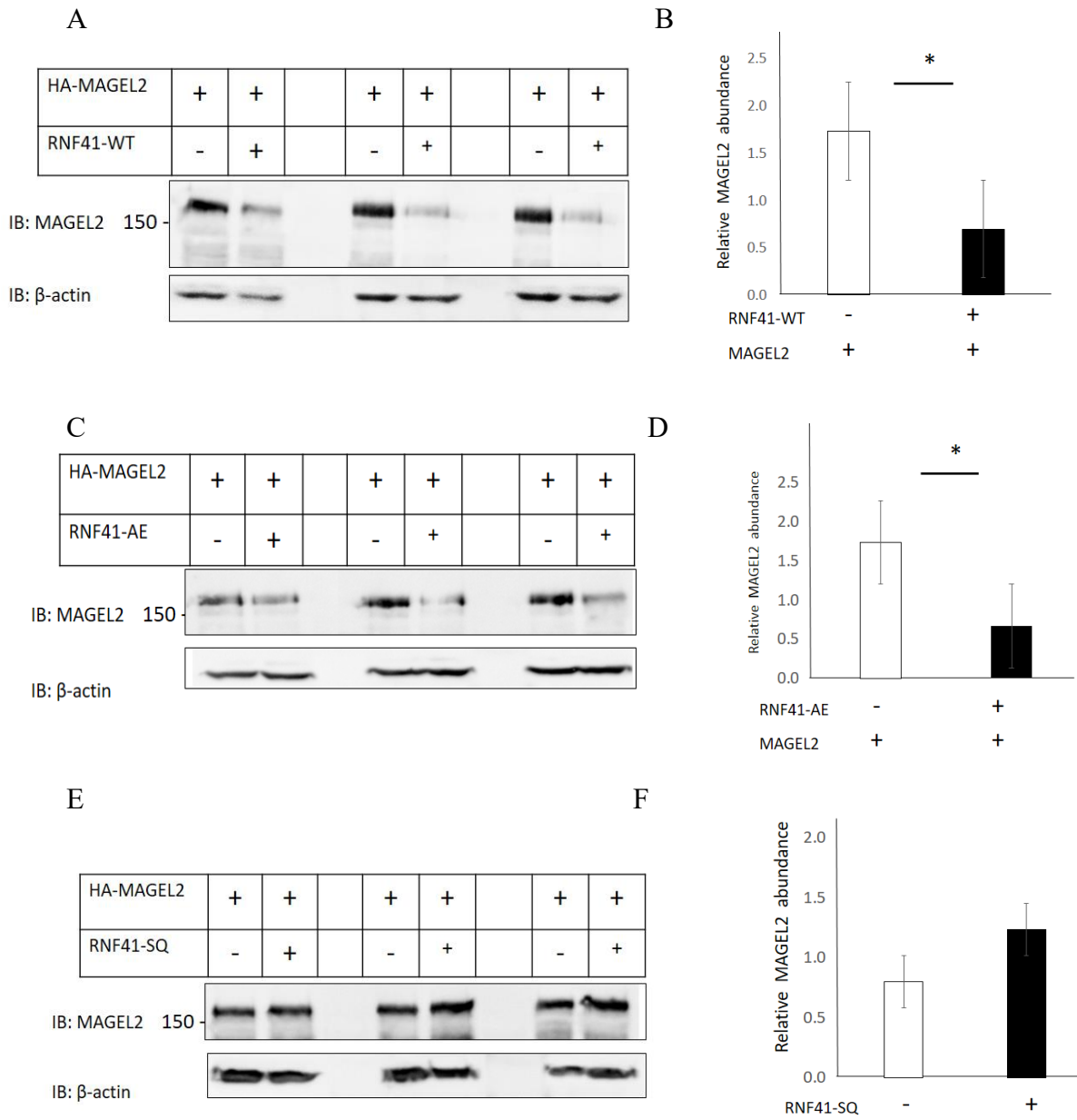


Figure 3.9 : Abundance of MAGEL2 with RNF41.

- A) Co-expression of RNF41-WT decreases MAGEL2 abundance.
- C) Co-expression of RNF-AE decreases MAGEL2 abundance.
- B), D) Quantification of the MAGEL2 abundance relative to the β -actin control. (mean \pm SD of biological triplicates). * P<0.05 different by student t-test
- E) Co-expression of RNF-SQ slightly increases MAGEL2 abundance, but not significantly.
- F) Quantification of the MAGEL2 abundance relative to the β -actin control. (mean \pm SD of biological triplicates)

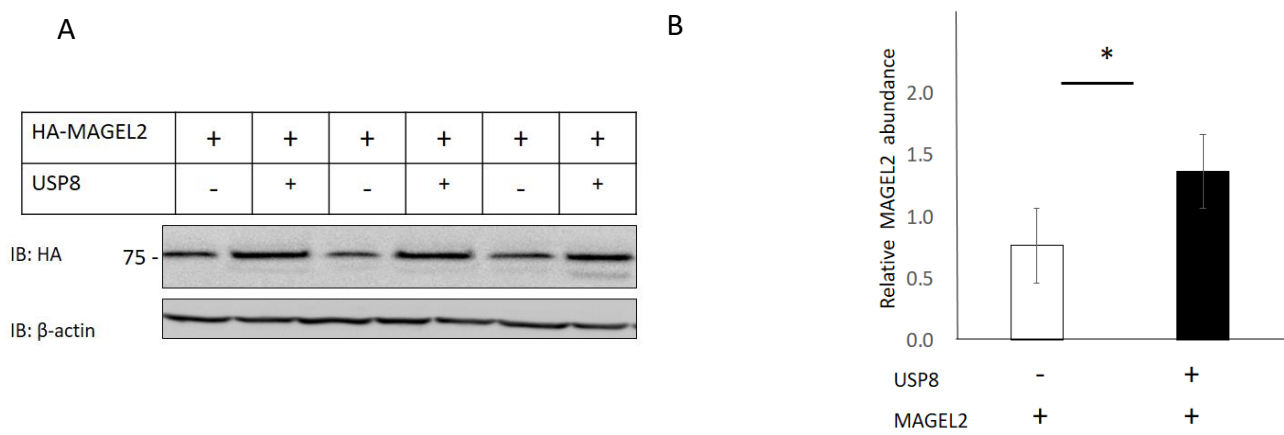


Figure 3.10 : Abundance of MAGEL2 with USP8.

A) Co-expression of USP8 increases the abundance of MAGEL2. Cell lysates were immunoblotted against anti-HA antibody.

B) Quantification of the MAGEL2 abundance relative to the β -actin control.

* P<0.05 different by student t-test

3.4 Mutations that disrupt the MHD of MAGEL2 disrupt the mutual effects of co-expression on stability.

MAGE proteins bind to E3 ligases through their conserved domain, which is the MAGE homology domain (MHD). To assess whether mutations in the MHD may change the results compared to wildtype MAGEL2, I used two different MAGEL2 mutant forms that have mutations in the conserved MHD and, that were already available in the laboratory. These mutant forms have similarities to the mutations found in the MHD of either MAGED2 or MAGEG1 and they produce a protein that ~70 kDa in size similar to the wild-type MAGEL2. The localization of these mutations in the MAGEL2 gene was described in Chapter 1 (Fig. 1.3).

A pathogenic missense mutation in MAGED2 (p.R446C) was identified in a patient with antenatal kidney disease (Laghmani et al., 2016). The corresponding arginine in the MAGEL2 gene (R1187) is highly conserved among the mammalian MAGEL2 genes, and this mutation is bioinformatically predicted to be very deleterious. A second MAGEL2 mutation, p.LL1031AA, replaces a highly conserved dileucine motif with two alanines, analogous to an engineered mutation in the MAGEG1 protein that disrupts its ability to bind to NSE1 (Doyle et al., 2010). As MAGE proteins bind to E3 ligases through their MHD, I tested whether mutations in this conserved MHD alter the mutual effect on the abundance of MAGEL2 and RNF41.

As shown in Figure 3.6A, co-expression of MAGEL2 increased the level of RNF41. In contrast co-expression of the MAGEL2p.LL1031AA (Fig. 3.11A) or MAGEL2p.R1187C (Fig. 3.11B) reduced RNF41 levels. To determine if the abundance of MAGEL2 changes with RNF41-WT, I co-transfected the mutant forms of MAGEL2 with and without RNF41 separately. Even though the wildtype RNF41 reduces levels of MAGEL2 (Fig. 3.9A), co-expression of RNF41 increased the levels of MAGEL2p.LL1031AA (Fig. 3.11D) or MAGEL2p.R1187C (Fig. 3.11E). As the two mutant forms, have point mutations in the MHD, these contrasting results suggest that defects in the MHD of MAGEL2 interfere with the mutual effect of RNF41 and MAGEL2 on each other's stability.

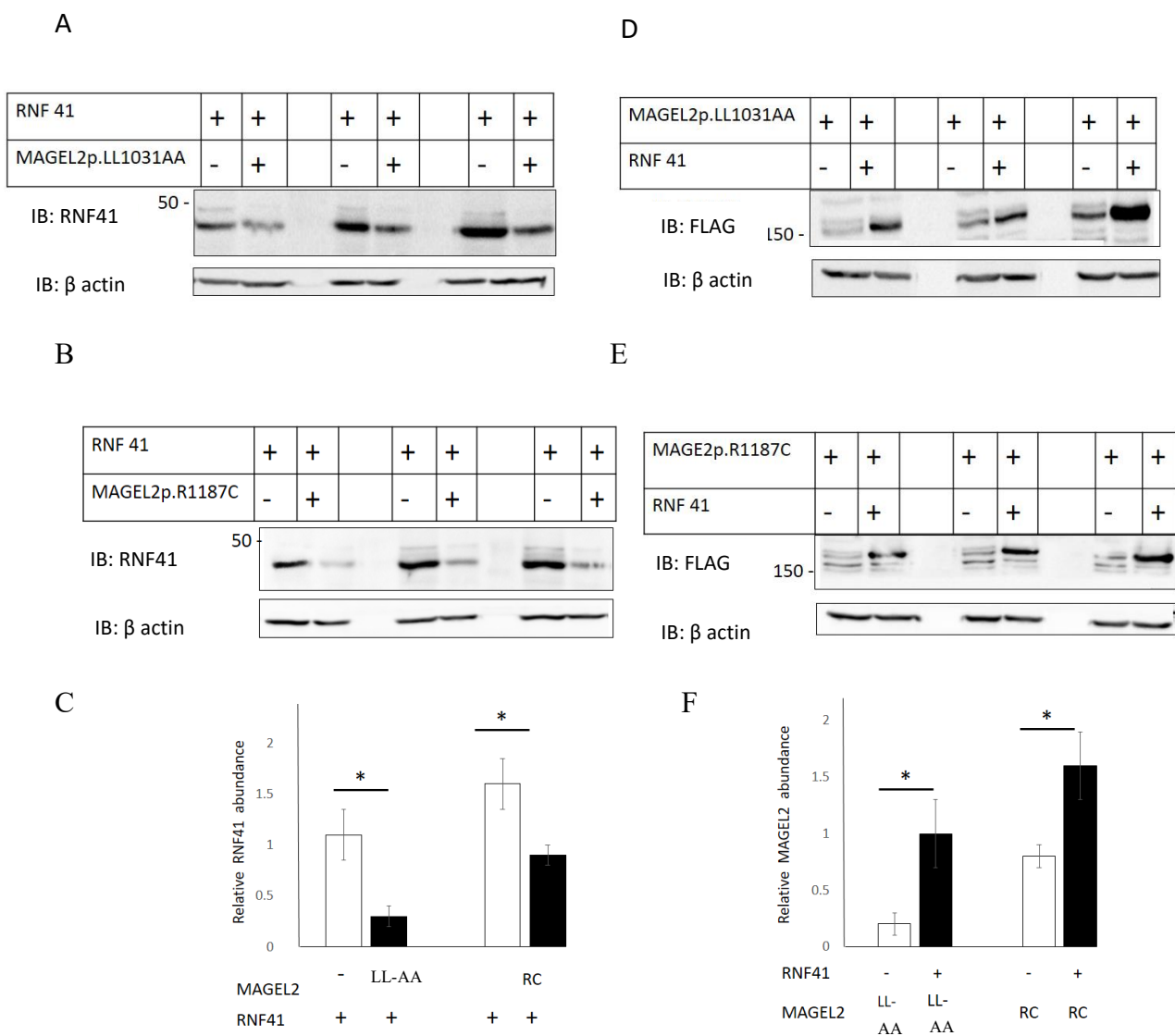


Figure 3.11 : Mutations that disrupt the MHD of MAGEL2 disrupt the mutual effects of co-expression on stability.

- A) Co-expression of the MAGEL2p.LL1031AA reduced RNF41 levels.
- B) Co-expression of the MAGEL2p.R1187C reduced RNF41 levels.
- C) Quantification of the RNF41 abundance relative to the β -actin control. (mean \pm SD of biological triplicates). * P<0.05 different by student t-test.
- D) Co-expression of RNF41 increased the level of MAGEL2p.LL103 1AA.
- E) Co-expression of RNF41 increased the levels of MAGEL2p.R1187C.
- F) Quantification of the MAGEL2 abundance relative to the β -actin control. (mean \pm SD of biological triplicates). * P<0.05 different by student t-test

3.5 MAGEL2 regulates the subcellular localization of RNF41, USP8 and the leptin receptor.

To understand whether MAGEL2 affects the subcellular localization of the other proteins such as RNF41 and USP8 that are involved in the leptin receptor trafficking and recycling, I performed an immunofluorescence assay. Before looking at the changes in the localization when these proteins were co-transfected, I looked at their normal distribution when they are singly transfected. MAGEL2 showed a diffuse pattern throughout the cytoplasm, with a minor proportion of the protein present in the nucleus in cultured U2OS cells (examples shown in Fig.3.12A) RNF41 showed a dispersed punctate pattern throughout the cytoplasm, with a proportion of the recombinant protein in a perinuclear location in cells (Fig.3.12B). Even though MAGEL2 and RNF41 are spread throughout the cytoplasm, both proteins were relocalized to perinuclear structures when they are co-transfected. The proteins were co-localized with each other as seen by the yellow signals in the cells (Fig. 3.13A). Co-expression of USP8-interacting proteins can alter its subcellular localization (De Ceuninck et al., 2013). Since RNF41 and MAGEL2 interacts with USP8, these different results might be due to an involvement of the endogenous USP8 levels. USP8 is located diffusely throughout the cytoplasm with some protein located at the plasma membrane and in punctate, perinuclear vesicles (Fig.3.14A). USP8 and RNF41 co-localize, and co-expression relocalizes both proteins to perinuclear structures when they are co-transfected. Consistent with previous results (De Ceuninck et al.,2013), co-expression of RNF41 relocalized USP8 from a diffuse cytoplasmic location to large intracellular vesicles (Fig. 3.14B). When MAGEL2 was co-transfected with RNF41 and USP8, this relocalization was no longer seen. Instead of the relocalization of USP8 in vesicles with RNF41, USP8 showed a more diffused pattern throughout the cytoplasm when co-transfected with MAGEL2 (Fig. 3.14C). This change in the localization pattern occurs from MAGEL2 expression. It appears that MAGEL2 reverses the stabilizing effect of USP8 on RNF41 and reverses the ability of RNF41 to relocalize USP8 to intracellular vesicles.

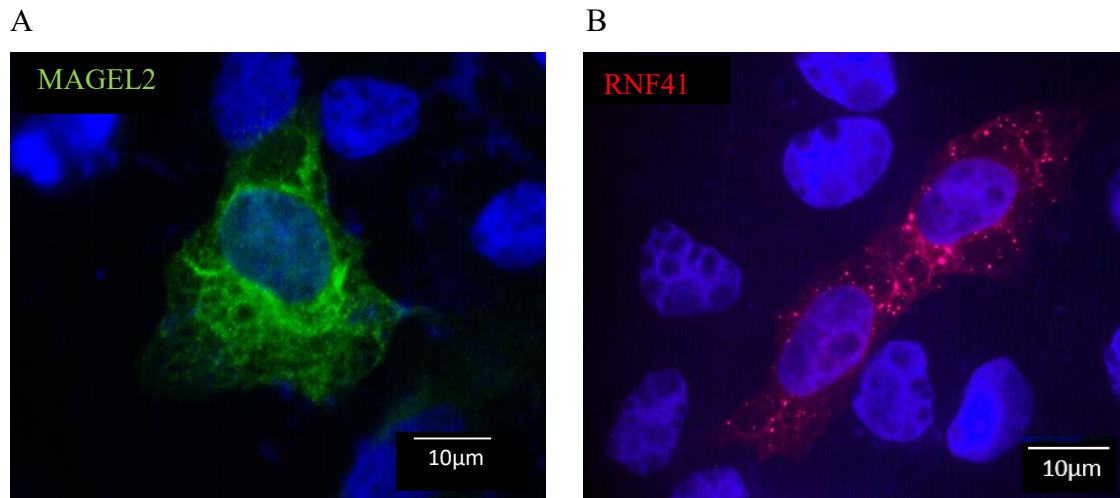


Figure 3.12 : Subcellular localization of MAGEL2 and RNF41.

U2OS cells were transfected with plasmids encoding epitope tagged HA-MAGEL2 and RNF41. Cells were fixed and stained against primary rabbit anti-HA and rabbit anti-RNF41 antibodies, and secondary Goat anti-Rabbit Alexa Fluor 488 and Alexa Fluor 594 antibodies.

- A) MAGEL2 has a diffused pattern throughout the cytoplasm (green)
- B) RNF41 has a dispersed punctate pattern throughout the cytoplasm (red)
nuclei were stained with Hoescht (blue)

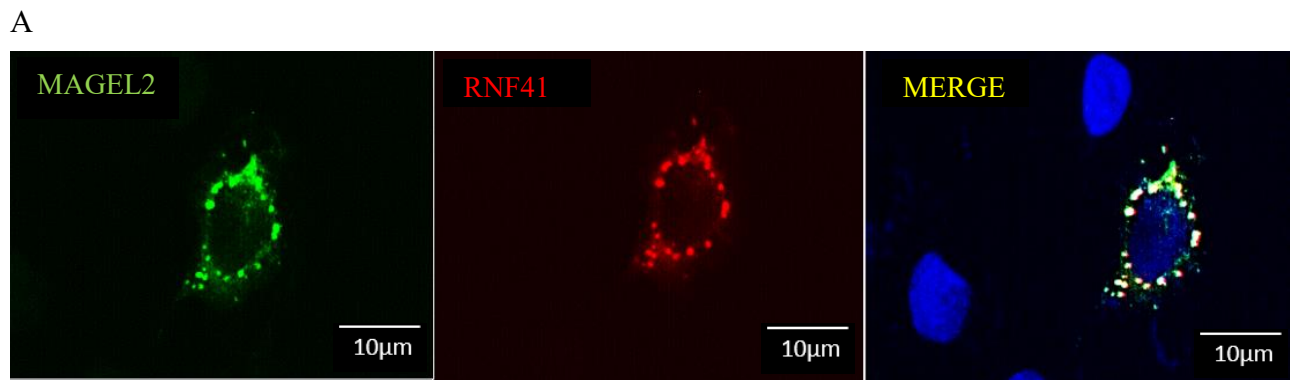


Figure 3.13 : Change in subcellular localization of MAGEL2 with RNF41.

Proteins were co-localized with each other, as indicated by the yellow signals in the cells and both proteins were relocalized to perinuclear structures when they are co-transfected. (MAGEL2-green, RNF41- red, nuclei were stained with Hoescht (blue)

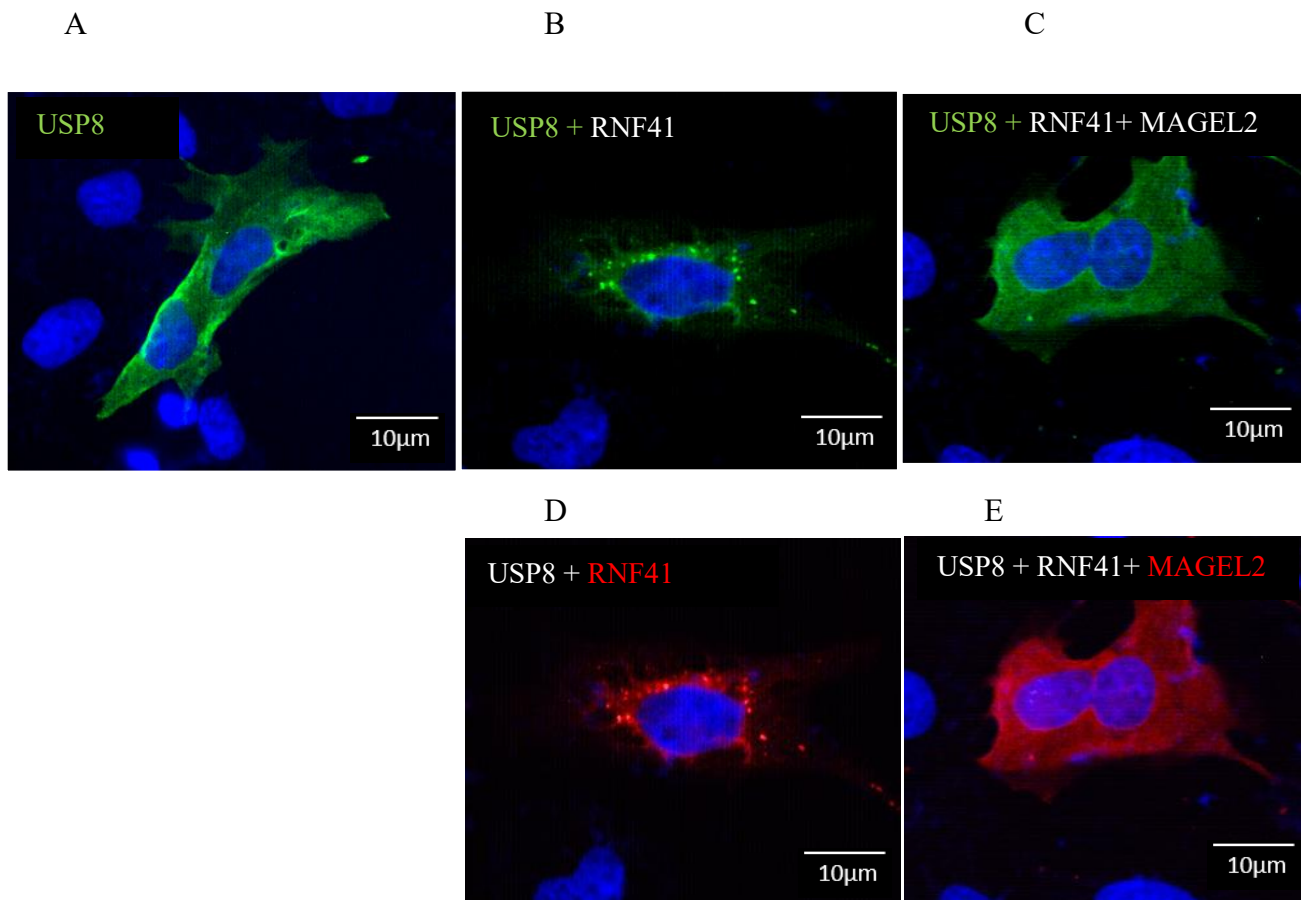


Figure 3.14 : Expression of HA-MAGEL2 reverses the stabilizing effect of USP8 on RNF41.

Cells were fixed with 4% PFA and stained against primary anti-USP8, anti-RNF41 and anti-HA primary antibodies and secondary Goat anti-Rabbit Alexa Fluor 488, Alexa Fluor 594 antibodies. Nuclei were stained with Hoescht (blue)

- A) USP8 was singly transfected and localized diffusely throughout the cytoplasm.
- B) USP8 was co-transfected with RNF41. This relocalized USP8 from a diffuse cytoplasmic location to large intracellular vesicles.
- C) USP8 was co-transfected with both RNF41 and MAGEL2. Instead of the relocalization of USP8 in vesicles with RNF41, USP8 showed a more diffused pattern throughout the cytoplasm when co-transfected with MAGEL2.
- D) Cells were stained against anti-RNF41 antibody to detect RNF41 expression (red).
- E) Cells were stained against anti-HA antibody to detect MAGEL2 expression (red).

To assess whether RNF41 and MAGEL2 regulate the trafficking of the leptin receptor, I performed immunofluorescence experiments. I examined the subcellular localization of the LepR in relation to early endosomes characterized by early marker EEA1 (Fig. 3.15). A portion of LepR accumulated on and co-localized with early endosomes. To assess if this LepR localization changes with the addition of other interacting proteins, I co-transfected LepR with RNF41, with MAGEL2 or with both RNF41 and MAGEL2. There was no change in the localization. A portion of the LepR was co-localized with the early endosomes indicating that after internalization of the LepR, it is transported to early endosomes independent from the other interacting proteins. Surprisingly, when LepR was co-transfected with RNF41 along with MAGEL2 or with MAGEL2 alone, a proportion of LepR was seen in the cell membrane, indicating that MAGEL2 has a role in recycling LepR back to the cell membrane (Fig. 3.15D).

Next to address the contribution of RNF41 and MAGEL2 in leptin receptor trafficking after internalization in a ligand-independent manner, I examined the subcellular localization of the LepR in relation to lysosomes characterized by late endosomal or lysosomal marker LAMP1 (Fig. 3.16). Another portion of LepR co-localizes with the lysosomal marker LAMP-1, which is evident from the yellow signals in the immunofluorescence. Surprisingly, when I co-transfected with RNF41, LepR did not colocalize with the lysosomes, but showed a more dispersed pattern. This disruption of co-localization by co-transfection with RNF41 was consistent with published evidence (Wauman and Tavernier, 2011). Interestingly, co-expression of both RNF41 and MAGEL2 or of MAGEL2 alone also showed similar results in which the co-localization of LepR with the lysosomal marker LAMP-1 was disrupted. This indicated that RNF41 and MAGEL2 might have a negative influence on LepR degradation as it was not localized with the lysosomes where degradation is initiated. This result is consistent with an important role for both RNF41 and MAGEL2 in the intracellular routing of LepR.

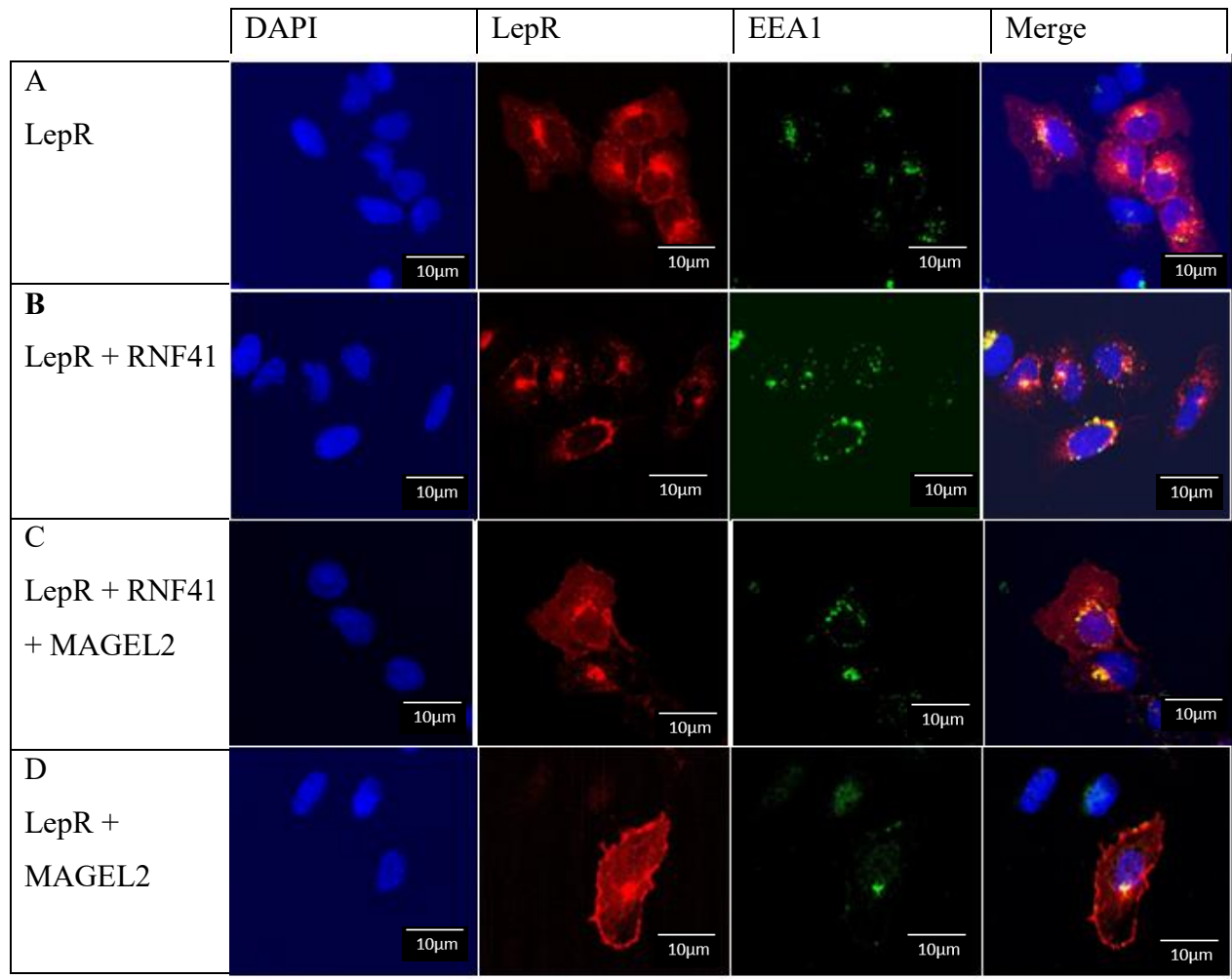


Figure 3.15: Change in subcellular localization of the LepR with other interacting proteins in relation to early endosomes labelled by antibody against EEA1.

(HA-LepR: red, EEA1: green, nuclei were stained with DAPI -blue)

- A) LepR was colocalized with the early endosomes.
- B) LepR co-localized with EEA1 after co-transflecting with RNF41.
- C) LepR co-localized with EEA1 after co-transflecting with both RNF41 and MAGEL2.
- A proportion of LepR was localized to the plasma membrane.
- D) LepR co-localized with EEA1 after co-transflecting with MAGEL2. LepR was localized more to the plasma membrane.

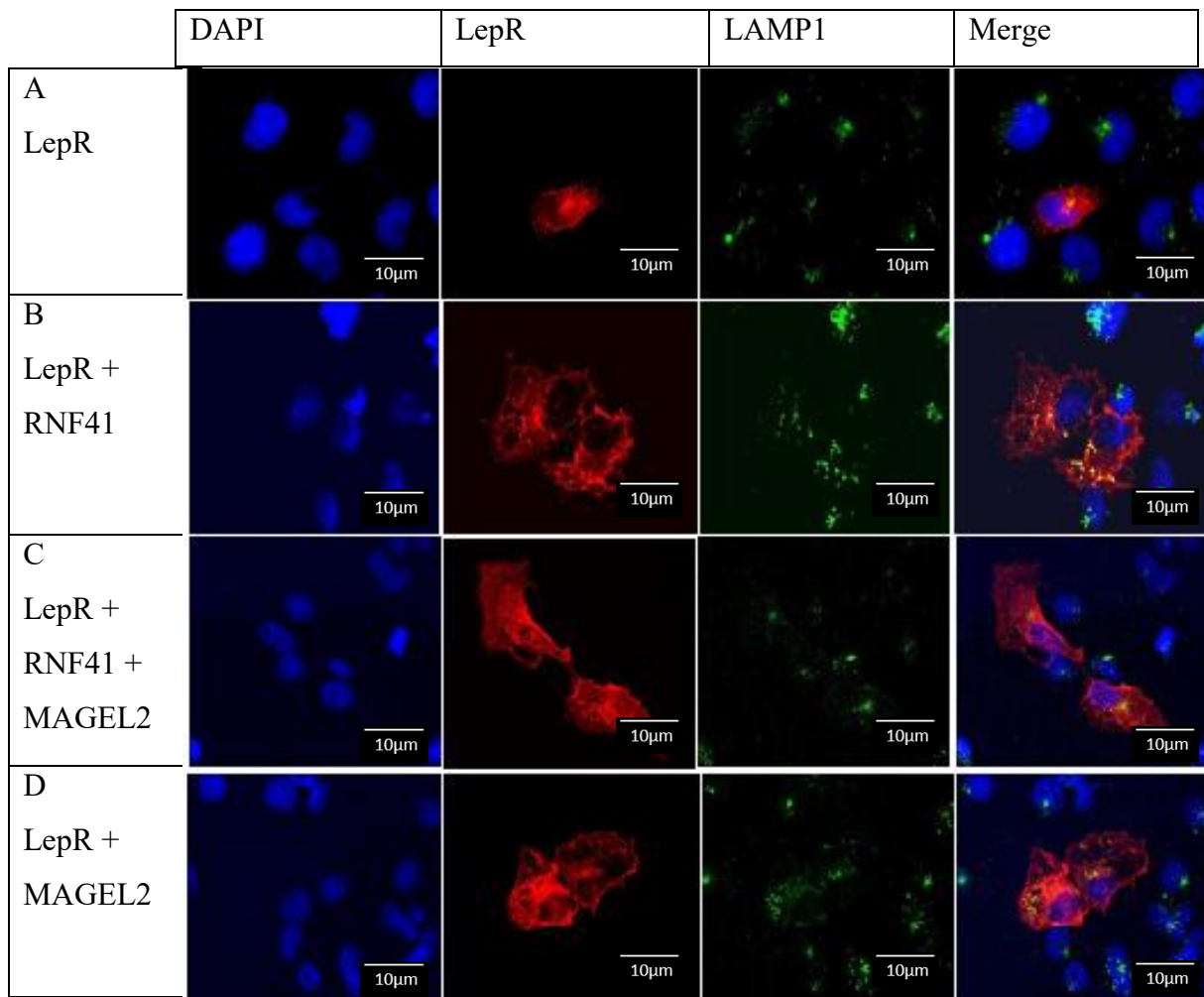


Figure 3.16 : Change in subcellular localization of the LepR with other interacting proteins in relation to late endosomes labelled by antibody against lysosomal marker LAMP1.

(HA-LepR: red, EEA1: green, nuclei were stained with DAPI -blue

- A) LepR was colocalized with lysosomes.
- B) LepR was not co-localized with LAMP1 after co-transfected with RNF41.
- C) LepR was not co-localized with LAMP1 after co-transfected with both RNF41 and MAGEL2, but a proportion of LepR was localized to the plasma membrane.
- D) LepR was not co-localized with LAMP1 after co-transfected with MAGEL2 but LepR was localized more towards the plasma membrane.

3.6 Abundance of LepR at the cell surface is sensitive to the presence of MAGEL2.

To determine whether the amount of LepR on the cell surface changes with the presence of MAGEL2 in a steady state, a cell surface biotinylation assay was performed. Cells were transfected with HA-LepR and co-transfected with MAGEL2. Next cells were surface labelled with Sulfo-NHS- SS-Biotin* in borate buffer. The biotinylated cell surface proteins were isolated using streptavidin precipitation, followed by immunoblotting using an anti-HA antibody to detect LepR. Comparison of protein levels in the cytosolic fraction (non-biotinylated protein) with the whole cell lysate (total protein amount) was used to calculate the percentage of LepR at cell surface. To verify membrane integrity during biotynaltion and to confirm that only surface proteins have been biotynalated, an anti- β actin antibody was used as a control for intracellular proteins to confirm that there was no actin in the biotinylated fraction (Fig.3.17).

$$\% \text{ Biotinylated} = \frac{\text{Total protein} - \text{non biotinylated protein}}{\text{Total protein}} \times 100\%$$

After analyzing the results, I observed that percentage of biotinylated LepR was significantly more when LepR is co-transfected with MAGEL2 than the level when LepR is transfected alone. There was an increase in the percentage of LepR in the cell surface with MAGEL2. This suggest that the abundance of LepR at the cell surface is sensitive to the presence of MAGEL2 and it indicated that MAGEL2 has a role in LepR trafficking in a steady state condition.

A

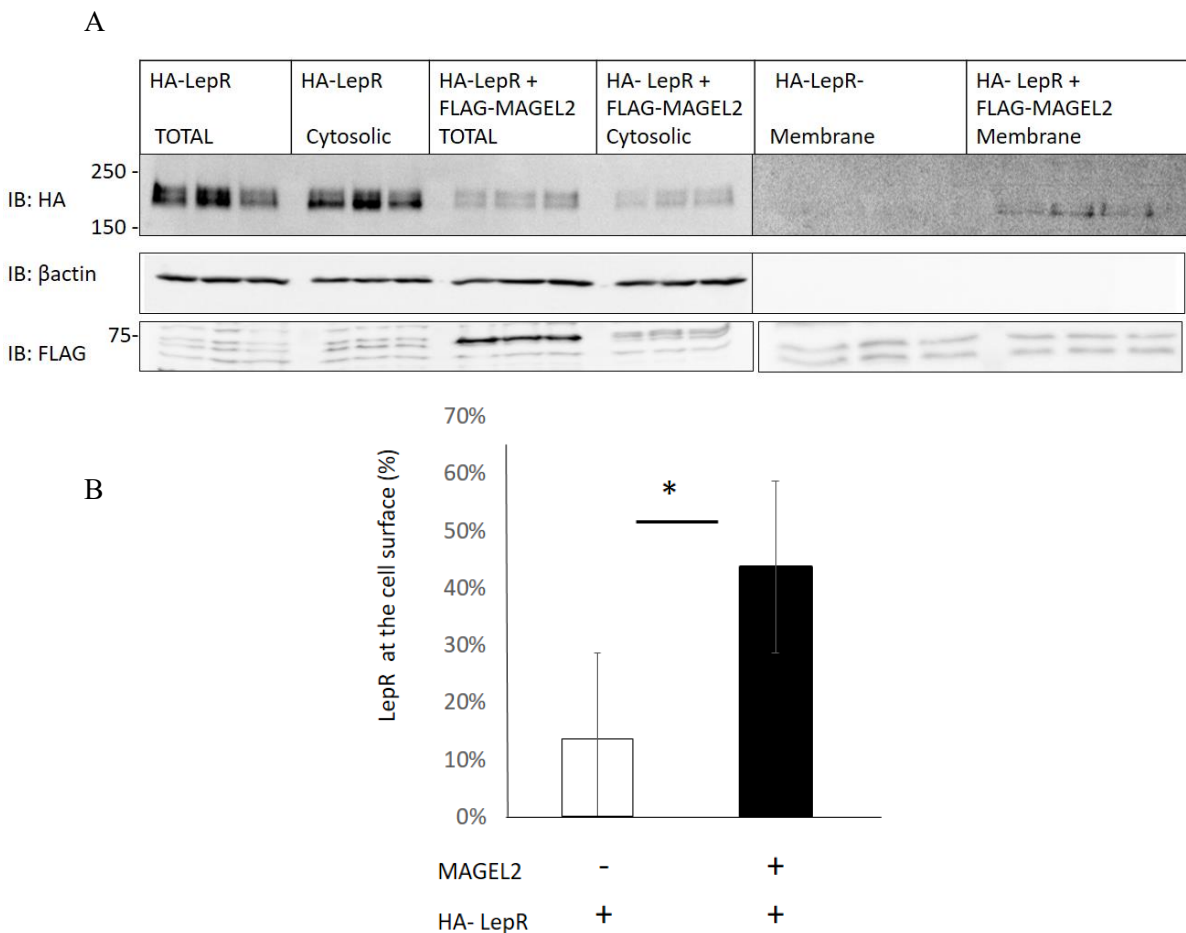


Figure 3.17: Abundance of LepR at the cell surface is sensitive to the presence of MAGEL2.

A) HEK cells were transfected with HA-LepR and co-transfected with FLAG-MAGEL2. Cell surface proteins were labeled with 1 mg/ml Sulfo-NHS- SS-Biotin. Protein in the cytosolic fraction and the whole cell lysate (total protein amount) were collected separately. The biotinylated cell surface proteins were isolated using streptavidin precipitation. Cell lysates were immunoblotted against anti-HA antibody to detect LepR.

B) Quantification of the percentage of LepR at the cell surface relative to the β-actin control.
mean ± SD, n=3, * P<0.05 student t-test

3.7 Lysosomal degradation of LepR (CTS formation) is prevented by RNF41 and MAGEL2

Rerouting of cytokine receptors such as LepR towards lysosomes for degradation or towards the cell membrane for recycling is regulated by RNF41 and USP8 (De Ceuninck et al., 2013). RNF41 blocks the formation of the LepR-CTS through a USP8-dependent mechanism that involves the destabilization of components of the ESCRT-0 complex (De Ceuninck et al., 2013). The decision to recycle LepR back to the plasma membrane or to direct them towards the lysosomes for degradation is largely a function of this ESCRT complex. When the LepR is targeted for lysosomal degradation, it can be detected by the formation of degradation products of the receptor. These degradation products of about 42 and 46 kDa are referred to as the C-terminal LR stubs (LepR-CTS). Chloroquine, which is an intra-lysosomal degradation inhibitor, was added to the cells 24 h after transfection to prevent further degradation of the CTS. To assess whether RNF41 or MAGEL2 has an effect on lysosomal degradation of LepR, I looked at the changes in the formation of LepR-CTS. I confirmed that expression of RNF41-WT prevents the formation of the LepR-CTS in cells treated with chloroquine (Fig. 3.18A) which was consistent with published evidence. To assess whether MAGEL2 has an influence in the LepR degradation, I co-transfected LepR with MAGEL2. Co-expression of MAGEL2 also reduced the formation of the LepR-CTS in the presence of chloroquine (Fig. 3.18B). A reduction in C-terminal stub (CTS) formation of LepR reflects reduced lysosomal degradation. From the above results, it was confirmed that RNF41 and MAGEL2 independently reduced lysosomal degradation of LepR.

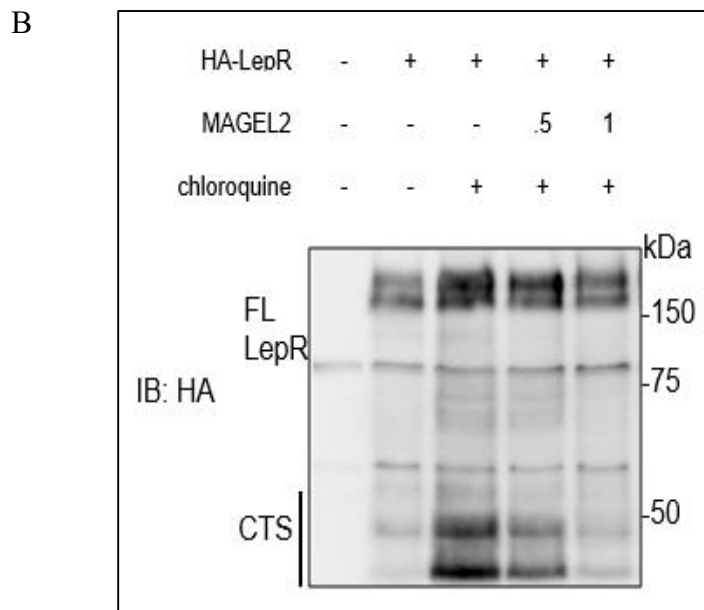
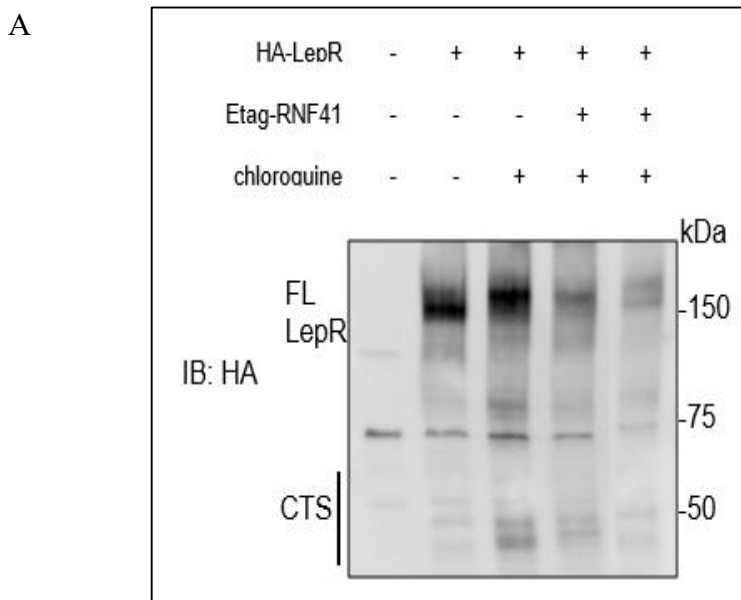


Figure 3.18 : Lysosomal degradation of LepR (CTS formation) is prevented by RNF41 and MAGEL2.

- A) Expression of RNF41 prevents the formation of the LepR CTS the presence of chloroquine.
- B) Expression of MAGEL2 reduced the formation of the LepR CTS in the presence of chloroquine. (CTS: C terminal stub, FL LepR: full length leptin receptor). (0.5 and 1 indicate the μ g of plasmid transfected).

To assess whether MAGEL2 has an effect on LepR degradation in the absence of chloroquine, I performed a cycloheximide assay. 24 h after transfection with HA-LepR alone or with both HA-LepR and MAGEL2, cells were treated with 40 µl of 5 mM cycloheximide to block *de novo* protein synthesis. The abundance of HA tagged LepR was measured every 30 min for 3 h after treatment. The abundance was monitored using immunoblotting with an anti-HA antibody. I detected that more than half of the total LepR was degraded at the end of 3 h, whereas LepR that was co-transfected with MAGEL2 degraded less than half of the starting LepR protein level. Also, co-expression of MAGEL2 increased the abundance of the LepR, in the absence of chloroquine, and increased the half-life of LepR from 87 min to 138 min (Fig. 3.19). This indicated that MAGEL2 can stabilize LepR within the cells and prevent it from degradation.

As explained previously, the decision of recycling LepR back to the plasma membrane or to direct them towards the lysosomes for degradation is largely a function of the ESCRT-0 complex. This complex consists of Hrs, STAM1 and STAM2 (also known as Hrs-binding protein). It has been previously published that heterologous expression of RNF41 destabilizes Hrs, STAM1 and STAM2 (De Ceuninck et al., 2013). I looked at the stabilization of the components of the ESCRT complex by MAGEL2. Interestingly, I found that heterologous expression of MAGEL2 also destabilized endogenous STAM1 in cultured cells, consistent with its role as an adapter protein for RNF41 activity (Fig. 3.20).

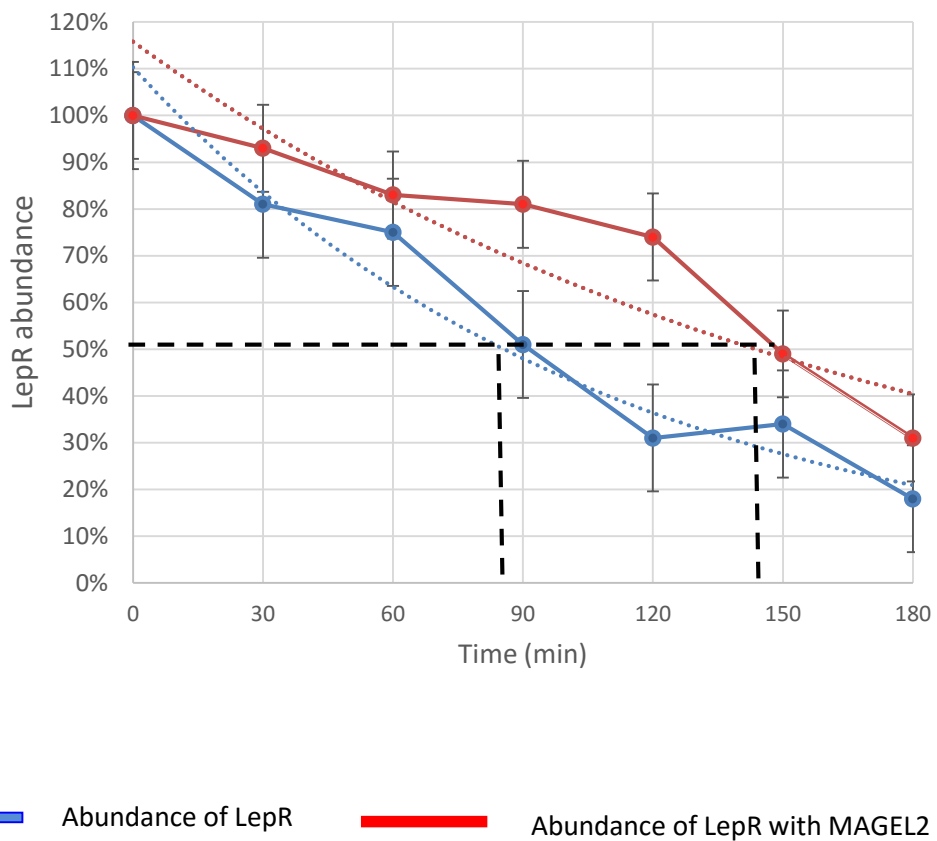
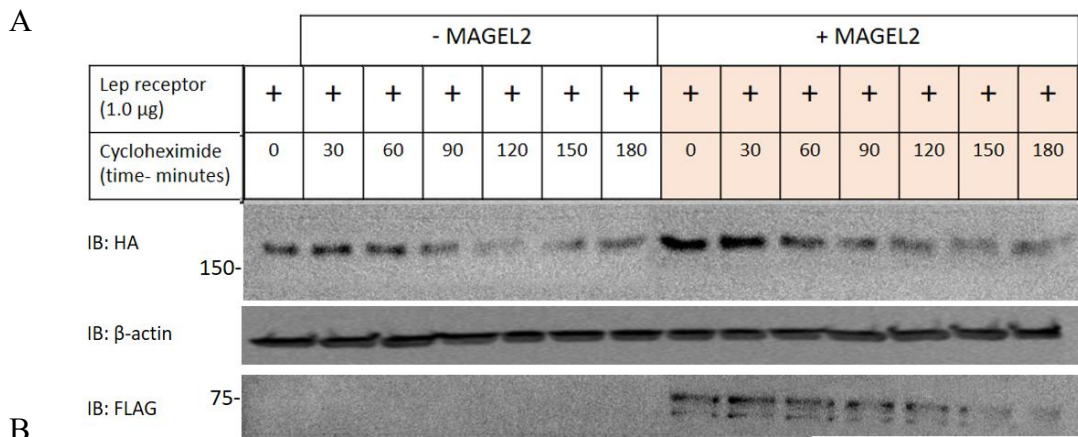
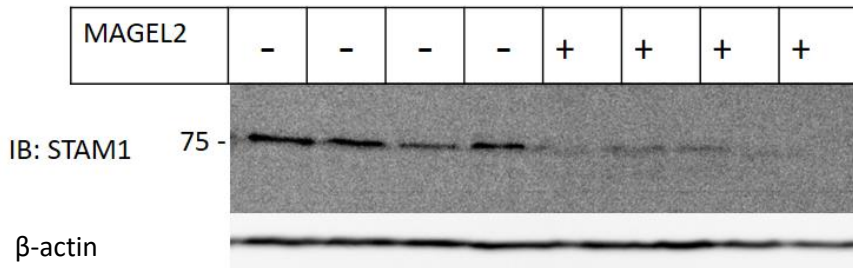


Figure 3.19 : Role of MAGEL2 in altering the stability of LepR.

- A) In the presence of cycloheximide, degradation of LepR was slower when MAGEL2 was co-expressed.
- B) MAGEL2 co-expression increased the half-life of RNF41 from 90 min to 140 min, indicating that MAGEL2 can stabilize LepR within the cells.

A



B

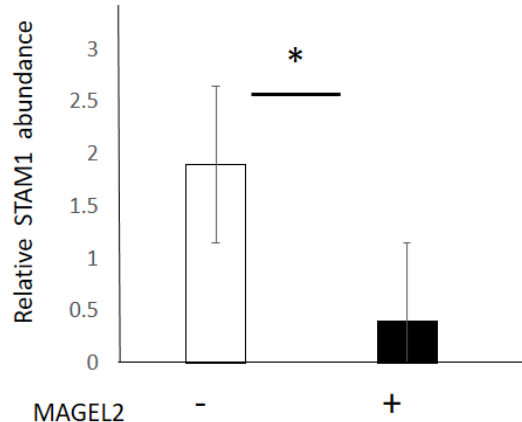


Figure 3.20 : Abundance of STAM1 with MAGEL2.

HEK cells were transfected with MAGEL2 and cell lysates were immunoblotted against rabbit anti-STAM1 primary antibody to detect the endogenous STAM1 levels.

A) Co-expression of MAGEL2 significantly decreased the abundance of STAM1.

B) Quantification of the STAM1 abundance relative to the β -actin control. (* P<0.05, Student t-test of biological quadruplicate, mean \pm SD)

3.8 Endogenous levels of murine Rnf41, Usp8, Stam1, LepR and neclin are altered in the brain of mice with a loss of function of *Magel2*.

Previous results were all generated by using cultured cell lines. Over-expression of MAGEL2 decreased the abundance of USP8 and increased the abundance of RNF41 in co-transfected cells (Fig. 3.5, Fig. 3.6A). To compare these results with the situation *in vivo*, I used *Magel2*-null mice and wildtype mice. I compared protein expression by analyzing the brain tissue, specifically hypothalamus and cortex samples.

It was predicted that inactivation of the *Magel2* gene would result in higher levels of Usp8 and lower levels of Rnf41 protein in tissues in *Magel2*-null mice. I prepared protein lysates from hypothalamus and cortex samples of wild-type and *Magel2*-null mice and compared the Rnf41 and Usp8 levels. As predicted, there was more Usp8 (Fig.3.21A) (hypothalamus) and less Rnf41 (Fig.3.21C, E) (hypothalamus and cortex) in brain protein lysates from *Magel2*-null mice. This suggests that *in vivo*, *Magel2* stabilizes Rnf41 and destabilizes Usp8.

To assess the changes in the stability of the ESCRT complex, I looked at Stam1 levels of hypothalamus and cortex samples in both *Magel2* null and wild type mice. Consistent with the results of the cultured cells where heterologous expression of MAGEL2 destabilized endogenous STAM1, there was increased levels of Stam1 in both hypothalamus and cortex samples from *Magel2* null mice compared to the wildtype mice (Fig.3.22A, C).

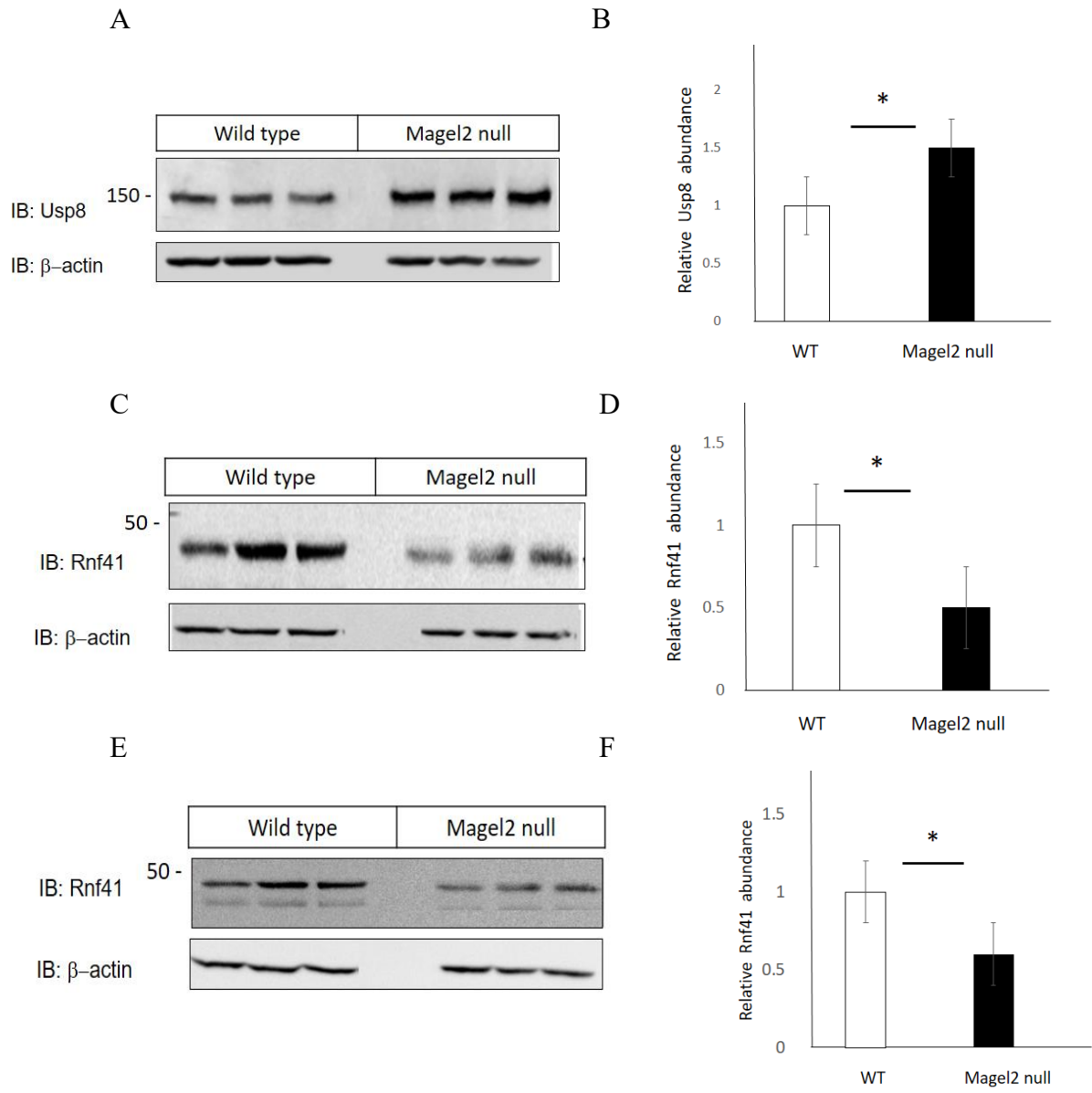


Figure 3.21 : Endogenous levels of murine Rnf41 and Usp8 are altered in the brain of mice with a loss of function of *Magel2*.

- A) Usp8 levels were higher in hypothalamus from *Magel2*-null mice.
- B) Quantification of the Usp8 level relative to the β -actin control. (mean \pm SD, n=3, * P<0.05 student t-test)
- C) Rnf41 levels were lower in hypothalamus from *Magel2*-null mice.
- E) Rnf41 levels were lower in cortex from *Magel2*-null mice.
- D) and F) Quantification of the Rnf41 level relative to the β -actin control. (mean \pm SD, n=3, * P<0.05 student t-test)

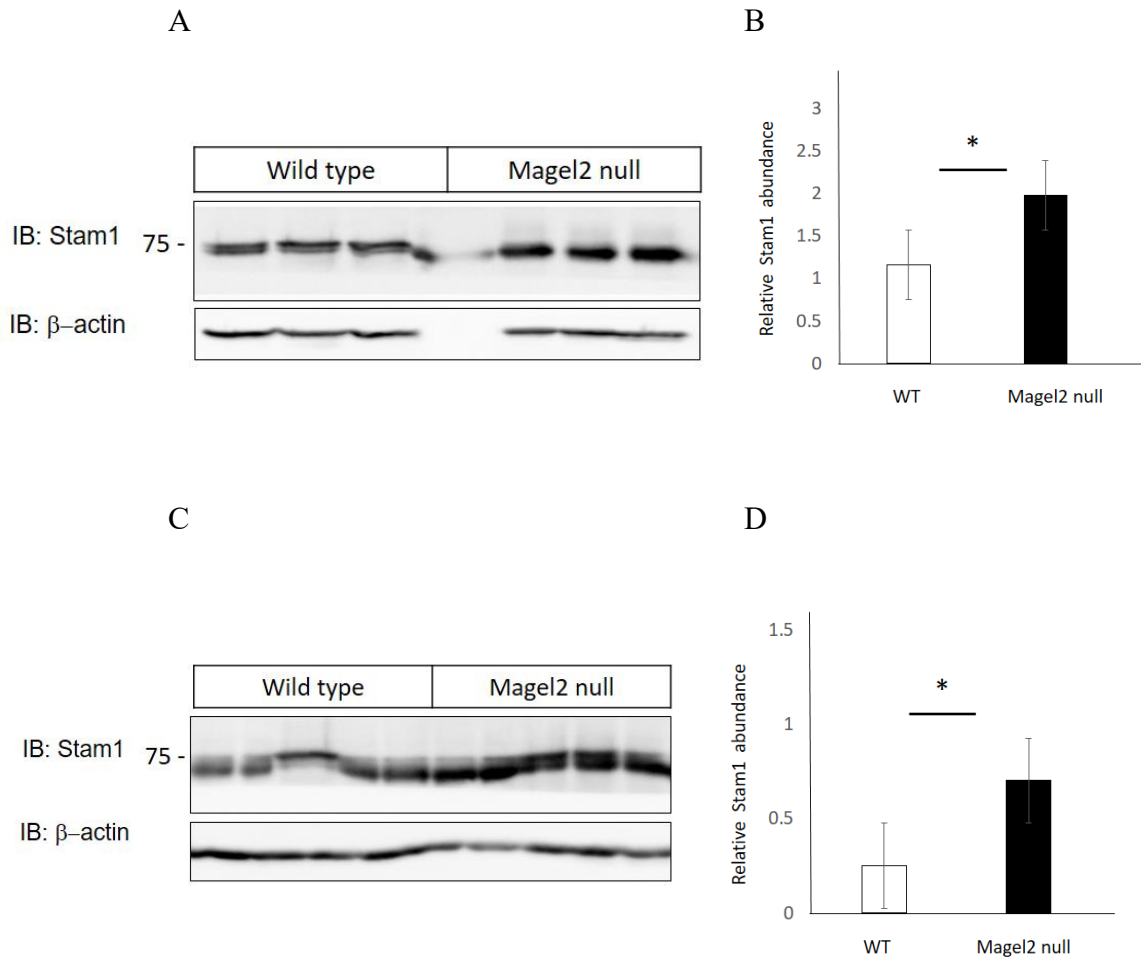


Figure 3.22 : Endogenous levels of murine Stam1 are altered in the brain of mice with a loss of function of *Magel2*.

- A) Stam1 levels were higher in hypothalamus from *Magel2*-null mice than wild type.
- B) Quantification of the Stam1 level relative to the β -actin control. (mean \pm SD, n=3, * P<0.05 student t-test)
- C) Stam1 levels were higher in cortex from *Magel2*-null mice than wild type.
- D) Quantification of the Stam1 level relative to the β -actin. (mean \pm SD, n=3, * P<0.05 student t-test)

I previously described that co-expression of MAGEL2 increased the abundance and half-life of LepR in co-transfected cells (Fig. 3.19). From this result, I predicted that there will be less LepR in *Magel2*-null mice than the wild type. To assess this, I used an anti-LepR antibody that detects the endogenous LepR levels in *Magel2*-null and wild type brain samples. The prediction was confirmed by immunoblot analysis as there was less LepR level in the hypothalamus of *Magel2*-null mice compared to wild-type littermates (Fig.3.23A). However, there was no difference in the abundance of the LepR in the cortex of *Magel2*-null mice compared to wild-type littermates (Fig.3.23C). Interactions and regulatory mechanisms involve in LepR trafficking among these proteins are far more complicated than expected. There are likely compensatory effects that impact the balance given the ability of different proteins to alter each other's abundance.

As NDN is another gene that is inactivated in the PWS region, I wanted to assess whether loss of *Magel2* could affect the abundance of necdin, which is also a part of the RNF41:USP8:MAGEL2 complex. Published evidence showed that the expression of the murine NDN gene is increased in the adult hypothalamus of *Magel2*-null mice (Kozlov et al., 2007). Recently our laboratory found out that necdin expression is increased 1.4-fold in RNA from *Magel2*-null adult cortex samples, and is the most significantly dysregulated gene in *Magel2*-null brain samples. This experiment used RNAseq to measure gene expression levels of adult cortex. Surprisingly, I detected that there were reduced levels of necdin protein in the brain tissues (cortex and hypothalamus) of *Magel2*-null mice compared to their wild type littermates (Fig. 3.24 A,C). From the BioID experiments I showed that necdin and MAGEL2 interact with each other. Therefore, from these contrasting results I suggest that these two MAGE proteins not only interact with each other but also regulate each other's abundance. Also, the increased RNA expression of necdin could be a result of a compensatory up-regulation relative to the instability of the necdin protein in the absence of *Magel2*.

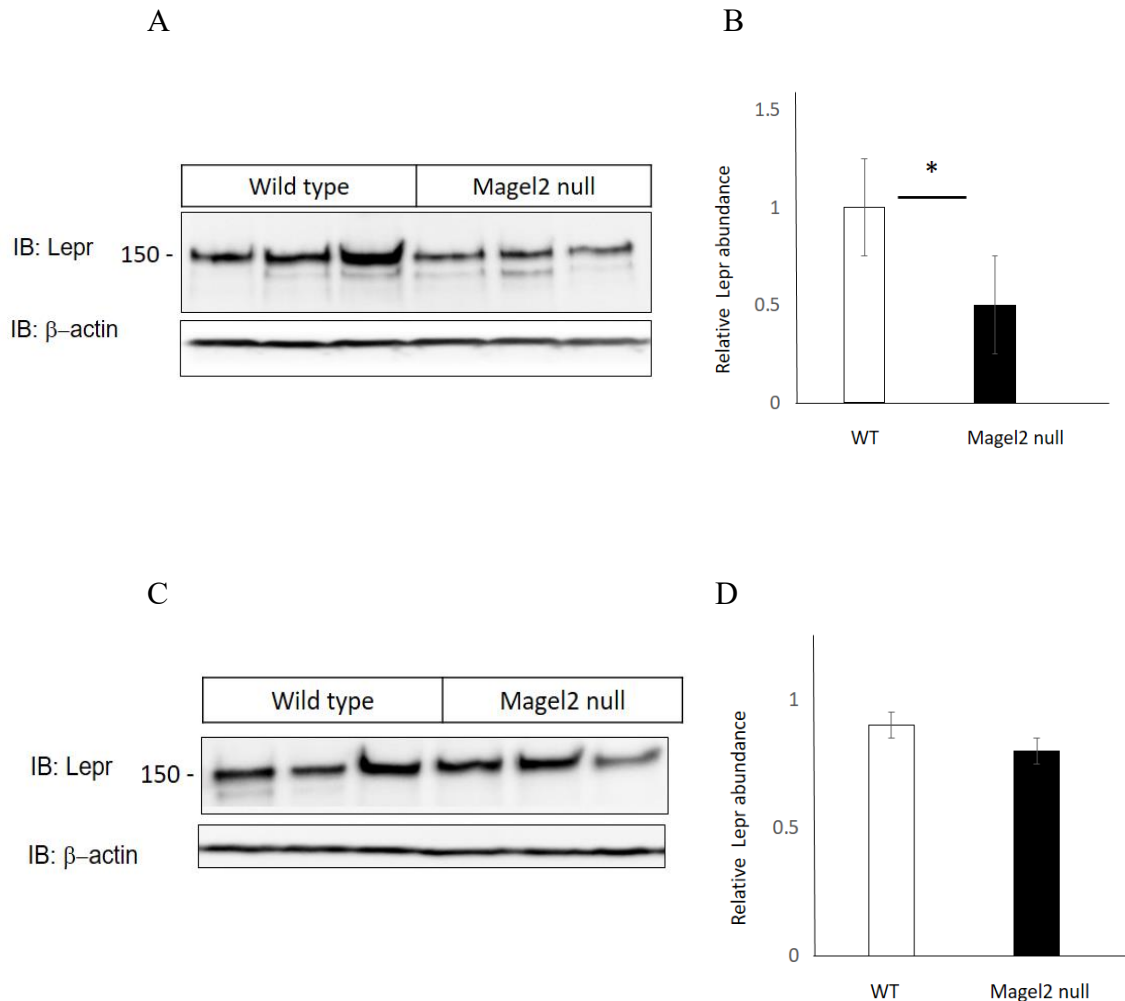


Figure 3.23 : Endogenous levels of murine Lepr is altered in the brain of mice with a loss of function of *Magel2*.

- A) Lepr levels were higher in hypothalamus from *Magel2*-null mice than wild type.
- B) Quantification of the Lepr level relative to the β -actin control. (mean \pm SD, n=3, * P<0.05 student t-test)
- C) No difference in Lepr levels in cortex from *Magel2*-null mice and wild type.
- D) Quantification of the Lepr level relative to the β -actin. (mean \pm SD, n=3, * P<0.05 student t-test)

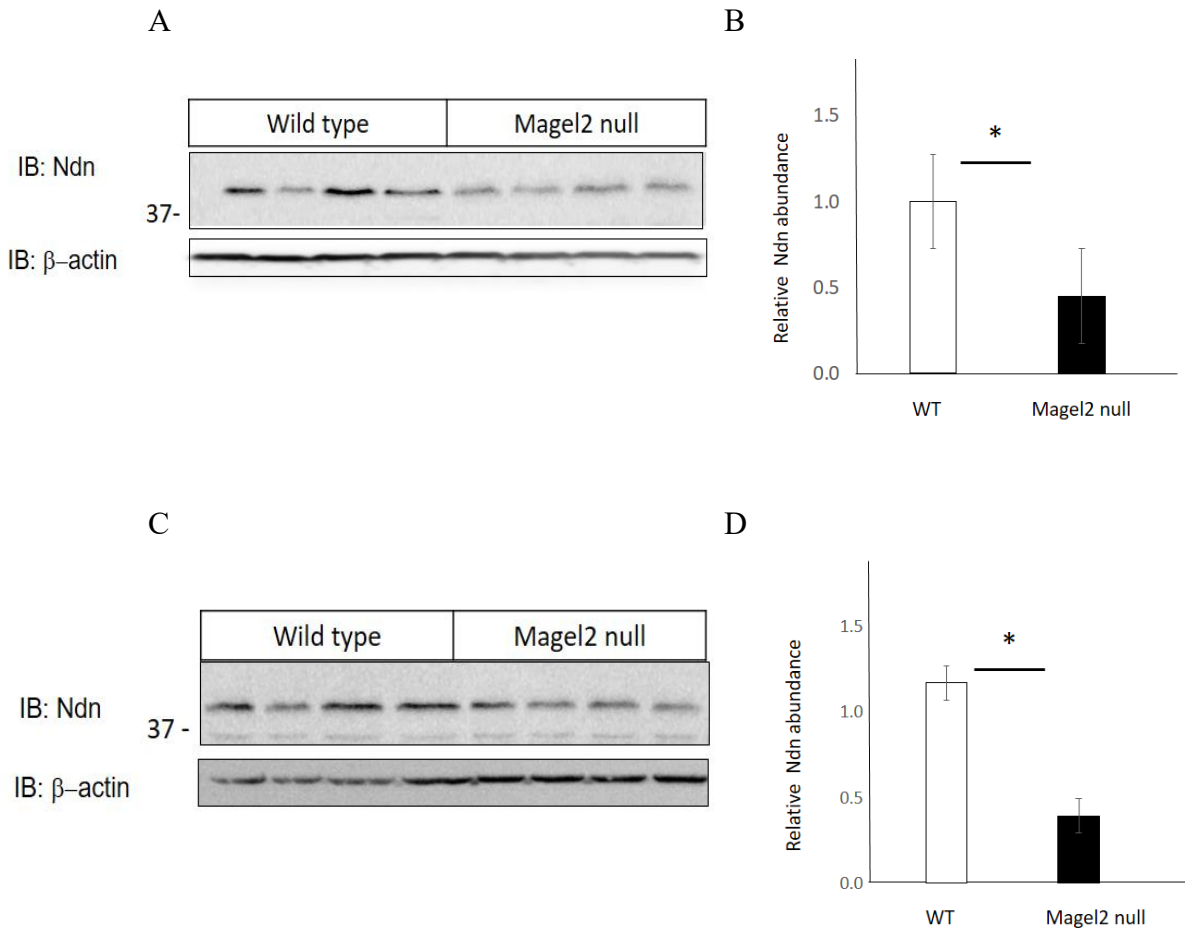


Figure 3.24 : Endogenous levels of murine necdin is altered in the brain of mice with a loss of function of *Magel2*.

- A) Necdin levels were lower in hypothalamus from *Magel2*-null mice than wild type.
- C) Necdin levels were lower in cortex from *Magel2*-null mice than wild type.
- B) and D) Quantification of the necdin level relative to the β -actin. (mean \pm SD, n=4, * P<0.05 student t-test)

Chapter 4 :Discussion

I hypothesized that MAGEL2 modifies the activity of RNF41-USP8 ubiquitination complex and modifies the regulation of intracellular sorting of leptin receptor. Therefore, loss of *MAGEL2* may contribute to obesity in PWS because it acts as an adaptor protein by bridging the leptin receptor to the ubiquitination complex RNF41- USP8. To support this hypothesis, I had to address several questions. Is there a relationship between MAGEL2 and leptin receptor associated proteins like RNF41 and USP8? Does MAGEL2 change the stability of the USP8-RNF41 complex? Does MAGEL2 bridge the leptin receptor with RNF41-USP8 complex? Does MAGEL2 modify the processing or degradation of the leptin receptors? Does MAGEL2 regulate the subcellular localization of leptin receptor, RNF41 and USP8? Does loss of *Magel2* alter the Rnf41-Usp8 -leptin receptor system in mice?

First to determine if MAGEL2 and necdin have a relationship with leptin receptor associated proteins such as USP8 and RNF41, I performed abundance experiments and BioID experiments. I found that MAGEL2 interacts strongly with necdin since necdin was biotinylated by BirA-MAGEL2 (Fig 3.1). To confirm this result I used BirA-necdin as the bait and MAGEL2 as the prey protein and got similar results (Fig 3.2). As both these proteins are members of the MAGE family of proteins that are inactivated in the PWS region, the interaction between MAGEL2 and necdin might be important.

I was interested to find out whether MAGEL2 and necdin contribute to the regulation of LepR trafficking along with the other associated proteins. Our collaborators confirmed that necdin interacts with the LepR, and MAGEL2 alone did not interact with LepR using a different method called MAPPIT (Fig 1.12). The method and all the MAPPIT results have been summarized previously in Introduction. I got similar results using the BioID assay. LepR and MAGEL2 were biotinylated by necdin (Fig 3.2) but LepR was not biotinylated by MAGEL2 (Fig 3.1D). I performed an abundance assay and a protein stability assay using cycloheximide and confirmed that MAGEL2 increases the abundance of LepR levels (Fig 3.19).

For my next set of experiments, I performed BioID to find whether MAGEL2 and necdin bridge the leptin receptor with RNF41 and USP8. I could not detect the interaction of USP8 and RNF41 with necdin by BioID (Fig 3.2). This result was consistent with the MAPPIT findings,

where they found that necdin forms a weaker complex with USP8 and RNF41. Consistent with the MAPPIT results, I found that MAGEL2 interacts strongly with USP8 (Fig. 3.1 A,B) as do USP7, EID1 and TRIM27, proteins previously shown to interact with MAGEL2 (Hao et al., 2015). The interaction between MAGEL2 and RNF41 was shown to be weak from the MAPPIT assay. I could not detect any RNF41 protein expression from the BioID technique either (Fig 3.1B). Biotinylation of RNF41 by MAGEL2 could only be detected in the presence of co-transfected protein USP8 and LepR, which may indicate an indirect interaction between the two proteins (Fig.3.1C). As these results were confirmed by BioID, where protein-protein interactions are based on close proximity, the interaction between MAGEL2 and RNF41 might be dependent on USP8 or LepR. This suggest that MAGEL2-USP8, RNF41 and LepR might be in a complex where all proteins are regulated by each other.

To determine if USP8 and RNF41 regulate each other's abundance, I looked at the changes of USP8 abundance with RNF41 and vice versa. I detected less USP8 protein when RNF41 was co-transfected (Fig 3.3). These results were consistent with the published evidence that showed endogenous USP8 levels were reduced in cultured cells by RNF41 (De Ceuninck et al., 2013). Similar results were obtained by using the RNF-SQ mutant form. RNF-SQ harbors two point mutations in its ring finger domain that are predicted to disrupt its binding to E2 ubiquitin conjugating enzymes, thereby impairing E3 ubiquitin ligase activity. This revealed that the E3 ubiquitin ligase activity of RNF41 is important to reduce USP8 levels, suggesting that USP8 is a substrate of RNF41. Conversely, RNF41 AE mutant expression no longer lowered USP8 protein levels (Fig 3.3). As RNF-AE mutant form does not bind to USP8, the above result indicated that suppression of USP8 by RNF41 depends on direct interaction between RNF41 and USP8. But in contrast, in a recent publication revealed that RNF41-AE mutant enhances endogenous USP8 levels, although it hardly interacts with USP8. This might be due to endogenous RNF41 levels (De Ceuninck et al., 2013). To examine whether abundance of RNF41 changes with USP8, I co-transfected cells with all three forms of RNF41 along with USP8. I found an increase in all the RNF41 levels, indicating that USP8 stabilizes RNF41 (Fig 3.4). From these above abundance results along with the MAPPIT results, I suggest that RNF41 and USP8 interact with each other and that they regulate each other. Previous studies have demonstrated that USP8 interacts with and stabilizes RNF41 levels (De Ceuninck et al., 2013). When USP8 levels are low, the activity will in turn be lower. This will cause RNF41 to be auto-ubiquitinated efficiently and target the proteins

for degradation through proteasomes. This will result in low levels of the RNF41. High levels of functional USP8 leads to stabilization of RNF41 by deubiquitination (Wu et al., 2004). Similar results were published regarding the stability of RNF41 protein levels by USP8 (Cao et al., 2007).

Conversely, RNF41 enhances USP8 ubiquitylation and in turn destabilizes USP8 (De Ceuninck et al., 2013). They showed that USP8 is a ubiquitination substrate of RNF41 and that USP8 physically interacts with RNF41. It was shown that RNF41 no longer interacts with USP8 when the specific binding site was mutated (Wu et al., 2004). From these above results, it was evident that there is tight regulation between RNF41 and USP8 by the proteins itself. However, it was important to confirm that RNF41 and USP8 proteins exist in a form of functional complex. By using HEK cell lines that endogenously express both these proteins, they were able to coimmunoprecipitate both proteins from lysates and confirmed that USP8 and RNF41 exist in a complex within cells (Wu et al., 2004). However, the mechanism by which the formation or activity of the RNF41-USP8 complex is regulated in cells remains an unanswered question.

To assess whether MAGEL2 regulates the stability of USP8-RNF41 complex, I transiently co-transfected MAGEL2 with a second construct expressing epitope tagged USP8 and RNF41 and looked at the changes in protein levels. Interestingly, co-transfection with MAGEL2 reversed the stabilizing effect of USP8 on RNF41 and its mutant forms (Fig 3.4). This suggest that MAGEL2 has an influence in the stability of RNF41 E3 ligase and USP8 deubiquitinase, and that MAGEL2 might interfere with their overall regulation.

A similar interaction between MAGEL2, TRIM27 E3 ubiquitin ligase and USP7 deubiquitinating enzyme was published recently (Hao et al., 2015). According to their results MAGEL2 binds to an E3 RING ubiquitin ligase, TRIM27, and enhances the ubiquitin ligase activity of TRIM27 (Doyle et al., 2010; Hao et al., 2013). The MAGEL2-TRIM27 complex localizes to endosomes, which then enhances endosomal protein recycling and trafficking. Through a set of *in vitro* binding studies and co-immunoprecipitation experiments they confirmed that USP7 is an integral component of the MAGEL2-TRIM27 complex (Hao et al., 2015). USP7 protects TRIM27 from auto-ubiquitination and proteosomal degradation. They confirmed that MAGEL2-TRIM27-USP7 form a stable protein complex (Hao et al., 2015).

As I found that MAGEL2 has an influence on the abundance of the RNF41-USP8 complex, I wanted to assess whether MAGEL2 modulates the stability of USP8 or RNF41 separately.

Results from this experiment showed that co-expression of MAGEL2 significantly reduced the abundance of USP8 (Fig. 3.5). Conversely, co expression of MAGEL2 increased the abundance of RNF41-WT (Fig 3.6A) as well as mutant forms (Fig.3.6C, 3.6E). This suggested that MAGEL2 indeed has an influence on both RNF41 and USP8 which was consistent with the MAPPIT results explained previously. From the results of the ubiquitination analysis, I found that MAGEL2 reduced the extent of RNF41 ubiquitination (Fig. 3.7), suggesting that MAGEL2 stabilizes RNF41 by diminishing its auto-ubiquitination or, alternatively, by increasing de-ubiquitination by endogenous DUBs such as USP8.

I confirmed that MAGEL2 stabilizes RNF41 protein expression by performing a cycloheximide assay by measuring the abundance of RNF41 every 30 min for 3 h after treatment with cycloheximide. Co-expression of MAGEL2 doubled the half-life of RNF41 from 73 min to 143 min indicating that MAGEL2 can stabilize RNF41 within the cells (Fig. 3.8). On the other hand, I found that expression of RNF41 affected abundance of MAGEL2 variably depending on the RNF41 construct used for the experiment. MAGEL2 protein levels were lower when co-expressed with RNF41-WT or RNF41-AE but unchanged with RNF41-SQ (Fig.3.9), suggesting that the ability of RNF41 to destabilize MAGEL2 requires ubiquitination activity. Conversely, co-expression of USP8 increased the abundance of MAGEL2 (Fig.3.10). Mutations that disrupt the MHD of MAGEL2 disrupted the mutual effects of RNF41 and MAGEL2 on each other's stability. Mutant MAGEL2 constructs were modeled on mutations found in the MHD of either MAGED2 or MAGEG1. As explained previously, co-expression of RNF41 lowers levels of wildtype MAGEL2, but in contrast RNF41 increased levels of the two MHD mutant versions of MAGEL2 (Fig.3.11D, E). Likewise, while wildtype MAGEL2 increased levels of RNF41, but co-expression of either MAGEL2p.R1187C or MAGEL2p.LL1031AA reduced RNF41 levels (Fig.3.11A, B). From these contrasting results, I suggest that defects in the MHD of MAGEL2 interfere with the mutual effect of RNF41 and MAGEL2 on each other's stability.

To understand whether MAGEL2 affects the subcellular localization of the proteins that are involved in the leptin receptor trafficking and recycling, I performed an immunofluorescence assay. I observed that cytoplasmically diffused USP8 was relocalized to large intracellular vesicles when co-transfected with RNF41 (Fig 3.14). The above mentioned change in localization was consistent with the previous results (De Ceuninck et al., 2013). However, when MAGEL2 was co-

transfected, this localization was reversed back and showed a more diffuse pattern throughout the cytoplasm. From the above result, I suggest that the expression of MAGEL2 reverses the stabilizing effect of USP8 on RNF41 by reversing the ability of RNF41 to relocalize USP8 to intracellular vesicles. To determine whether MAGEL2 regulates the subcellular localization of LepR along with RNF41 and USP8, I performed an immunofluorescence assay. The main aim was to visualize if MAGEL2 could reverse the altered leptin receptor levels at the cell surface, in its trafficking process. Before looking at the changes in the subcellular localization of LepR, I found that most of the LepR was expressed in the cytoplasmic region and generally weak signals on the cell surface when it is transfected alone. This was consistent with the published evidence where LepR was observed at three locations corresponding to a perinuclear compartment, a peripheral compartment, and the plasma membrane. They confirmed that cell surface staining was weak, therefore LepR cannot be detected in cell surface, especially when the LepR expression level is lower (Belouzard et al., 2004).

I used different markers to visualize the changes of subcellular localization of the LepR with other associated proteins. In relation to early endosomes characterized by early marker EEA1, a portion of LepR was co-localized with early endosomes (Fig 3.15). This co-localization remained same with the addition of RNF41 or MAGEL2. This indicated that LepR is transported to early endosomes independent from the other interacting proteins. Surprisingly, when LepR was co-transfected with RNF41 along with MAGEL2 and MAGEL2 alone, a higher proportion of LepR was seen in the cell surface or on the cell membrane. This might either be due to recycling of receptor back to the cell membrane or it might also be due to less internalization of LepR when MAGEL2 is present.

In relation to lysosomes characterized by late endosomal or lysosomal marker LAMP1 another portion of LepR was co-localized with LAMP1, which is evident from the yellow signals in the immunofluorescence (Fig 3.16). This colocalization was impaired in the presence of RNF41, indicating that RNF41 may suppress LepR from being degraded by lysosomes. Also, I observed that co-localization of LepR with lysosomes was impaired and more LepR was seen at the cell membrane in the presence of both RNF41 and MAGEL2 or in the presence of MAGEL2 alone. This indicated that RNF41 and MAGEL2 might have a negative influence on LepR degradation as it was not localized with the lysosomes where degradation is initiated. These findings suggest an important role of both RNF41 and MAGEL2 in the intracellular routing of

LepR. In order to characterize the dynamics of leptin receptors between intracellular compartments and the cell surface, further experiments should be done. To further expand this experiment, I could have used USP8 and look at the changes of subcellular localization of the LepR along with EEA1 and LAMP1 markers of internal compartments. Also, it would be better to involve MAGEL2 along with USP8. As USP8 stabilizes the ESCRT-0 complex and enhances the degradation pathway for LepR, I should be able to observe a colocalization of LepR with both EEA1 and LAMP1. By observing the previous evidence, in the presence of MAGEL2, this co-localization should only be seen with EEA1, but not with LAMP1, indicating that MAGEL2 has a negative influence in LepR degradation. Also, to confirm if MAGEL2 reroutes LepR back to the cell surface, I could have used membrane markers like cadherin and observed whether LepR colocalizes with the plasma membrane in the presence of MAGEL2.

To make the immunofluorescence results clearer, I performed cell surface biotinylation assay, where percentage of receptors at the cell surface is calculated in a steady state in relation to total and cytosolic protein expression levels. All the steps upto lysing of cells were done on ice, in order to prevent receptor internalization. After analyzing the results, I observed that percentage of biotinylated LepR was significantly more in the presence of MAGEL2 (Fig 3.17). From the above result, I suggest that the abundance of LepR at the cell surface is sensitive to MAGEL2. This result was consistent with the previously described immunofluorescence results where LepR was expressed more in the cell membrane in the presence of MAGEL2. Therefore, I suggest that MAGEL2 has a role in LepR trafficking in a steady state level. To get a better understanding, it would be better if I tested the change in the cell surface expression of LepR with an increasing dose of MAGEL2. If MAGEL2 has an impact on surface expression, my prediction will be a dose dependent increase of LepR expression at the cell surface. Other than overexpression of MAGEL2, stable cell lines which knocked down MAGEL2 expression by RNA interference (shRNA) can be used to assess the role of MAGEL2 proteins in the modulation of LepR cell surface expression by comparison. Other than MAGEL2, I could use USP8 and RNF41, to examine its role in the regulation and stability of LepR by measuring the changes in cell surface LepR expression.

A change in the number of internalized receptors recycled to the cell surface could also lead to an alteration of the steady state number of receptors present at the cell surface. Antibody uptake experiment and LepR endocytosis assay are two other experiments that will be useful. Observing the changes in the internalization rate of LepR in the presence or absence of MAGEL2,

would give a clear idea whether MAGEL2 has a negative influence in LepR endocytosis leading to higher cell surface expression or vice versa. In the antibody uptake experiment, the cells must be incubated at 37 °C for 20 min, in order for the cell surface LepR to be internalized. Intracellular localization of internalized LepR tagged with epitope can be detected by immunofluorescence by double-labeling with an anti-EEA1 (early endosome marker), CD63 (MVB marker), TGN46 (trans golgi network marker) or anti-LAMP-1 (late endosomal or lysosomal marker). The change in LepR localization can then be compared in the presence or absence of MAGEL2. If internalized LepR do not accumulate in endocytic compartments of these cells in the presence of MAGEL2, specially within the late endosome or lysosomes where degradation occurs, it suggests that LepR are probably recycled back to the plasma membrane, resulting in their increased expression at the cell surface. Therefore, it remains to be determined if the relative levels of the intracellular and cell surface pools of leptin receptor could be modulated in response to the presence of MAGEL2, and if defects in this regulation may alter leptin sensitivity.

The interaction of LepR with trafficking proteins like USP8 and RNF41 regulates its intracellular trafficking, and consequently its cell surface expression. This concept has been studied previously. RNF41 E3 ligase leads to an increase of LepR recycling to the plasma membrane than lysosomal targeting (Wauman and Tavernier, 2011). The activity of E3 ligases is counterbalanced by the activity of USP8 deubiquitylating enzymes (DUBs) (De Ceuninck et al., 2013). LepR turnover can also be observed by the formation of the CTS. To monitor LR degradation, I incubated cells with chloroquine, an inhibitor of intralysosomal degradation. This led to the stabilization the degradation products or the CTS. Suppression of CTS reflects reduced lysosomal degradation.

It has been published that RNF41 blocks the LepR-CTS formation (Wauman et al., 2011). This might be due to the reduction of endogenous USP8 by RNF41. I observed similar results indicating that lysosomal degradation of LepR is prevented by RNF41 (Fig 3.18A). Co-expression of USP8 reverses the inhibitory effect of RNF41 on LR CTS formation in a dose-dependent manner and restore CTS generation (De Ceuninck et al., 2013). This sensitivity to the dosage of USP8 might be due to compensation for the loss of endogenous USP8 levels upon RNF41 expression. I detected that MAGEL2 also reduced the formation of the LepR-CTS in the presence of chloroquine (Fig. 3.18B). I performed a protein stability assay using cycloheximide and found that co-expression of MAGEL2 increased the abundance of the LepR, and increased the LepR

half-life (Fig.3.19). Similar results were obtained at least three independent experiments. From these results, I suggest that MAGEL2 stabilizes LepR within the cells and protects it from lysosomal degradation. Therefore, in the absence of MAGEL2 there will be an increase in the rate of LepR degradation leading to less cell surface expression and less leptin signaling.

The decision to recycle endocytosed receptors back to the plasma membrane or to direct them towards the lysosomes for degradation is largely a function of ESCRT complex. Therefore, it acts as an important checkpoint that determines the fate of receptors such as leptin receptor. The ESCRT-0 complex consists of Hrs and STAM1. Direct binding of USP8 to STAM proteins deubiquitylates and stabilizes the ESCRT-0 complex (Niendorf et al., 2007). It was published that RNF41 indirectly destabilizes the ESCRT-0 complex through suppression of USP8. This statement was supported by the reduction in endogenous Hrs and STAM1 protein levels in the presence of RNF41 (De Ceuninck et al., 2013). The balance between USP8 and RNF41 E3 ligase expression and activity, eventually defines cell surface expression of leptin receptors at steady-state. I found that in the presence of MAGEL2, the abundance of STAM1 is reduced, indicating that MAGEL2 is destabilizing the ESCRT-0 complex (Fig 3.20). Previously I explained that co-expression of MAGEL2 reduces the USP8 abundance and co-expression of RNF41-WT increase MAGEL2 abundance. From these results, I suggest that in the presence of MAGEL2, the stability of the ESCRT complex by USP8 is suppressed and the destabilization of ESCRT complex by RNF41 is improved.

As all the above results were gained from cultured cells *in vitro*, so I wanted to compare them with *in vivo* results. Therefore, I used *Magel2*-null mice where *Magel2* is knocked out and wild type mice as controls. Energy balance is regulated by specialized neurons within the hypothalamus of the brain. They sense circulating signals of energy stores such as leptin. Also, *Magel2* is most prominently expressed in the hypothalamus. Therefore, in order to confirm the predicted changes in different proteins in the presence or absence of *Magel2*, hypothalamus samples from wild type and mutant mice were used. I compared the endogenous levels of murine Rnf41, Usp8, Stam1, LepR and necdin between wild type and *Magel2*-null mice. As predicted, there was more Usp8 (Fig.3.21A) and less Rnf41 (Fig.3.21C) in hypothalamus from *Magel2*-null mice. This suggests that *in vivo*, *Magel2* stabilizes Rnf41 and destabilizes Usp8. These results were consistent with the previous *in vitro* results. Cells from a *Usp8*-null mouse model were

shown to have a strong destabilization of Stam1 (Niendorf et al., 2007). Consistent with the results of the cultured cells where heterologous expression of MAGEL2 destabilized endogenous STAM1, there was increased levels of Stam1 in hypothalamus samples in *Magel2*-null mice than the wildtype mice (Fig.3.22A). USP8 indirectly promote LepR degradation through its regulation of the ESCRT complex (Berlin et al., 2010). In contrast, after looking at my results, I suggest that MAGEL2 may indirectly prevent LepR degradation through its regulation of the ESCRT machinery.

I previously described that co-expression of MAGEL2 increased the abundance and half-life of LepR in co-transfected cells. From this result, I predicted that there will be less Lepr in *Magel2*-null mice than the wild type. The predication was confirmed by immunoblot analysis as there was less Lepr level in the hypothalamus of *Magel2*-null mice compared to wild-type littermates (Fig.3.23A). Leprs are expressed in several hypothalamic regions including the ARC, VMH, DMH, PVN and LHA (Suzuki et al., 2012). However, the arcuate nucleus is the key hypothalamic region involved in energy balance regulation and it is leptin's main site of action (Mercer et al., 2013; Woods and D'Alessio, 2008). To identify the changes in the expression levels of Lepr specifically at the ARC would be beneficial to narrow down the result. Other than the use of mouse models, future studies can be done in postmortem samples of the hypothalamus from humans with PWS to examine changes in LepR expression with control samples.

Previous work with the *Magel2*-null mice identified defects in signaling of leptin hormone crucial to hypothalamic control of energy metabolism. These mutant mice have increased circulating leptin, suggesting a reduced sensitivity to leptin hormone (Bischof et al., 2007). This explanation was supported, from the finding that adult mutant mice, unlike wildtypes, fail to reduce food intake in response to externally administered leptin (Mercer et al., 2013). To further understand the cause of this leptin insensitivity, our laboratory previously examined whether leptin is able to bind its receptor (LepR) in the ARC and initiate a downstream signaling cascade by phosphorylating STAT3, and whether LepR is activated. The phosphorylated STAT3 expression in neurons is a marker of LepR activation. They published that, although leptin treatment increased the number of phosphorylated STAT3 neurons in ARC in both wild type and mutant mice, leptin-treated *Magel2* mutants had fewer phosphorylated STAT3 neurons than leptin-treated wildtypes (Mercer et al., 2013). They suggested that the reduced phosphorylated STAT3 activation in

Magel2-null mice could be due to decrease in the number of leptin-responsive neurons in the ARC, or reduced transport across the blood brain barrier (Faouzi et al., 2007). Immunohistochemical analysis revealed that *Magel2*-null mice have a reduced number of POMC neurons in the ARC than the wildtype (Mercer et al., 2013). Although it supports the former findings, it does not rule out the possibility that loss of leptin sensitivity could be caused by defects in intracellular trafficking that could lead to altered or decreased LepR expression at the cell surface. This constitutes an important issue since the pool of LepR at the cell surface could determine the sensitivity of the cell to leptin. Cell surface expression of LepR is a highly dynamic process that, besides *de novo* synthesis, involves endocytosis irrespective of ligand triggering, followed by sorting to recycling vesicles, signaling endosomes or MVBs and lysosomes for degradation. The molecular basis of how cells establish an appropriate number of receptors at their cell surface is not yet understood clearly. The interaction of LepR with trafficking proteins like USP8, RNF41 and MAGEL2 may regulate its intracellular trafficking, and consequently its cell surface expression and ability to bind leptin.

I reasoned that MAGEL2 could interact with components of the RNF41-USP8- LepR complex to regulate LepR function and ultimately appetite and body weight. In this study, I found that MAGEL2 acts as adaptor protein by bridging the leptin receptor to the ubiquitination complex RNF41-USP8 and that co-expression of MAGEL2 alters the stability and intracellular routing of LepR, along with RNF41 and USP8. Complementary results were obtained *in vivo* using *Magel2*-null and wild type mice. In mice, *Magel2* is mainly expressed in the central nervous system, with highest expression levels in the hypothalamus (Lee et al., 2003). I found out that, the abundance of Rnf41, Usp8 and the leptin receptor are altered in brain tissues from mice lacking *Magel2*. Thus, loss of *Magel2* disrupts the normal equilibrium of leptin receptor internalization, trafficking and degradation, likely accounting for the progressive loss of leptin sensitivity observed in the *Magel2*-null mouse model of Prader-Willi syndrome.

To assess whether LepR deficiency is a primary abnormality in PWS, RT-PCR was used to examine LepR expression in the lymphocytes of the PWS patients (Goldstone et al., 2002). Because LepR mRNA is expressed in lymphocytes from PWS patients, they concluded that leptin receptor deficiency does not appear to be a primary consequence of the gene defects observed in PWS. These findings do not, however, exclude the possibility of absent LepR expression in the hypothalamus of PWS patients, due to hypothalamus-specific defect or due to low surface

expression to perform its function. Several *in vitro* studies with transfected leptin receptors have confirmed the existence of a large intracellular LepR pool rather than at the cell surface (Belouzard et al., 2004). This might be due to a rapid turnover of leptin receptor or that the levels of LepR cell surface expression is lowered by a regulation via other interacting proteins. The functional meaning of this distribution, and the relationship between the intracellular pools of receptor and the cell surface, where the interaction with leptin occurs, have not yet been investigated, and very little is known about its intracellular trafficking. However, defining the mechanism of LepR trafficking is a critical step toward understanding the regulation of it by RNF41-USP8 complex along with MAGEL2.

PWS is an imprinted genetic obesity disorder characterized by abnormalities of growth and metabolism (Bischof et al., 2007). Children with PWS become severely obese because of reduced voluntary activity, low metabolic rate and increased food intake. They also exhibit growth hormone deficiency, excessive daytime sleepiness, endocrine dysregulation and infertility (Colmers and Wevrick, 2013). The hyperphagia, obesity, and impaired sex hormones observed in PWS patients are also seen in patients with leptin deficiency and leptin receptor defects. This increases the possibility that defects in leptin pathways in the brain may explain these phenotypes in PWS patients (Goldstone et al., 2002).

Leptin leads to regulation of a range of biological functions and processes, including energy intake and expenditure, body fat, neuroendocrine systems, autonomic function, and insulin and glucose balance (Bjørbaek, 2009; Morton et al., 2005). Other than that, leptin interacts with the reproductive axis at multiple sites, with stimulatory effects at the hypothalamus and pituitary and inhibitory effects at the gonads (ovaries and testis) (Mantzoros, 2000; Moschos et al., 2002). Similar to the *ob/ob* and *db/db* mice, obese patients that have mutations in the leptin gene or the leptin receptor gene have also been demonstrated to have reproductive dysfunction (Mantzoros, 2000). Moreover, leptin administration to these mouse models results in maturation of the reproductive tract, by increasing gonadal hormones. Loss of *Magel2* alters reproductive function in both male and female obese mice. They have impaired leptin signaling and impaired leptin response in the hypothalamus (Mercer and Wevrick, 2009). However, the exact role of leptin in reproductive abnormalities associated with obesity remains to be shown in future studies.

It has been published that appetite suppressing response to exogenous leptin was impaired in *Magel2*-null mice. These mice fail to activate the POMC neurons in the ARC in the presence of

leptin. These indicated that POMC neurons, which are responsible for appetite suppressing effect, are unresponsive for leptin. Contrastingly, the NPY neurons are hyperpolarized and inhibited in the presence of leptin in normal conditions. NPY neurons showed no difference in its response in both wild type and *Magel2*-null mice (Mercer et al., 2013). This indicated that *Magel2* is not required for normal NPY signaling. Therefore, more experiments should be targeted on hypothalamic POMC neurons that showed a significant difference in its activation. Future experiments are required to determine the underlying cause of the unresponsiveness of POMC neurons to leptin in *Magel2*-null mice. Since the pool of LepR at the cell surface determines the sensitivity of the neuronal cell to leptin, low expression of LepR at the cell surface might be a possibility for the above phenomena. It would be interesting to see whether there is a change in the LepR levels in the POMC positive neurons using hypothalamic sections of both wild type and *Magel2*-null mice and compare the co-localization using double-immunofluorescence labelling.

Recently it was shown that increased LepR cell surface expression increases cellular leptin signaling and prevents obesity development in mice (Kim et al., 2014). *In vitro* studies have shown that LepR is endocytosed constitutively in a ligand-independent manner (Barr et al., 1999) indicating that the down-regulation of this receptor is not mediated by ligand induced internalization. Therefore, understanding the mechanism and regulation of the leptin receptor trafficking clearly, will open new avenues in improving the LepR cell surface expression. Ultimately this can be considered as an interesting anti-obesity therapeutic strategy for PWS.

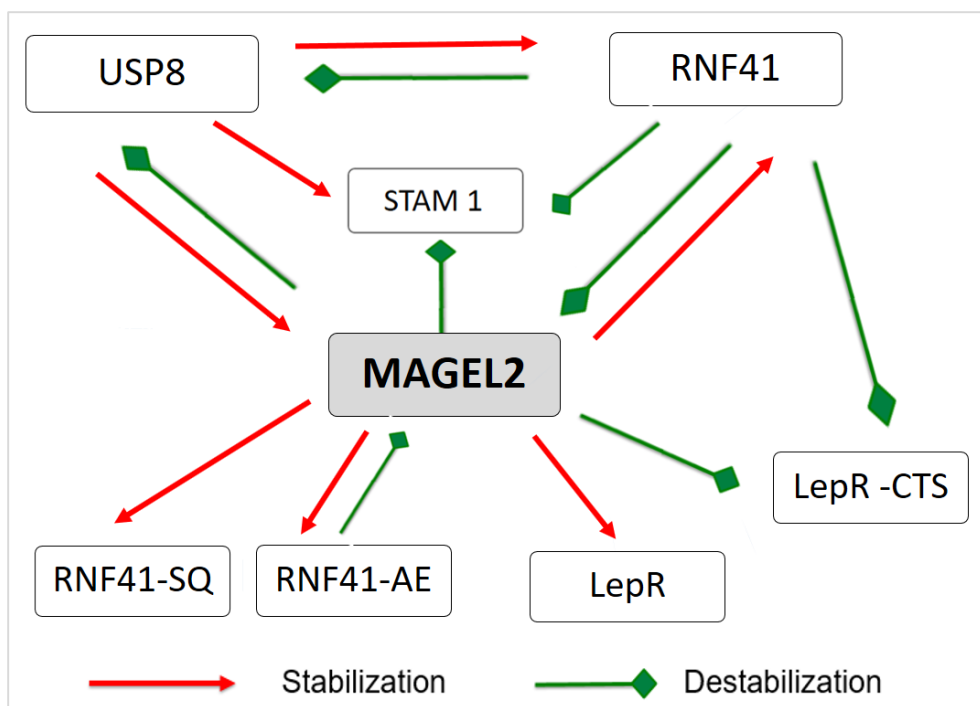


Figure 4.1: Summary of the abundance results.

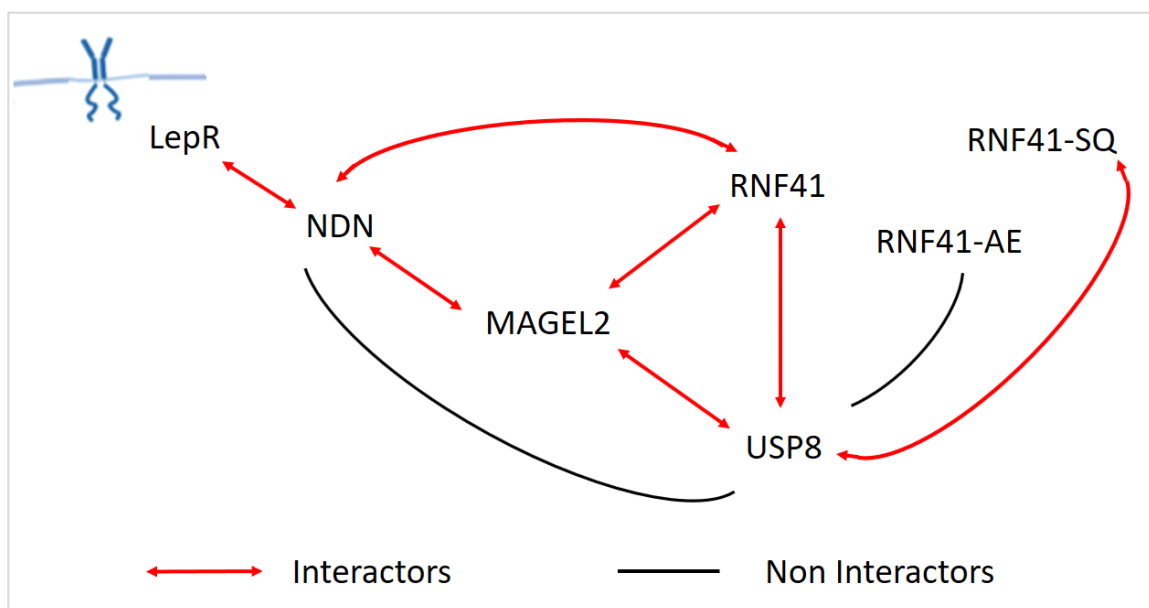
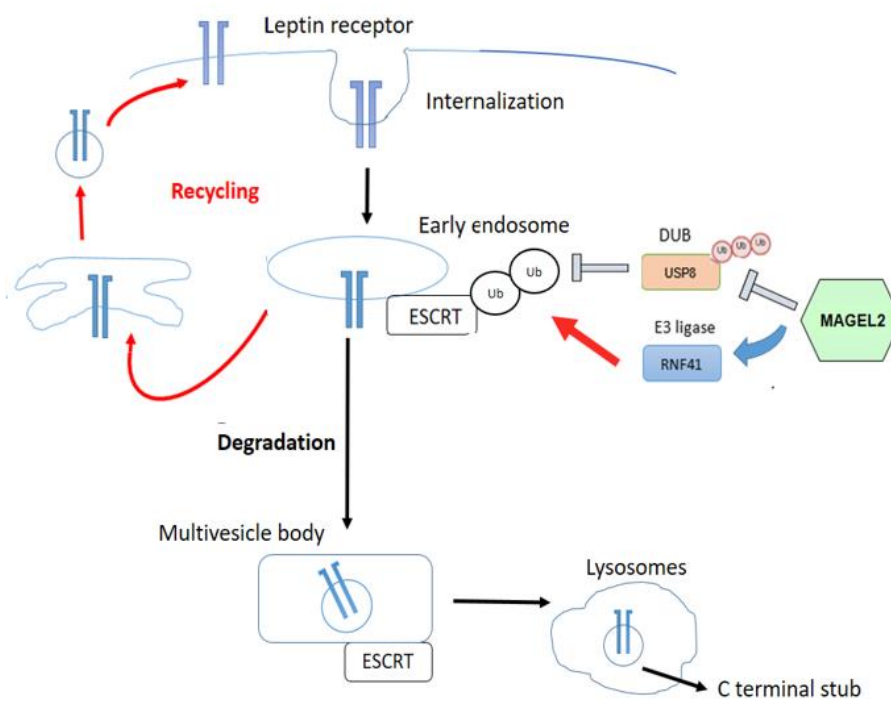


Figure 4.2 : Summary of the interaction results.

A



B

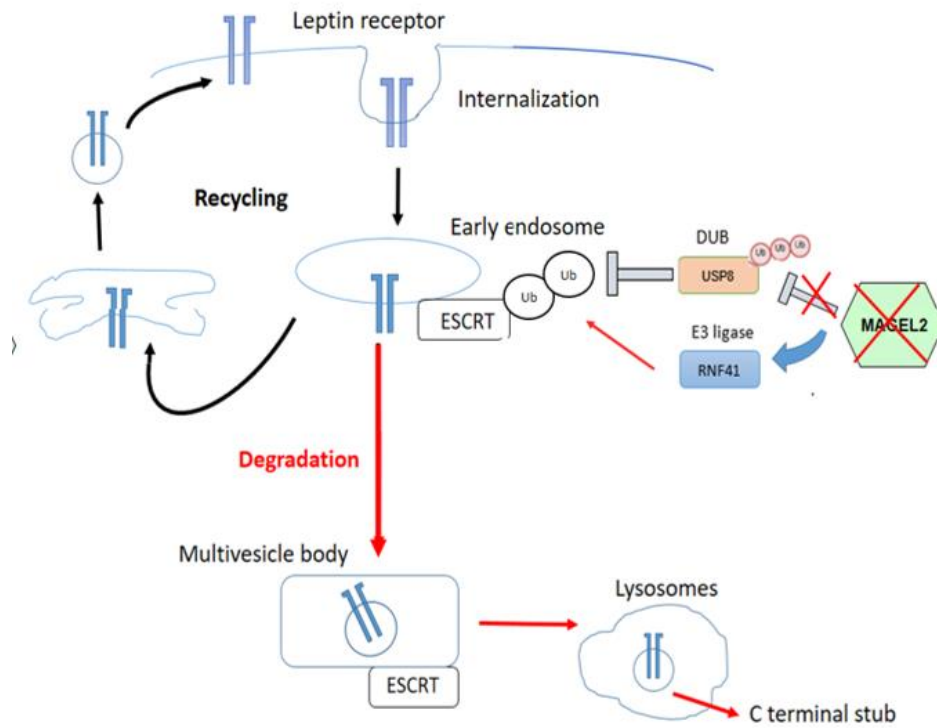


Figure 4.3 : Model for leptin receptor trafficking in the presence (A) or absence (B) of MAGEL2.

References

- Allison, M.B., and Myers, M.G. (2014). 20 years of leptin: connecting leptin signaling to biological function. *J. Endocrinol.* *223*, T25–35.
- d’Azzo, A., Bongiovanni, A., and Nastasi, T. (2005). E3 ubiquitin ligases as regulators of membrane protein trafficking and degradation. *Traffic Cph. Den.* *6*, 429–441.
- Banks, A.S., Davis, S.M., Bates, S.H., and Myers, M.G. (2000). Activation of downstream signals by the long form of the leptin receptor. *J. Biol. Chem.* *275*, 14563–14572.
- Barker, P.A., and Salehi, A. (2002). The MAGE proteins: emerging roles in cell cycle progression, apoptosis, and neurogenetic disease. *J. Neurosci. Res.* *67*, 705–712.
- Barr, V.A., Lane, K., and Taylor, S.I. (1999). Subcellular localization and internalization of the four human leptin receptor isoforms. *J. Biol. Chem.* *274*, 21416–21424.
- Bates, S.H., Stearns, W.H., Dundon, T.A., Schubert, M., Tso, A.W.K., Wang, Y., Banks, A.S., Lavery, H.J., Haq, A.K., Maratos-Flier, E., et al. (2003). STAT3 signalling is required for leptin regulation of energy balance but not reproduction. *Nature* *421*, 856–859.
- Belouzard, S., Delcroix, D., and Rouillé, Y. (2004). Low levels of expression of leptin receptor at the cell surface result from constitutive endocytosis and intracellular retention in the biosynthetic pathway. *J. Biol. Chem.* *279*, 28499–28508.
- Berlin, I., Higginbotham, K.M., Dise, R.S., Sierra, M.I., and Nash, P.D. (2010). The deubiquitinating enzyme USP8 promotes trafficking and degradation of the chemokine receptor 4 at the sorting endosome. *J. Biol. Chem.* *285*, 37895–37908.
- Bischof, J.M., Stewart, C.L., and Wevrick, R. (2007). Inactivation of the mouse Magel2 gene results in growth abnormalities similar to Prader-Willi syndrome. *Hum. Mol. Genet.* *16*, 2713–2719.
- Bjørbaek, C. (2009). Central leptin receptor action and resistance in obesity. *J. Investig. Med. Off. Publ. Am. Fed. Clin. Res.* *57*, 789–794.
- Bjørbaek, C., Elmquist, J.K., Michl, P., Ahima, R.S., van Bueren, A., McCall, A.L., and Flier, J.S. (1998). Expression of leptin receptor isoforms in rat brain microvessels. *Endocrinology* *139*, 3485–3491.
- Boccaccio, I., Glatt-Deeley, H., Watrin, F., Roëckel, N., Lalande, M., and Muscatelli, F. (1999). The human MAGEL2 gene and its mouse homologue are paternally expressed and mapped to the Prader-Willi region. *Hum. Mol. Genet.* *8*, 2497–2505.
- Boguszewski, C.L., Paz-Filho, G., and Velloso, L.A. (2010). Neuroendocrine body weight regulation: integration between fat tissue, gastrointestinal tract, and the brain. *Endokrynol. Pol.* *61*, 194–206.

- Bush, J.R., and Wevrick, R. (2012). Loss of the Prader-Willi obesity syndrome protein neitin promotes adipogenesis. *Gene* *497*, 45–51.
- Butler, M.G. (2011). Prader-Willi Syndrome: Obesity due to Genomic Imprinting. *Curr. Genomics* *12*, 204–215.
- Butler, A.A., and Cone, R.D. (2002). The melanocortin receptors: lessons from knockout models. *Neuropeptides* *36*, 77–84.
- Butler, M.G., Theodoro, M.F., Bittel, D.C., and Donnelly, J.E. (2007). Energy expenditure and physical activity in Prader-Willi syndrome: comparison with obese subjects. *Am. J. Med. Genet. A* *143A*, 449–459.
- Cao, Z., Wu, X., Yen, L., Sweeney, C., and Carraway, K.L. (2007). Neuregulin-induced ErbB3 downregulation is mediated by a protein stability cascade involving the E3 ubiquitin ligase Nrdp1. *Mol. Cell. Biol.* *27*, 2180–2188.
- Cassidy, S.B. (1997). Prader-Willi syndrome. *J. Med. Genet.* *34*, 917–923.
- Cassidy, S.B., and Driscoll, D.J. (2008). Prader-Willi syndrome. *Eur. J. Hum. Genet.* *17*, 3–13.
- Cassidy, S.B., Schwartz, S., Miller, J.L., and Driscoll, D.J. (2012). Prader-Willi syndrome. *Genet. Med. Off. J. Am. Coll. Med. Genet.* *14*, 10–26.
- Chapman, E.J., and Knowles, M.A. (2009). Neitin: a multi functional protein with potential tumor suppressor role? *Mol. Carcinog.* *48*, 975–981.
- Chomez, P., De Backer, O., Bertrand, M., De Plaen, E., Boon, T., and Lucas, S. (2001). An overview of the MAGE gene family with the identification of all human members of the family. *Cancer Res.* *61*, 5544–5551.
- Clément, K., Vaisse, C., Lahllou, N., Cabrol, S., Pelloux, V., Cassuto, D., Gourmelen, M., Dina, C., Chambaz, J., Lacorte, J.M., et al. (1998). A mutation in the human leptin receptor gene causes obesity and pituitary dysfunction. *Nature* *392*, 398–401.
- Colmers, W.F., and Wevrick, R. (2013). Leptin signaling defects in a mouse model of Prader-Willi syndrome. *Rare Dis.* *1*.
- Considine, R.V., and Caro, J.F. (1997). Leptin and the regulation of body weight. *Int. J. Biochem. Cell Biol.* *29*, 1255–1272.
- De Ceuninck, L., Wauman, J., Masschaele, D., Peelman, F., and Tavernier, J. (2013). Reciprocal cross-regulation between RNF41 and USP8 controls cytokine receptor sorting and processing. *J. Cell Sci.* *126*, 3770–3781.
- Deshaires, R.J., and Joazeiro, C.A.P. (2009). RING domain E3 ubiquitin ligases. *Annu. Rev. Biochem.* *78*, 399–434.

- Doyle, J.M., Gao, J., Wang, J., Yang, M., and Potts, P.R. (2010). MAGE-RING protein complexes comprise a family of E3 ubiquitin ligases. *Mol. Cell* *39*, 963–974.
- Fang, S., and Weissman, A.M. (2004). A field guide to ubiquitylation. *Cell. Mol. Life Sci.* *CMLS* *61*, 1546–1561.
- Faouzi, M., Leshan, R., Björnholm, M., Hennessey, T., Jones, J., and Münzberg, H. (2007). Differential accessibility of circulating leptin to individual hypothalamic sites. *Endocrinology* *148*, 5414–5423.
- Farooqi, I.S., Keogh, J.M., Yeo, G.S.H., Lank, E.J., Cheetham, T., and O’Rahilly, S. (2003). Clinical spectrum of obesity and mutations in the melanocortin 4 receptor gene. *N. Engl. J. Med.* *348*, 1085–1095.
- Farooqi, I.S., Wangensteen, T., Collins, S., Kimber, W., Matarese, G., Keogh, J.M., Lank, E., Bottomley, B., Lopez-Fernandez, J., Ferraz-Amaro, I., et al. (2007). Clinical and molecular genetic spectrum of congenital deficiency of the leptin receptor. *N. Engl. J. Med.* *356*, 237–247.
- Feng, Y., Gao, J., and Yang, M. (2011). When MAGE meets RING: insights into biological functions of MAGE proteins. *Protein Cell* *2*, 7–12.
- Frederich, R.C., Hamann, A., Anderson, S., Löllmann, B., Lowell, B.B., and Flier, J.S. (1995). Leptin levels reflect body lipid content in mice: evidence for diet-induced resistance to leptin action. *Nat. Med.* *1*, 1311–1314.
- Funcke, J.-B., von Schnurbein, J., Lennerz, B., Lahr, G., Debatin, K.-M., Fischer-Posovszky, P., and Wabitsch, M. (2014). Monogenic forms of childhood obesity due to mutations in the leptin gene. *Mol. Cell. Pediatr.* *1*, 3.
- Glenn, C.C., Driscoll, D.J., Yang, T.P., and Nicholls, R.D. (1997). Genomic imprinting: potential function and mechanisms revealed by the Prader-Willi and Angelman syndromes. *Mol. Hum. Reprod.* *3*, 321–332.
- Goldstone, A.P., Brynes, A.E., Thomas, E.L., Bell, J.D., Frost, G., Holland, A., Ghatei, M.A., and Bloom, S.R. (2002). Resting metabolic rate, plasma leptin concentrations, leptin receptor expression, and adipose tissue measured by whole-body magnetic resonance imaging in women with Prader-Willi syndrome. *Am. J. Clin. Nutr.* *75*, 468–475.
- Grugni, G., Crinò, A., Bosio, L., Corrias, A., Cuttini, M., De Toni, T., Di Battista, E., Franzese, A., Gargantini, L., Greggio, N., et al. (2008). The Italian National Survey for Prader-Willi syndrome: an epidemiologic study. *Am. J. Med. Genet. A* *146A*, 861–872.
- Gunay-aygun, M., Schwartz, S., Heeger, S., Riordan, M.A., Cassidy, S.B., Background, A., and Pws, P. (2001). Criteria and Proposed Revised Criteria. *Pediatrics* *108*, 1–5.
- Hao, Y.-H., Doyle, J.M., Ramanathan, S., Gomez, T.S., Jia, D., Xu, M., Chen, Z.J., Billadeau, D.D., Rosen, M.K., and Potts, P.R. (2013). Regulation of WASH-dependent actin polymerization and protein trafficking by ubiquitination. *Cell* *152*, 1051–1064.

- Hao, Y.-H., Fountain, M.D., Fon Tacer, K., Xia, F., Bi, W., Kang, S.-H.L., Patel, A., Rosenfeld, J.A., Le Caignec, C., Isidor, B., et al. (2015). USP7 Acts as a Molecular Rheostat to Promote WASH-Dependent Endosomal Protein Recycling and Is Mutated in a Human Neurodevelopmental Disorder. *Mol. Cell* *59*, 956–969.
- Holm, V.A., Cassidy, S.B., Butler, M.G., Hanchett, J.M., Greenswag, L.R., Whitman, B.Y., and Greenberg, F. (1993). Prader-Willi syndrome: consensus diagnostic criteria. *Pediatrics* *91*, 398–402.
- Jay, P., Rougeulle, C., Massacrier, A., Moncla, A., Mattei, M.G., Malzac, P., Roëckel, N., Taviaux, S., Lefranc, J.L., Cau, P., et al. (1997). The human neccidin gene, NDN, is maternally imprinted and located in the Prader-Willi syndrome chromosomal region. *Nat. Genet.* *17*, 357–361.
- Jovic, M., Sharma, M., Rahajeng, J., and Caplan, S. (2010). The early endosome: a busy sorting station for proteins at the crossroads. *Histol. Histopathol.* *25*, 99–112.
- Kamikubo, Y., Dellas, C., Loskutoff, D.J., Quigley, J.P., and Ruggeri, Z.M. (2008). Contribution of leptin receptor N-linked glycans to leptin binding. *Biochem. J.* *410*, 595–604.
- Kim, T.-H., Choi, D.-H., Vauthier, V., Dam, J., Li, X., Nam, Y.-J., Ko, Y., Kwon, H.J., Shin, S.H., Cechetto, J., et al. (2014). Anti-obesity phenotypic screening looking to increase OBR cell surface expression. *J. Biomol. Screen.* *19*, 88–99.
- Kozlov, S.V., Bogenpohl, J.W., Howell, M.P., Wevrick, R., Panda, S., Hogenesch, J.B., Muglia, L.J., Van Gelder, R.N., Herzog, E.D., and Stewart, C.L. (2007). The imprinted gene Magel2 regulates normal circadian output. *Nat. Genet.* *39*, 1266–1272.
- Laghmani, K., Beck, B.B., Yang, S.-S., Seaayfan, E., Wenzel, A., Reusch, B., Vitzthum, H., Priem, D., Demaretz, S., Bergmann, K., et al. (2016). Polyhydramnios, Transient Antenatal Bartter's Syndrome, and MAGED2 Mutations. *N. Engl. J. Med.* *374*, 1853–1863.
- Ledbetter, D.H., Mascarello, J.T., Riccardi, V.M., Harper, V.D., Airhart, S.D., and Strobel, R.J. (1982). Chromosome 15 abnormalities and the Prader-Willi syndrome: a follow-up report of 40 cases. *Am. J. Hum. Genet.* *34*, 278–285.
- Lee, S., Walker, C.L., and Wevrick, R. (2003). Prader-Willi syndrome transcripts are expressed in phenotypically significant regions of the developing mouse brain. *Gene Expr. Patterns GEP* *3*, 599–609.
- Lee, S., Walker, C.L., Karten, B., Kuny, S.L., Tennese, A.A., O'Neill, M.A., and Wevrick, R. (2005). Essential role for the Prader-Willi syndrome protein neccidin in axonal outgrowth. *Hum. Mol. Genet.* *14*, 627–637.
- Li, X.-M., Yan, H.-J., Guo, Y.-S., and Wang, D. (2016). The role of leptin in central nervous system diseases. *Neuroreport* *27*, 350–355.

MacDonald, H.R., and Wevrick, R. (1997). The necdin gene is deleted in Prader-Willi syndrome and is imprinted in human and mouse. *Hum. Mol. Genet.* *6*, 1873–1878.

MacDonald, C., Buchkovich, N.J., Stringer, D.K., Emr, S.D., and Piper, R.C. (2012). Cargo ubiquitination is essential for multivesicular body intraluminal vesicle formation. *EMBO Rep.* *13*, 331–338.

Maillard, J., Park, S., Croizier, S., Vanacker, C., Cook, J.H., Prevot, V., Tauber, M., and Bouret, S.G. (2016). Loss of Magel2 impairs the development of hypothalamic Anorexigenic circuits. *Hum. Mol. Genet.* *25*, 3208–3215.

Mantzoros, C.S. (2000). Role of leptin in reproduction. *Ann. N. Y. Acad. Sci.* *900*, 174–183.

Margetic, S., Gazzola, C., Pegg, G.G., and Hill, R.A. (2002). Leptin: a review of its peripheral actions and interactions. *Int. J. Obes. Relat. Metab. Disord. J. Int. Assoc. Study Obes.* *26*, 1407–1433.

Maruyama, E. (1996). Biochemical characterization of mouse brain necdin. *Biochem. J.* *314* (*Pt 3*), 895–901.

Maruyama, K., Usami, M., Aizawa, T., and Yoshikawa, K. (1991). A novel brain-specific mRNA encoding nuclear protein (necdin) expressed in neurally differentiated embryonal carcinoma cells. *Biochem. Biophys. Res. Commun.* *178*, 291–296.

Mayor, S., Parton, R.G., and Donaldson, J.G. (2014). Clathrin-Independent Pathways of Endocytosis. *Cold Spring Harb. Perspect. Biol.* *6*.

Mejlachowicz, D., Nolent, F., Maluenda, J., Ranjatoelina-Randrianaivo, H., Giuliano, F., Gut, I., Sternberg, D., Laquerrière, A., and Melki, J. (2015). Truncating Mutations of MAGEL2, a Gene within the Prader-Willi Locus, Are Responsible for Severe Arthrogryposis. *Am. J. Hum. Genet.* *97*, 616–620.

Mercer, R.E., and Wevrick, R. (2009). Loss of the Prader-Willi Syndrome candidate gene Magel2 alters appetite energy balance. *Can. J. Diabetes* *33*, 185.

Mercer, R.E., Michaelson, S.D., Chee, M.J.S., Atallah, T.A., Wevrick, R., and Colmers, W.F. (2013). Magel2 is required for leptin-mediated depolarization of POMC neurons in the hypothalamic arcuate nucleus in mice. *PLoS Genet.* *9*, e1003207.

Miller, J.L., Lynn, C.H., Driscoll, D.C., Goldstone, A.P., Gold, J.-A., Kimonis, V., Dykens, E., Butler, M.G., Shuster, J.J., and Driscoll, D.J. (2011). Nutritional phases in Prader-Willi syndrome. *Am. J. Med. Genet. A.* *155A*, 1040–1049.

Montague, C.T., Farooqi, I.S., Whitehead, J.P., Soos, M.A., Rau, H., Wareham, N.J., Sewter, C.P., Digby, J.E., Mohammed, S.N., Hurst, J.A., et al. (1997). Congenital leptin deficiency is associated with severe early-onset obesity in humans. *Nature* *387*, 903–908.

- Morris, D.L., and Rui, L. (2009). Recent advances in understanding leptin signaling and leptin resistance. *Am. J. Physiol. Endocrinol. Metab.* *297*, E1247–1259.
- Morton, G.J., and Schwartz, M.W. (2011). Leptin and the central nervous system control of glucose metabolism. *Physiol. Rev.* *91*, 389–411.
- Morton, G.J., Gelling, R.W., Niswender, K.D., Morrison, C.D., Rhodes, C.J., and Schwartz, M.W. (2005). Leptin regulates insulin sensitivity via phosphatidylinositol-3-OH kinase signaling in mediobasal hypothalamic neurons. *Cell Metab.* *2*, 411–420.
- Morton, G.J., Cummings, D.E., Baskin, D.G., Barsh, G.S., and Schwartz, M.W. (2006). Central nervous system control of food intake and body weight. *Nature* *443*, 289–295.
- Moschos, S., Chan, J.L., and Mantzoros, C.S. (2002). Leptin and reproduction: a review. *Fertil. Steril.* *77*, 433–444.
- Muscatelli, F., Abrous, D.N., Massacrier, A., Boccaccio, I., Le Moal, M., Cau, P., and Cremer, H. (2000). Disruption of the mouse Necdin gene results in hypothalamic and behavioral alterations reminiscent of the human Prader-Willi syndrome. *Hum. Mol. Genet.* *9*, 3101–3110.
- Nicholls, R.D., Knoll, J.H., Butler, M.G., Karam, S., and Lalande, M. (1989). Genetic imprinting suggested by maternal heterodisomy in nondeletion Prader-Willi syndrome. *Nature* *342*, 281–285.
- Niendorf, S., Oksche, A., Kissner, A., Löhler, J., Prinz, M., Schorle, H., Feller, S., Lewitzky, M., Horak, I., and Knobeloch, K.-P. (2007). Essential role of ubiquitin-specific protease 8 for receptor tyrosine kinase stability and endocytic trafficking in vivo. *Mol. Cell. Biol.* *27*, 5029–5039.
- Prader, A., Labhart, A., and Willi, H. (1956). Ein syndrome von adipositas, kleinwuchs, kryptorchismus und oligophrenie nach myotonierartigem zustand im neugeborenenalter. *Schweiz Med Wochenschr* *66*, 1260–1261.
- Pravdivyi, I., Ballanyi, K., Colmers, W.F., and Wevrick, R. (2015). Progressive postnatal decline in leptin sensitivity of arcuate hypothalamic neurons in the Magel2-null mouse model of Prader-Willi syndrome. *Hum. Mol. Genet.* *24*, 4276–4283.
- Rahmouni, K., Sigmund, C.D., Haynes, W.G., and Mark, A.L. (2009). Hypothalamic ERK mediates the anorectic and thermogenic sympathetic effects of leptin. *Diabetes* *58*, 536–542.
- Roujeau, C., Jockers, R., and Dam, J. (2014). New pharmacological perspectives for the leptin receptor in the treatment of obesity. *Front. Endocrinol.* *5*, 167.
- Row, P.E., Prior, I.A., McCullough, J., Clague, M.J., and Urbé, S. (2006). The ubiquitin isopeptidase UBPY regulates endosomal ubiquitin dynamics and is essential for receptor down-regulation. *J. Biol. Chem.* *281*, 12618–12624.

- Schaaf, C.P., Gonzalez-Garay, M.L., Xia, F., Potocki, L., Gripp, K.W., Zhang, B., Peters, B.A., McElwain, M.A., Drmanac, R., Beaudet, A.L., et al. (2013). Truncating mutations of MAGEL2 cause Prader-Willi phenotypes and autism. *Nat. Genet.* *45*, 1405–1408.
- Schrader, E.K., Harstad, K.G., and Matouschek, A. (2009). Targeting proteins for degradation. *Nat. Chem. Biol.* *5*, 815–822.
- Schwartz, M.W., Woods, S.C., Porte, D., Seeley, R.J., and Baskin, D.G. (2000). Central nervous system control of food intake. *Nature* *404*, 661–671.
- Shields, S.B., Oestreich, A.J., Winistorfer, S., Nguyen, D., Payne, J.A., Katzmann, D.J., and Piper, R. (2009). ESCRT ubiquitin-binding domains function cooperatively during MVB cargo sorting. *J. Cell Biol.* *185*, 213–224.
- de Souza, L.B., and Ambudkar, I.S. (2014). Trafficking mechanisms and regulation of TRPC channels. *Cell Calcium* *56*, 43–50.
- Stunkard, A.J. (1996). Current views on obesity. *Am. J. Med.* *100*, 230–236.
- Sun, L., and Chen, Z.J. (2004). The novel functions of ubiquitination in signaling. *Curr. Opin. Cell Biol.* *16*, 119–126.
- Suzuki, K., Jayasena, C.N., and Bloom, S.R. (2012). Obesity and appetite control. *Exp. Diabetes Res.* *2012*, 824305.
- Sweeney, G. (2002). Leptin signalling. *Cell. Signal.* *14*, 655–663.
- Tauber, M., Diene, G., Mimoun, E., Cabal-Berthoumieu, S., Mantoulan, C., Molinas, C., Muscatelli, F., and Salles, J.P. (2014). Prader-Willi syndrome as a model of human hyperphagia. *Front. Horm. Res.* *42*, 93–106.
- Tcherpakov, M., Bronfman, F.C., Conticello, S.G., Vaskovsky, A., Levy, Z., Niinobe, M., Yoshikawa, K., Arenas, E., and Fainzilber, M. (2002). The p75 neurotrophin receptor interacts with multiple MAGE proteins. *J. Biol. Chem.* *277*, 49101–49104.
- Uetsuki, T., Takagi, K., Sugiura, H., and Yoshikawa, K. (1996). Structure and expression of the mouse neccdin gene. Identification of a postmitotic neuron-restrictive core promoter. *J. Biol. Chem.* *271*, 918–924.
- Wauman, J., and Tavernier, J. (2011). Leptin receptor signaling: pathways to leptin resistance. *Front. Biosci. Landmark Ed.* *16*, 2771–2793.
- Wauman, J., De Ceuninck, L., Vanderroost, N., Lievens, S., and Tavernier, J. (2011). RNF41 (Nrdp1) controls type 1 cytokine receptor degradation and ectodomain shedding. *J. Cell Sci.* *124*, 921–932.
- Woods, S.C., and D'Alessio, D.A. (2008). Central control of body weight and appetite. *J. Clin. Endocrinol. Metab.* *93*, S37-50.

- Wright, M.H., Berlin, I., and Nash, P.D. (2011). Regulation of endocytic sorting by ESCRT-DUB-mediated deubiquitination. *Cell Biochem. Biophys.* *60*, 39–46.
- Wu, X., Yen, L., Irwin, L., Sweeney, C., and Carraway, K.L. (2004). Stabilization of the E3 ubiquitin ligase Nrdp1 by the deubiquitinating enzyme USP8. *Mol. Cell. Biol.* *24*, 7748–7757.
- Xia, Q., and Grant, S.F. (2013). The genetics of human obesity. *Ann. N. Y. Acad. Sci.* *1281*, 178–190.